ORNL-6938

ornl

OAK RIDGE NATIONAL LABORATORY

LOCKHEED MARTIN

CHARACTERIZATION AND PROCESS DEVELOPMENT OF CYANATE ESTER RESIN AND COMPOSITE

B. J. Frame
Engineering Technology Division
Oak Ridge National Laboratory

March 1998

MANAGED AND OPERATED BY
LOCKHEED MARTIN ENERGY RESEARCH CORPORATION
FOR THE UNITED STATES
DEPARTMENT OF ENERGY

ORNL-27 (3-96)

DISCLAIMER

DISCLAIMER

Portions of this document may be illegible electronic image products. Images are produced from the best available original document.

ORNL-6938

CHARACTERIZATION AND PROCESS DEVELOPMENT OF CYANATE ESTER RESIN AND COMPOSITE

B. J. Frame
Engineering Technology Division
Oak Ridge National Laboratory

March 1998

Prepared by the
Oak Ridge National Laboratory
Oak Ridge, Tennessee 37831-8048

Managed by
LOCKHEED MARTIN
ENERGY RESEARCH CORPORATION
for the
U.S. DEPARTMENT OF ENERGY
under contract DE-AC05-96OR22464

CONTENTS

TABLES

FIGURES

LIST OF ACRONYMS AND ABBREVIATIONS

ASTM	American Society of Testing and Materials
cps	centipoise
CV	Coefficient of Variation
CTE	Coefficient of Thermal Expansion
DMA	Dynamic Mechanical Analysis
DSC	Differential Scanning Calorimetry
EDX	Energy Dispersive X-ray
FTIR	Fourier Transform Infrared
G′	storage modulus
G″	loss modulus
H	Enthalpy
ID	Inner Diameter
IR	infrared
ksi	10^3 pounds per square inch
Msi	10^6 pounds per square inch
N_2	Nitrogen
NOL	Naval Ordinance Laboratory
ORNL	Oak Ridge National Laboratory
OD	Outer Diameter
PAN	polyacrylonitrile
psi	pounds per square inch
RH	Relative Humidity
RTM	Resin Transfer Molding
SBS	Short Beam Shear
SEM	Scanning Electron Microscope
T_g	glass transition temperature
T_p	peak temperature
Zr	Zirconium

ABSTRACT

Cyanate ester (or polycyanate) resins offer advantages as composite matrices because of their high thermal stability, low outgassing, low water absorption and radiation resistance. This report describes the results of a processing study to develop high-strength hoop-wound composite by the wet-filament winding method using Toray T1000G carbon fiber and YLA RS-14A polycyanate resin as the constituent materials. Process trials, tests and analyses were conducted in order to gain insight into factors that can affect final properties of the cured cyanate ester resin and its composites. The study shows that the cyanate ester resin has a broad process envelope but that an inert-atmosphere cure is essential for obtaining optimum resin and composite properties. Minimizing moisture exposure prior to cure is also crucial as it affects the T_g of the resin and composite. Recommendations for reducing moisture contact with the resin during wet-winding are presented. High fiber volume fraction (~80%) composites wound and cured with these methods yielded excellent hoop tensile strengths (660 to 670 ksi average with individual rings failing above 700 ksi), which are believed to be the highest recorded strengths for this class of materials. The measured transverse properties were also exceptional for these high fiber fraction composites. Based on the available data, this cyanate ester resin system and its composites are recommended for space and vacuum applications only. Further testing is required before these materials can be recommended for long term use at elevated temperatures in an ambient air environment. The results of all analyses and tests performed as part of this study are presented as well as a baseline process for fabricating thick, stage-cured composites. The manufacture of a 1 in. thick composite cylinder made with this process is also described.

1. INTRODUCTION

The Oak Ridge National Laboratory (ORNL)is involved in the development of affordable composites structures for military, aerospace and transportation applications. As part of this continuing activity, ORNL evaluates new materials and combinations of materials for use in such applications as pressure vessels, flywheel energy storage systems, and aircraft structures. Process development and the determination of the thermomechanical properties of the composite are key factors in the design of successful high performance applications.

This report documents the results of a processing study to develop high-strength hoop-wound composite by the wet-filament winding method using Toray T1000G carbon fiber and YLA RS-14A polycyanate resin as the constituent materials. It is a continuation of the work previously performed and reported by ORNL.[1,2] Material characterization and process trials conducted as part of these studies indicated that the properties of the YLA RS-14 cyanate ester resin were sensitive to factors that include the process environment and cure profile.

In this study, process trials, tests, and analyses were conducted in order to gain better insight into factors that can affect final properties of the cured RS-14 cyanate ester resin and its composites. Emphasis was placed on defining a process for fabrication of thick (0.75 in. or greater) composites made with this material. The results of all analyses and tests performed as a part of this study are presented in this report. The fabrication of a thick T1000G/RS-14 composite cylinder is also described.

The results of a limited physical aging study conducted with neat RS-14 resin panels are also presented. Based on these data, this cyanate ester resin system and its composites are recommended for space and vacuum applications only. Further testing is required before these materials can be recommended for long term use at elevated temperatures in an ambient air environment.

This report is subdivided into three subtasks: (1) RS-14/ RS-14A Resin Optimization Study, (2) Composite Process Trials and (3) Thick T1000G/RS-14 Demonstration Cylinder Fabrication.

2. RS-14/RS-14A RESIN OPTIMIZATION STUDY

The objective of the RS-14/RS-14A Resin Optimization Study subtask was to further investigate process variables identified in previous studies[1,2] that can influence the properties of composites wet-wound with RS-14 cyanate ester resin. These include the presence of moisture and humidity during winding and cure, carbamate formation, surface oxidation arising from the presence of air during postcures at elevated temperature and the cure cycle. The sensitivity of the neat RS-14 resin properties to each of the above was determined in order to establish "thresholds" or limits at which resin (and composite) properties are compromised. This information will establish a process envelope for manufacturing composite hardware.

As a result of the work performed in this subtask, a discovery was made concerning the RS-14 resin formulation. These results persuaded the resin manufacturer, YLA Incorporated, to reformulate the resin. The new formulation, named RS-14A, was introduced approximately half way through the course of these studies.

2.1 RS-14A Resin

A description of events leading to the introduction of RS-14A resin is presented in this section.

2.1.1 RS-14 Resin and Specimen Appearance

The initial material characterization work performed in these studies was conducted using YLA RS-14 resin from Reference (Lot) No. FB3K702. This resin lot was manufactured (blended) by YLA on September 26, 1995, and has been stored continuously in a freezer since its procurement.

Observations made while handling the resin and during sample fabrication yielded unexpected findings. Cast RS-14 resin panels had a sprinkling of red-brown spots or flecks across the surface. The resin panels are cured in an upright position in a mold. The greatest concentration of red-brown flecks was found along the edge of the panel that corresponded to the bottom of the mold while very few flecks were observed at the edge corresponding to the top of the mold. The distribution of red-brown flecks in between the two edges increased going from top to the bottom.

The general appearance of the panel was as if a particulate was settling out of the resin during the cure cycle.

Resin that was centrifuged in a glass test tube and then cured exhibited similar characteristics. A concentration, or patch, of red-brown substance was observed at the bottom of the specimen suggesting that a heavier material had been separated from the resin. Examination under an optical microscope indicated that there were bubbles or porosity in the vicinity of this red-brown substance. Since bubbles would be expected to rise to the top of the test tube during centrifugation, it is reasonable to conclude that they were formed during the cure of the RS-14 resin.

At the same time, a "gritty" residue of light colored particles was observed in the residue lining the walls of the metal quart cans after the RS-14 resin was poured from its container. The visual appearance was as if sand had been mixed with the resin.

These phenomena were not noticed in previous studies with the RS-14 resin. One reason for this is that the RS-14 resin panels fabricated in this study were postcured in an autoclave under a nitrogen (inert) environment. In previous ORNL studies, the RS-14 panels were cured and postcured in air which tends to darken the surface. Red-brown flecks in these specimens would have been impossible to detect visually. The RS-14 resin panels cured in an inert atmosphere, however, tend to remain a light tan color so that the red-brown flecks stand out noticeably.

The majority of thermal and mechanical properties obtained from this lot of RS-14 resin did not suggest that its properties were degraded and these results are presented in later sections of this report. However, a few groups of resin tensile specimens provided evidence that the red-brown flecks were capable of acting as flaws or stress concentrators in the cured resin, thereby reducing the ultimate strength and elongation of individual specimens.

2.1.2 RS-14 Resin Tensile Data

Tensile testing of dogbone specimens cut from the RS-14 resin panels showed that some specimens were failing at significantly lower strengths and elongations than comparable specimens from the same set. Many of the fracture surfaces of these low-strength specimens revealed the presence of a red-brown spot which appeared to be the site for failure initiation. The spots were large enough to be visible to the human eye. Most of the spots were round but some were elongated

or even irregularly shaped.

Table 2.1.2-1 summarizes the individual tensile data for those sets of RS-14 tensile specimens that exhibited red-brown spots at the fracture surfaces. The tensile strengths of specimens with this artifact are, for the most part, significantly lower than for the remainder of the sample set. The red-brown spot appears to be a flaw, or initiation site for early tensile failure.

Closer examination of the fracture surfaces show that the failure occurs symmetrically through the mid-plane of the red-brown feature so that both halves of the tensile specimen have matching spots. Even when the spot is not round, there is a mirror image of its shape duplicated on the other half of the specimen. Photographs of this phenomena are provided in Figure 2.1.2-1. This suggests that failure is occurring at the midplane of the flaw.

Examination of the red-brown spots under an optical microscope showed that the spots are not large bubbles or voids. Instead, both halves of the tensile specimen show that there is a continuous film or skin of resin across the surface of the spots. However, tilting the specimen slightly under the microscopes shows that there is porosity or bubbles ***just beneath*** the surfaces of the spots.

2.1.3 SEM/EDX Analysis

Selected tensile specimens were submitted for Scanning Electron Microscope (SEM) and Energy Dispersive X-ray (EDX) analyses. Figure 2.1.3-1 shows the results of the SEM investigation. The area associated with the red-brown spots are riddled with small bubbles that is suggestive of gas porosity.

EDX analysis of the spots for elements Z=11 to 92 indicated that these spots are also rich in the element zirconium. X-Ray dot maps for the element zirconium (Figure 2.1.3-2) illustrate the concentration of zirconium at the fracture surface which precisely duplicates the footprint of the spots.

Table 2.1.2-1. Tensile specimens with red spots at fracture surface.

Sample ID	Tensile Strength (psi)	Red Spot
RX-1	**(4x380°F; N2 // 510°F; N2)**	
1	5715	Yes
2	5317	Yes
3	11267	
4	4859	Yes
5	4991	Yes
6	12078	
7	7135	Yes
8	12397	
9	4678	Yes
AVG:	7604	
% CV	43.7	
RX-2	**(380°F; N2 // 510°F; N2)**	
1	11181	
2	13841	
3	12760	
4	12115	
5	13117	
6	9531	Yes
7	9445	Yes
8	8519	
9	10333	Yes
10	9566	Yes
11	13486	
12	13202	
13	12779	
14	12208	
15	13034	
16	13435	
17	9635	
AVG:	11658	
%CV	15.2	
RX-7	**(380°F; N2 // 480°F; N2)**	
1	12279	
2	10609	Yes
3	10547	
4	12376	
5	13156	
6	7449	(outlier)
7	13016	
8	12172	Yes
9	12138	
10	12573	
AVG:	12096	
% CV	7.7	

Sample ID	Tensile Strength (psi)	Red Spot
RX-4	**(380°F; N2 // 4x510°F; N2)**	
1	12222	Yes
2	13267	
3	10140	
4	12387	
5	4268	(outlier)
6	12572	
7	11385	Yes
8	12331	
9	12527	
10	11588	
AVG:	12046	
% CV	7.5	
RX-5	**(380°F; Air // 510°F; N2)**	
1	11772	
2	5321	Yes
3	10791	Yes
4	11880	
5	10675	
6	6970	
7	10084	
8	11205	
9	7698	Yes
10	7067	Yes
AVG:	9346	
%CV	25.2	
RX-22	**(380°F; N2 // 480°F; N2)**	
1	11501	
2	12750	
3	11588	
4	11922	
5	12264	
6	6380	Yes ; (outlier)
7	12505	
8	11540	
9	11621	
10	11165	
AVG:	11,873	
% CV	4.4	

Note: Calculations for average tensile strength do not include outliers

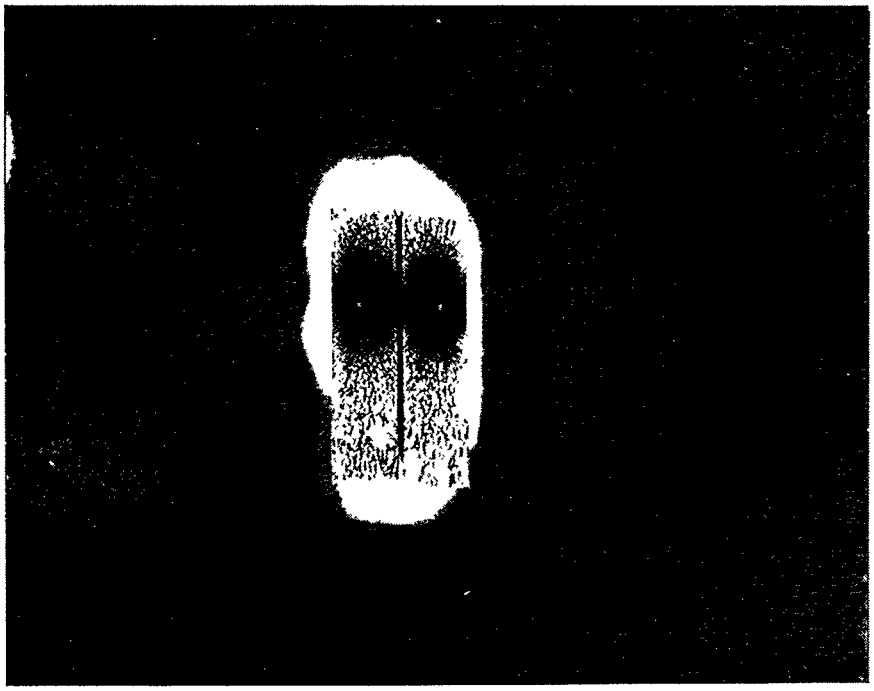

(a) Specimen RX-5, No. 2

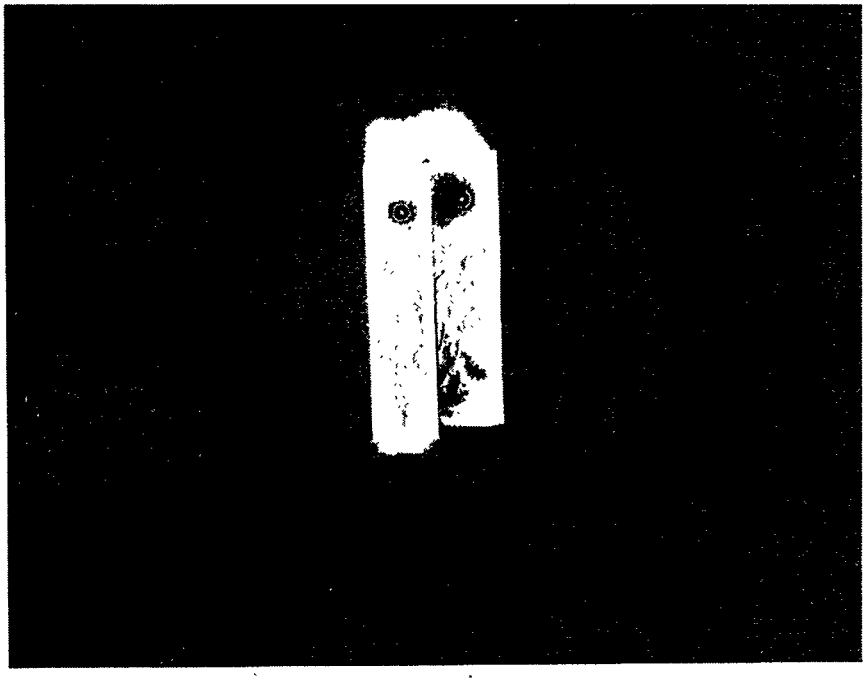

(b) Specimen RX-2, No. 7

Figure 2.1.2-1. Fracture surface of RX-14 tensile specimens with red-brown spots.

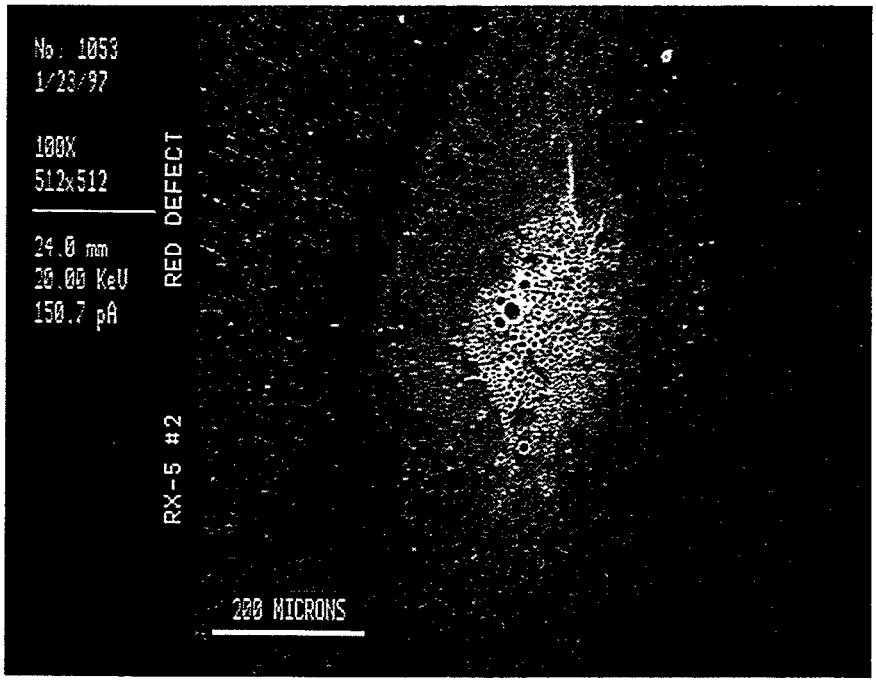

(a) 100X

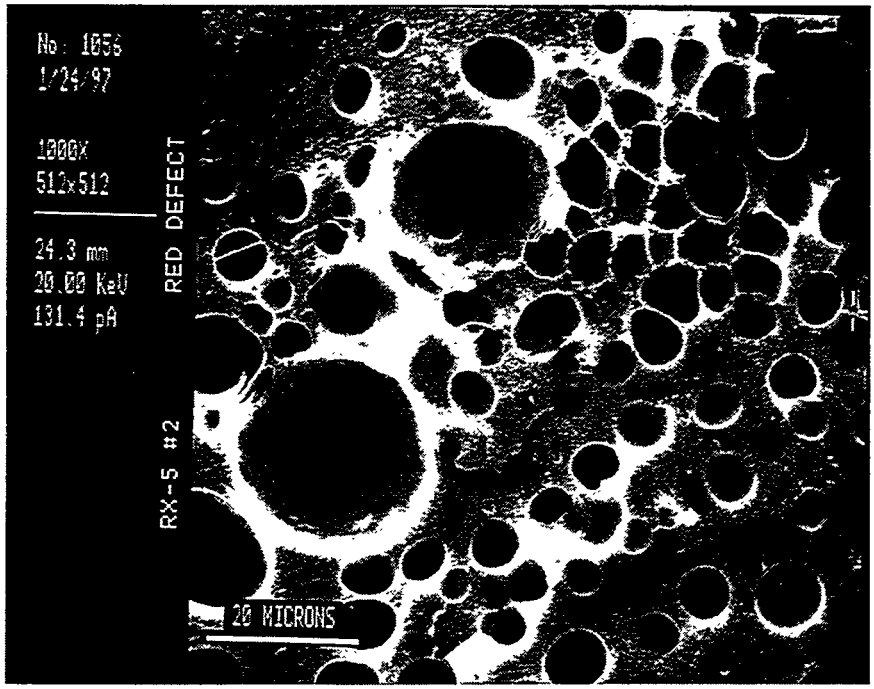

(b) 1000X

Figure 2.1.3-1. SEM of red-brown spots on fracture surface of RX-5, No. 2 tensile specimen.

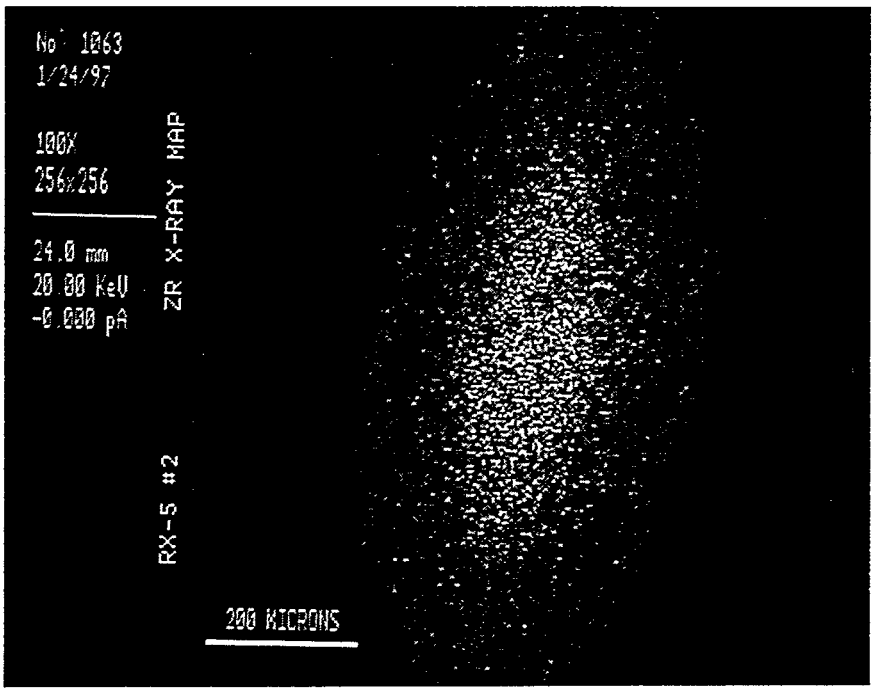

(a) Specimen RX-5, No. 2

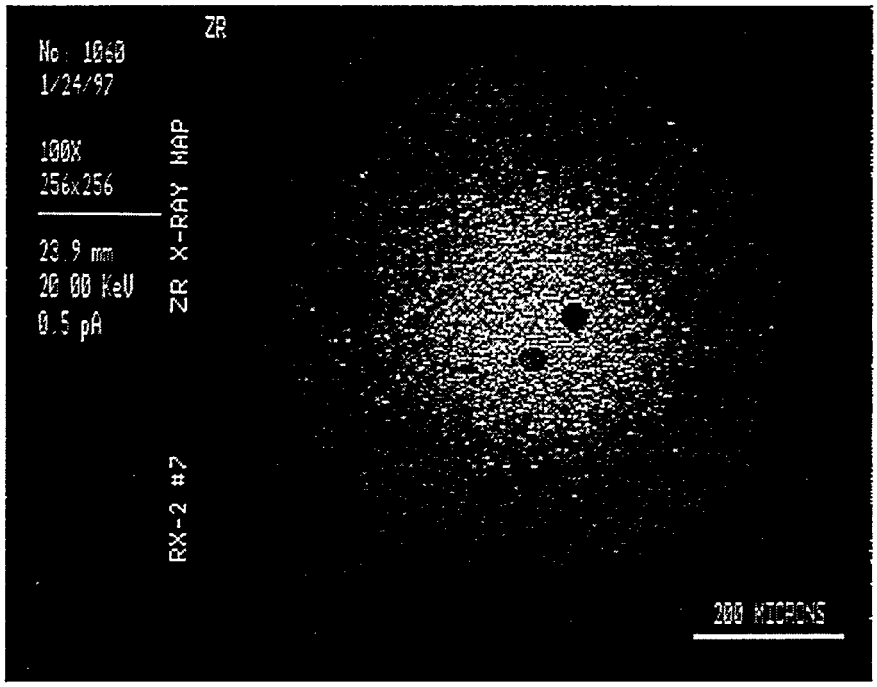

(b) Specimen RX-2, No. 7

Figure 2.1.3-2. Zr X-ray map of red-brown spots at fracture surfaces of RX-14 tensile specimens.

2.1.4 Zirconate Coupling Agent

At the conclusion of the SEM/EDX analyses of the tensile specimen fracture surfaces, YLA Incorporated was informed of the results and consulted to identify possible sources of zirconium contamination in the RS-14 resin. After a review of their processing and equipment, YLA traced the zirconium to a coupling agent that they had been adding to the RS-14 resin in order to improve fiber wettability for resin transfer molding (RTM).

The coupling agent is neopently(diallyl)oxy,tri(dioctyl)phosphato zirconate. It is an orange-red liquid and comprises roughly 0.35 wt % of the RS-14 resin formulation. This is significantly higher than the ~50 ppm level of cobalt (III) acetylacetonate catalyst which is also added to the resin. YLA began adding the coupling agent in response to comments made by another customer that the original formulation was not wetting glass fiber adequately in their RTM process.

Based on ORNL findings, however, YLA became concerned that the zirconate coupling agent might be catalyzing a curing reaction with the RS-14 resin in the storage container, thereby shortening the shelf life of the resin. This would confirm that the "grit" observed in the resin residue is actually small particles of partially cured resin. Another concern is that the coupling agent may catalyze a reaction with any moisture that is present to produce carbamates during cure. Indeed, one of the characteristics of the zirconium-rich spots observed at the fracture surfaces of the tensile specimens was high porosity. The centrifuged RS-14 resin that produced bubbles in the vicinity of the red-brown patches at the bottom of the test tube also suggest possible carbamate formation associated with this material.

YLA elected to remove the zirconate coupling agent from all future batches of RS-14 it produces. If its customers decide that they still want the coupling agent in RS-14 resin, YLA will recommend that they add it themselves at their own facilities or will prepare a custom blend for them. YLA calls the new resin formulation RS-14A. The RS-14A resin is the same as the original RS-14 system with the exception that it no longer contains the zirconate coupling agent.

ORNL procured approximately 50 lb of RS-14A resin for evaluation and to complete the remainder of this study. This resin was prepared as Reference (Lot) No. FB5K176 and was manufactured (blended) by YLA on February 14, 1997.

Essentially, few differences were found between the RS-14 and RS-14A neat resin and composite properties. Neat resin panels cast from the new RS-14A resin lot did not have the red-brown spots observed with the old lot of RS-14 resin and the resin residue remaining in the metal cans was free of the "grit" or partially polymerized resin. Data and analyses comparing the properties of RS-14A to RS-14 resin and composites are presented in later sections of this report.

2.2 Resin Properties with Cure Cycle

This portion of the Resin Optimization subtask is a continuation of process development activities conducted and reported by ORNL.[2] Those studies indicated a higher-than-expected variability in the uncured RS-14 resin's mechanical and thermal properties. Process variables targeted for future investigation included the cure cycle, the reaction rate, exposure to air during cure and postcure, and the presence of moisture during the cure cycle. In this study, each of these variables was investigated individually to assess its impact and significance to cured RS-14/RS-14A resin and (ultimately) composite properties.

2.2.1 DSC Analyses

Differential Scanning Calorimeter (DSC) analyses were performed on uncured RS-14 resin to investigate the effects of ramp rate, precure temperature and postcure temperature on the resin cure profile and ultimate T_g.

The advantage of DSC analysis is that the cure temperature, ramp rate and environment can be very precisely controlled. The cure of large resin and composite samples in an oven is subject to some inaccuracy because of thermal gradients in the oven chamber and lags in the heatup rate associated with the sample size and the thermal mass of the tooling or mold. DSC, on the other hand, employs small (~10 mg) resin weights that are placed in a well instrumented sample cell. The process temperature and heatup rate are therefore known to a greater degree of precision. In addition, the sample holder is continuously purged with a stream of dry nitrogen throughout testing to minimize resin side reactions with air and ambient humidity. DSC has the added advantage that it is a relatively inexpensive analysis to run compared to the cost of fabricating and testing resin panels.

The analyses were performed using a Perkin Elmer DSC-7 Differential Scanning Calorimeter. A nominal 10 to 11 mg sample of resin was sealed in aluminum pans prior to being placed in the DSC sample cell. Information measured for the uncured RS-14/RS-14A resin included the exothermic heat of reaction (delta H), the onset and peak temperatures from the enthlapy cure profile, and the resin sample glass transition temperature (T_g) after cure.

Table 2.2.1-1 summarizes the DSC analysis results for ten cure profiles conducted with the RS-14 resin. The cure cycles evaluated include a 3 hr precure at 135°C (275°F) followed by a 4 hr postcure at 265°C (509°F); a 3 hr precure at 190°C (374°F) followed by a 4 hr postcure at 265°C; and cure cycles where the precure step is eliminated and the resin is ramped directly to the postcure temperatures of 250°C (482°F) or 265°C for 4 hr. Ramp rates to the precure temperature evaluated are 1° and 4°C/min. The effect of ramp rate to the postcure temperature was tested at 1°, 2°, and 4°C/min. After postcure all of the samples were cooled back to 25°C and then ramped at 5°C/min to 300°C to determine the resin's T_g.

Table 2.2.1-1. DSC T_g data for RS-14 resin.

Cure	135°C		190°C		250°C		265°C		T_g	
	Ramp (°C/min)	Hold (hrs)	Ramp (°C/min)	Hold (hrs)	Ramp (°C/min)	Hold (hrs)	Ramp (°C/min)	Hold (hrs)	(°C)	(°F)
#1							1	4	253	488
#2							2	4	256	493
#3-1							4	4	255	491
#3-2							4	4	253	488
#4					1	4			256	493
#5-1					2	4			254	489
#5-2					2	4			256	493
#6					4	4			255	491
#7-1	1	3					1	4	253	487
#7-2	1	3					1	4	255	491
#8	4	3					1	4	254	489
#9			1	3			1	4	254	489
#10-1			4	3			1	4	256	492
#10-2			4	3			1	4	256	493

The DSC analyses showed that the T_g obtained from all of the cure cycles was essentially the same and in the range of 253°–256°C (487°–493°F). These results were reproducible within 2°C for selected cure profiles that were retested. The data indicate that the precure temperature (or lack of a precure step) as well as the resin heat up rate have no impact on the RS-14 resin's ultimate T_g.

It is interesting that there was also no difference in the T_g of the resin samples postcured at 250° and 265°C. Ordinarily a polymer's ultimate T_g will depend on its last cure temperature. It is believed that the long (4 hr) soak at the 250°C postcure temperature is the factor that enabled the cyclotrimerization reaction to proceed to same degree of conversion as for samples postcured at 265°C.

Table 2.2.1-2 are the data from the enthalpy profiles for the RS-14 samples ramped directly to the postcure temperature without a precure step. (The Perkin Elmer DSC-7 introduces a discontinuity, or "step" into the baseline profile when it switches from one cure segment to the next. The delta H values of cure profiles with multiple steps are therefore difficult to interpret and are not included in this table.) The data are from the portion of the enthalpy curve corresponding to temperature ramp only and do not include the exothermic heat evolved during the thermal soak at the postcure temperature. A typical enthalpy profile for the RS-14A resin is provided in Figure 2.2.1-1.

Table 2.2.1-2. DSC enthalpy data for RS-14 resin.

Cure	135°C		190°C		250°C		265°C		Onset	Tp	Delta H
	Ramp (°C/min)	Hold (hrs)	Ramp (°C/min)	Hold (hrs)	Ramp (°C/min)	Hold (hrs)	Ramp (°C/min)	Hold (hrs)	(°C)	(°C)	J/gm
#1							1	4	145	174	-774
#2							2	4	158	187	-624
#3-1							4	4	172	201	-519
#3-2							4	4	171	201	-539
#4					1	4			147	174	-616
#5-1					2	4			161	187	-536
#5-2					2	4			158	187	-538
#6					4	4			171	201	-472

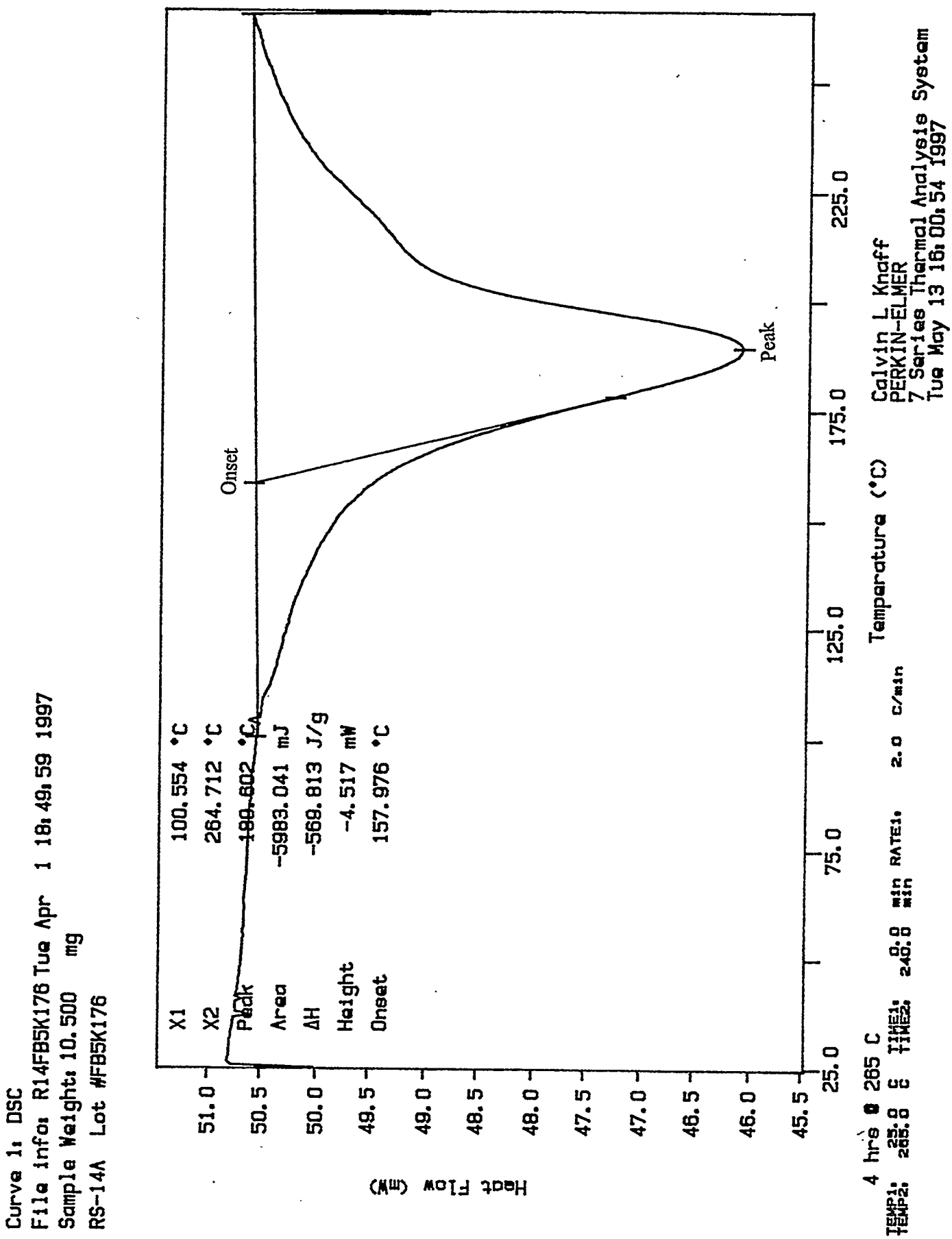

Figure 2.2.1-1. DSC curve of RS-14A cure.

The literature[3] report that although DSC is a widely applied method for determining the conversion of cyanate ester resins, changes in heat capacity of the polymer during reaction, poor heat contact between sample and pan, and other experimental difficulties associated with the DSC baseline definition (curvature) all can produce a great scatter in the enthalpy data. Based on literature values,[4] an enthalpy of -100 to -110 kJ/cyanate equivalence is typical for cyanate ester resins. YLA calculates the cyanate equivalent weight for the RS-14 and RS-14A resin to be on the order of 178 g/equivalence. This suggests that the measured delta H values should be on the order of -561 to -618 J/g. These calculated delta H values are in the proximity of the enthalpy data summarized in Table 2.2.1-2.

The data show that the faster the heat up rate, the lower the delta H measured during the ramp to the postcure temperature. That is as expected because there is less time for the cyclotrimerization reaction to proceed. Therefore a greater percentage of the cure must occur during the thermal soak at the postcure temperature. Similarly, the onset and peak temperatures for the enthalpy curve occur at higher temperatures with increasing ramp rate because there is less time at the lower temperature for conversion to occur.

Table 2.2.1-3 is a comparison of the DSC data for RS-14A and RS-14 resin. Both resins were heated at 2°C/min from 25° to 265°C and held at the upper temperature for 4 hr. The samples were then cooled to 25°C and rescanned at 5°C/min to 300°C to obtain the T_g.

Table 2.2.1-3. DSC analysis of RS-14 and RS-14A resin.

Resin	Sample	Onset (°C)	Peak (°C)	Delta H (J/gm)	T_g (°C)
RS-14	1	158	187	-624	256
RS-14A	1	158	189	-570	270
	2	162	189	-598	270

Samples heated at 2°C/minute from 25°C to 265°C and held for 4 hours at 265°C.
Sample rescanned at 5°C/minute to obtain T_g.

The onset and peak temperatures obtained from the enthalpy profiles are comparable for RS-14 and RS-14A resin. The delta H values for both resins agree within 10% which is considered good, considering the data scatter inherent with this measurement.

The T_g of the RS-14A resin is 270°C (518°F) which is significantly higher than the 256°C (493°F) T_g of the RS-14 resin. It is not known whether this difference is due to normal batch-to-batch variability for these materials or because the RS-14 came from an older lot of resin. Removal of the zirconate coupling agent from the resin formulation may also have had an effect on the RS–14A resin's T_g.

The degree of conversion for a polymeric reaction can be estimated based on the fraction of heat evolved as determined from the DSC enthalpy profile. Using this approach, the delta H for the samples ramped to 250°C can be normalized with respect to the delta H values for the samples ramped to 265°C for a given ramp rate. The results are summarized in Table 2.2.1-4 and show that the estimated degree of conversion (cure) for the RS-14 resin heated to 250°C was nominally 80–88% of its conversion at 265°C. Restated, the heat liberated during ramps to 250°C at a given ramp rate is roughly 80–88% of the heat liberated in ramping to 265°C for the same ramp rate.

Table 2.2.1-4. RS-14 heat evolved during ramp to temperature.

Ramp (°C/min)	Delta H (J/gm)		Percent* heat evolved to 250°C
	250°C	265°C	
1	-616	-774	80
2	-536	-624	86
4	-472	-539	88

*Delta H between ambient to 265°C is assumed to be 100 percent.

DSC analyses were also conducted on the RS-14A resin to estimate the degree of conversion from the precure step of the cure cycle. Samples of RS-14A resin were ramped at 2°C/min from 25°C to either 135° or 190°C (275° or 374°F) and held at that temperature for 3 hr. The samples were then cooled to 25°C and reheated at 2°C/min to 265°C to obtain the residual heat of reaction.

The residual heat of reaction was then normalized with respect to the delta H values obtained for samples heated directly to the postcure temperature without a precure step.

The data are summarized in Table 2.2.1-5 and show that the measurable exothermic heat of reaction for an RS-14A sample that has been precured 3 hr at 190°C is between 2 to 9% of its original (non-precured) value. The polymer still undergoes cross linking above 190°C and at the postcure temperature to increase its final T_g but there is not much heat liberated with these reactions.

Table 2.2.1-5. Residual delta H with precure temperature for RS-14A resin.

Precure*	Delta H** (J/gm)	Percentage of total Delta H
(none)	-570	
	-598	
	Average: -584	100
135°C	-150	26
	-177	30
190°C	-11	2
	-54	9

*Precure is 2°C/minute ramp to temperature and hold 3 hours.

**Sample ramped after precure at 2°C/minute to 265°C to measure residual delta H.

By comparison, the delta H for an RS-14A sample that has been precured 3 hr at 135°C still liberates 25 to 30% of its original (non-precured) heat. This residual heat may have significance for thick parts where transport mechanisms to conduct excess heat out of the composite are limited.

2.2.2 Cast Panel Properties

RS-14 and RS-14A resin panels were cast and cured to determine the impact of the process cycle and environment on cured resin properties. After cure, the panels were evaluated for tensile properties, density and by Dynamic Mechanical Analysis (DMA).

2.2.2.1 Panel Fabrication

Emphasis in this study was placed on control of the curing environment and measurement of its effect on cured resin properties. In order to achieve this, all panels were cured in an autoclave that was purged with dry nitrogen gas prior to initiating the cure cycle.

Nominal 9 in. × 14 in. × 1/8 in. thick panels were fabricated according to the following procedure. The cyanate ester resin was preheated to ~170°F in an oven and then evacuated in a vacuum desiccator for ~10 min to remove the bulk of any entrapped air. The resin was then poured into a preheated metal mold.

The mold was sealed in an autoclave and the autoclave chamber was purged for 1 hr at room temperature with 2–3 psi dry nitrogen. The autoclave vent was cracked slightly during purging so that the nitrogen would eventually displace the air in the autoclave's chamber. After one hr at room temperature, the cure cycle was initiated but purging with nitrogen was continued an additional 3–4 hr into the cure. At that point, the autoclave vent was sealed to prevent the inadvertent re-entry of air into the autoclave when it entered the cool-down portion of the cure cycle.

The cure process variables studied were (1) a 280°F versus a 380°F precure step prior to postcure; (2) a cure cycle with no precure step that ramps directly to the postcure temperature; (3) a 480°F versus a 510°F postcure temperature.

The 280°F precure temperature was selected for investigation because previous studies[1] showed that this is the minimum temperature required to effectively gel the RS-14 cyanate ester resin. The 380°F precure temperature, however, has also been used to process T1000G/RS-14 cylinders in previous studies and was also the precure temperature recommended by YLA.

Eliminating the precure step is of potential benefit for a production scenario because it represents a significant time saving to the cure process. However, it is known from work conducted with epoxies that the precure step can be an important part of a resin's cure cycle because it provides time for resin gelation to occur and for a gradual liberation of the exothermic heat of reaction associated with cure. The significance of the precure step to the cyanate ester cyclotrimerization reaction was unknown and investigated.

Similarly, the 480°F postcure temperature was selected for study because DSC studies indicated that RS-14 resin postcured at this temperature would achieve the same T_g as resin postcured at the higher temperature. Previously T1000G/RS-14 cylinders have been postcured at 510°F in an effort to maximize the resin and composite's T_g.

The times at process temperature for this study were maintained at 3 hr for the precure segment and 4 hr for the postcure segment of the cure cycle. Ramp rates to precure and postcure temperature were 2°–3°F/min.

After cure, the resin panels were allowed to cool to room temperature in the autoclave while the nitrogen atmosphere was maintained. The panels were then removed from the mold and evaluated.

2.2.2.2 Tensile Properties

Tensile testing was accomplished per ASTM D-638 (*Tensile Properties of Rigid Plastics*) using dogbone specimens cut from the panels. The gagelength sections of all of the specimens was polished lightly with sandpaper to reduce surface flaws and marks from the cutting operation. The specimen modulus and elongation were measured using an extensometer clipped to the gagelength.

RS-14 and RS-14A resin tensile data as a function of cure cycle are summarized respectively in Tables 2.2.2.2-1 and 2.2.2.2-2. The average tensile strengths exclude the values of specimens that had red-brown spots at the fracture surface or were statistical outliers. The Statistical Analysis Program for MIL-HDBK-17 (STAT17), Revision 3.1, November 4, 1992 was used to analyze sample sets for outliers as well as batch-to-batch variability. STAT17 determines the statistically based mechanical properties according to procedures outlined in MIL-HDBK-17 on Polymer Matrix Composites.

The lowest RS-14 average tensile strength is from panel RX-5 which was 11,125 ksi with a 6.8% coefficient of variation. RX-5 was precured for 3 hr at 380°F in air and postcured for 4 hr at 510°F in nitrogen. The exposure to air is not considered to be a significant factor due to the fact

Table 2.2.2.2-1. RS-14 resin tensile properties with cure cycle.

Panel ID	Cure Cycle	No. of Specimens	Strength (psi)	Elongation (%)	Modulus** (ksi)
RX-2*	380°F; N2 // 510°F; N2	13	12,255 (12.9)	5.1 (26.1)	406 (3.2)
RX-5*	380°F; Air // 510°F; N2	5	11,125 (6.8)	3.5 (10.7)	425 (0.9)
RX-6	280°F; N2 // 480°F; N2	10	13,023 (3.5)	5.8 (12.3)	395 (2.9)
RX-7*	380°F; N2 // 480°F; N2	6	12,589 (3.3)	4.9 (8.0)	390 (5.3)
RX-8	280°F; N2 // 510°F; N2	9	12,388 (3.0)	4.5 (5.8)	388 (4.3)
NRS14	280°F; N2 // 510°F; N2	7	12,551 (4.3)	5.2 (12.6)	396 (3.5)
RX-9	510°F; N2	10	11,685 (10.6)	4.2 (19.8)	401 (6.0)
RX-10	480°F; N2	10	12,734 (5.6)	5.5 (15.5)	391 (4.2)
RX-22*	380°F; N2 // 480°F; N2	9	11,878 (4.4)	4.1 (8.3)	396 (2.9)
RX-24	280°F; N2 // 480°F; N2	10	12,264 (3.0)	4.8 (7.2)	377 (2.1)

* Strength and elongation data exclude specimens with visible red spots at fracture surfaces
** Average of 7 or more specimens
( ) Number in parentheses is percent coefficient of variation

Table 2.2.2.2-2. RS-14A resin tensile properties with cure cycle.

Panel ID	Cure Cycle	No. of Specimens	Strength (psi)	Elongation (%)	Modulus (ksi)
RX-29	380°F; N2 // 480°F; N2	9	12,122 (5.3)	4.6 (10.9)	377 (1.8)
RX-33	280°F; N2 // 480°F; N2	10	12,820 (4.5)	5.5 (12.0)	372 (1.3)

( ) Number in parentheses is percent coefficient of variation

that the precure was conducted in the mold, and resin exposure to the atmosphere would have been limited. A more reasonable explanation is that the sample size is only five specimens after excluding specimens with red-brown spots at the fracture surface or statistical outliers and may not be representative of the RS-14 resin's properties.

Excluding panel RX-5, the remainder of the data show that the RS-14 average tensile strength is on the order of 11.7 to 13.0 ksi. The elongation at failure ranges between 4.1 to 5.8% and the modulus is 377 to 406 ksi.

The average tensile strengths for the data sets (excluding RX-5) agree within 10% of one another and there is otherwise no apparent difference in average tensile strength for RS-14 resin that is (1) precured at 280°F versus 380°F prior to postcure; (2) cured without a precure step; and (3) postcured at 480°F versus 510°F. There is also good agreement between the modulus and elongation at failure data for all of the cure cycles.

STAT17 was used to analyze the data sets for batch-to-batch variability and found that the data sets were statistically different. Excluding the lower strength data sets from panels RX-9 and RX-22 as well as RX-5 yielded the same result. The reason for this is unknown. Otherwise, the variability encountered in this study appears to be typical for neat resin tensile data in general.

One significant observation is that the RS-14 panels that were postcured at 480°F in nitrogen remained a light tan color, or the same color as the precured resin. RS-14 panels that were postcured at 510°F in nitrogen, on the other hand, turned a dark brown color. The darkening was not due to oxidation as a result of an imperfect nitrogen purge because the color change went all the way through the panel thickness as opposed to being only at the surface. This indicates a change occurs with elevated temperature in the bulk RS-14 resin.

The RS-14A average tensile strength measured 12.1 and 12.8 ksi for the two cure cycles evaluated. The elongation at failure was 4.6 to 5.5% and the modulus was 377 and 372 ksi. The data in Tables 2.2.2.2-1 and 2.2.2.2-2 show that the RS-14A and RS-14 tensile strength and elongation data are basically equivalent. However, the RS-14A tensile modulus is slightly lower than that of the RS-14 resin.

2.2.2.3 Density

Density measurements were made via ASTM D792 (Tests for Specific Gravity and Density of Plastics by Displacement) using a 2 in. × 3 in. section of resin panel. Tables 2.2.2.3-1 and 2.2.2.3-2 are respectively a compilation of all of the RS-14 and RS-14A neat resin densities measured in this study. The density data for the panels that were fabricated as part of this study to evaluate resin properties as a function of cure cycle are combined with the data from panels from the thermal cycling (Section 2.3) studies.

The data show that (1) the RS-14 and RS-14A densities are equivalent to each other and (2) the resin density does not change with cure cycle. The nominal resin density for all of the panels is on the order of 1.20 g/cm^3. This agrees with information provided by YLA Incorporated.

2.2.2.4 DMA

DMA was accomplished using a Rheometrics Dynamic Spectrometer with the rectangular torsion test geometry. The samples were tested with a fixed frequency of 6.28 rad/sec and a commanded strain of 0.03%. A temperature sweep was performed from 30° to 300°C with a heat up rate of 5°C/min. Data were taken at 5°C intervals with a 1 min soak time at each test temperature prior to taking the measurement. The data recorded for each test temperature includes G', G" and tan delta.

Tables 2.2.2.4-1 and 2.2.2.4-2 are, respectively, a compilation of the RS-14 and RS-14A resin DMA results. The DMA results of the panels that were fabricated as part of this study to evaluate resin properties as a function of cure cycle are combined with the data from panels from the thermal cycling studies (Section 2.3).

The shear modulus data reported in Tables 2.2.2.4-1 and 2.2.2.4-2 are of the G' storage (elastic component) modulus taken at room temperature. The T_g was calculated three ways. With the G' line-fit method, the T_g was calculated from the G' versus temperature curve by extrapolating

Table 2.2.2.3-1. RS-14 neat resin density.

Panel ID	Cure Cycle	Density (g/cm3)	Comment
RX-1	4x380°F; N2 // 510°F; N2	1.2060	Four thermal cycles @ 380°F in N2
RX-2	380°F; N2 // 510°F; N2	1.1995	
RX-3	4x380°F; Air // 510°F; N2	1.2094	Four thermal cycles @ 380°F in air
RX-4	380°F; N2 // 4x510°F; N2	1.2099	Four thermal cycles @ 510°F in N2
RX-5	380°F; Air // 510°F; N2	1.2041	Precured in air
RX-6	280°F; N2 // 480°F; N2	1.1975	
RX-7	380°F; N2 // 480°F; N2	1.1983	
RX-8	280°F; N2 // 510°F; N2	1.2020	
RX-9	510°F; N2	1.2024	
RX-10	480°F; N2	1.1982	
RX-21	4x380°F; N2 // 480°F; N2	1.2046	Four thermal cycles @ 380°F in N2
RX-22	380°F; N2 // 480°F; N2	1.2026	
RX-24	280°F; N2 // 480°F; N2	1.2003	
RX-25	280°F; N2 // 4x480°F; N2	1.2092	Four thermal cycles @ 480°F in N2

Table 2.2.2.3-2. RS-14A neat resin density.

Panel ID	Cure Cycle	Density (g/cm3)	Comment
RX-28	4x380°F; N2 // 480°F; N2	1.1988	Four thermal cycles @ 380°F in N2
RX-29	380°F; N2 // 480°F; N2	1.1992	
RX-30	4x280°F; Air // 480°F; N2	1.2011	Four thermal cycles @ 280°F in air
RX-31	280°F; Air // 480°F; N2	1.1996	Precured in air
RX-32	280°F; N2 // 4x480°F; N2	1.2047	Four thermal cycles @ 480°F in N2
RX-33	280°F; N2 // 480°F; N2	1.1980	

Table 2.2.2.4-1. RS-14 resin DMA properties with cure cycle.

Panel ID	Cure Cycle	G' @ 82°F (ksi)	Tg (°F) G' Line-Fit	Tg (°F) G" Peak	Tg (°F) Tan Delta Peak
RX-1*	4x380°F; N2 // 510°F; N2	166	467	478	496
RX-2	380°F; N2 // 510°F; N2	157	487	496	524
RX-3**	4x380°F; Air // 510°F; N2	170	453	469	488
RX-4*	380°F; N2 // 4x510°F; N2	177	468	478	506
RX-5	380°F; Air // 510°F; N2	165	472	478	506
RX-6	280°F; N2 // 480°F; N2	159	485	487	524
RX-7	380°F; N2 // 480°F; N2	153	488	496	524
RX-8	280°F; N2 // 510°F; N2	157	493	496	533
NRS14	280°F; N2 // 510°F; N2	NA	474	487	514
RX-9	510°F; N2	155	489	496	533
RX-10	480°F; N2	160	486	496	524
RX-21*	4x380°F; N2 // 480°F; N2	158	470	482	509
RX-22	380°F; N2 // 480°F; N2	157	478	491	519
RX-24	280°F; N2 // 480°F; N2	158	492	499	527
RX-25*	280°F; N2 // 4x480°F; N2	163	475	489	508

*** Thermally cycled in nitrogen**
****Thermally cycled in air**

Table 2.2.2.4-2. RS-14A resin DMA properties with cure cycle.

Panel ID	Cure Cycle	G' @ 82°F (ksi)	Tg (°F) G' Line-Fit	Tg (°F) G" Peak	Tg (°F) Tan Delta Peak
RX-28*	4x380°F; N2 // 480°F; N2	152	505	518	536
RX-29	380°F; N2 // 480°F; N2	153	506	517	535
RX-30**	4x280°F; Air // 480°F; N2	159	495	515	533
RX-31	280°F; Air // 480°F; N2	150	504	515	534
RX-32*	280°F; N2 // 4x480°F; N2	157	505	516	534
RX-33	280°F; N2 // 480°F; N2	152	504	515	542

*** Thermally cycled in nitrogen**
**** Thermally cycled in air**

the straight line portions before and after the "knee" in the curve and interpreting T_g as the point on the temperature axis at which the two lines intersect. T_gs' were also calculated from the peaks of the G" (loss modulus) and tan delta (G"/G') versus temperature curves. A typical RS-14A DMA plot with T_g calculations is provided in Figure 2.2.2.4-1.

Excluding the thermal cycling data, the RS-14 T_g ranges from 472° to 493°F (G' line-fit method), 478° to 499°F (G" peak) and 506° to 533°F (tan delta peak). The lowest T_g data from this set was measured from panel RX-5 which was precured for 3 hr at 380°F in air and postcured for 4 hr at 510°F in nitrogen. As discussed in the preceding section, this panel also had the lowest average tensile strength.

The RS-14A T_g data range from 504° to 506°F (G' line-fit method), 515° to 517°F (G" peak), and 534° to 542°F (tan delta peak) for panels that were not part of the thermal cycling study. These T_g are significantly higher than the T_g data from the RS-14 panels. There is also less spread between the maximum and minimum T_g values for each of the G' line-fit, G" peak and tan delta peak calculation methods. These results confirm the DSC analyses of RS-14A and RS-14 resin in Section 2.2.1 which also showed that the RS-14A resin had a significantly higher T_g than the RS-14 resin.

The data in Table 2.2.2.4-1 show that there was no difference in the T_g between RS-14 samples that were postcured at 480° and 510°F in nitrogen. This is comparable to the DSC results summarized in Section 2.2.1. Ordinarily a polymer's ultimate T_g will depend on its last cure temperature. It is believed that the long (4 hr) soak at the 480°F postcure temperature is the factor that enabled the cyclotrimerization reaction to proceed to same degree of conversion as for samples postcured at 510°F.

Similarly, there was no consistent difference in the panel T_g from curing the resin with a 280° and 380°F precure step, or from eliminating the precure step and ramping directly to the postcure temperature. These data, too, match the DSC results in Section 2.2.1.

Excluding the data from the thermally cycled panels, the RS-14 and RS-14A shear modulus is in the range of 150 to 165 ksi. There is no clear correlation between the shear modulus and the cure cycle used to fabricate the panels. The shear moduli for RS-14 and RS-14A resin are essentially equivalent.

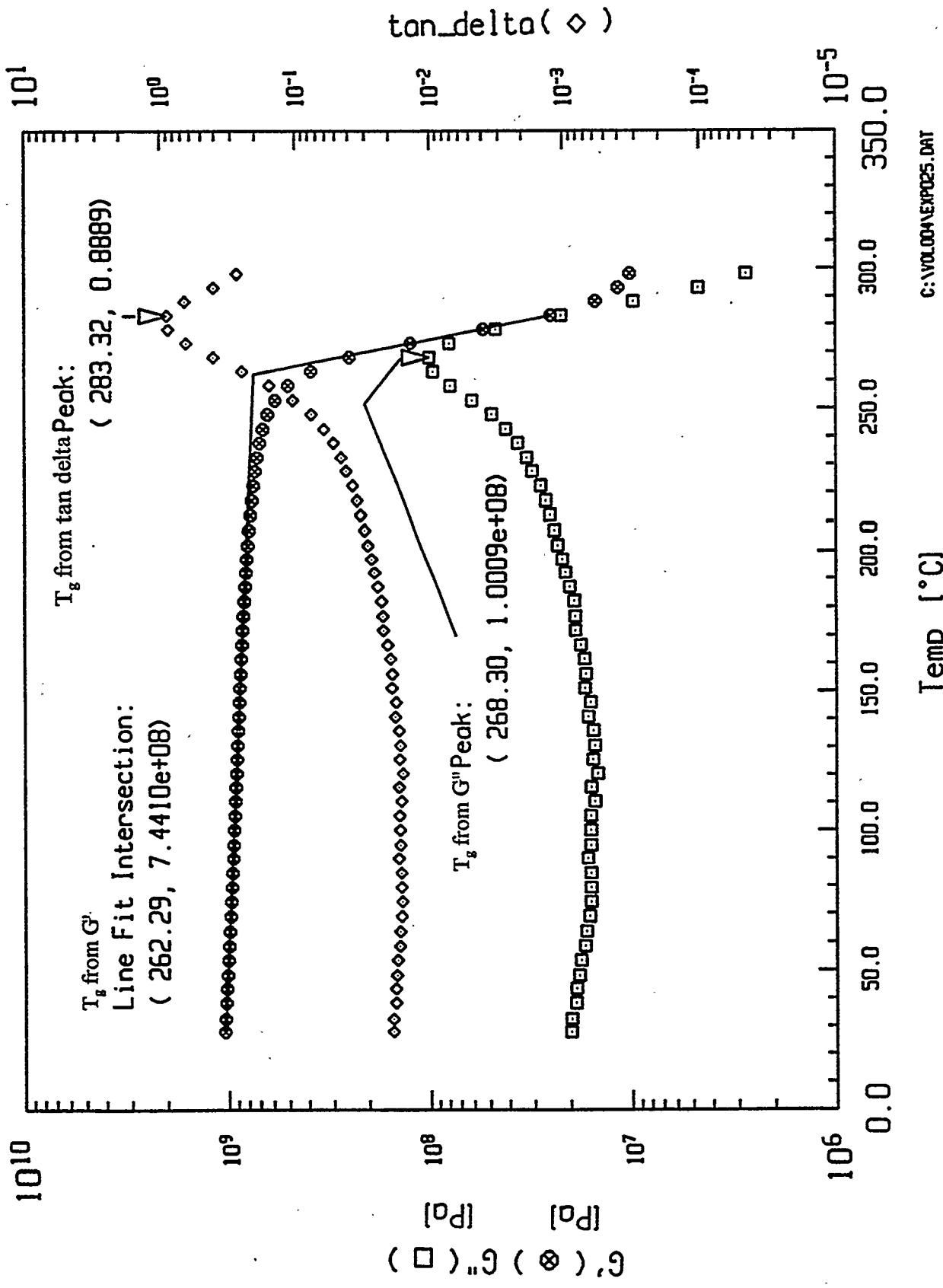

Figure 2.2.2.4-1. DMA plot for panel RX-33.

2.3 Thermal Cycling Trials

The objective of the resin thermal cycling trials was to determine the effects of multiple precure and postcure cycles on the RS-14/RS-14A resin's properties. In addition, thermal cycling trials were conducted in both air and inert environments to determine the minimum temperature threshold at which surface oxidation occurs. This work supports the development of a process for wet-filament-winding thick, stage cured composite.

2.3.1 Procedure

RS-14 and RS-14A panels designated for cure and thermal cycling in a nitrogen environment were cast and cured per the procedures described in Section 2.2.2. The panels were then removed from the mold and laid flat on a metal surface plate in the autoclave. Cycling was accomplished while purging the autoclave with nitrogen using the same procedure used to cure the resin panels.

Panels designated for cure and thermal cycling in air were fabricated and tested with the same procedure ***except*** that the autoclave was not purged with nitrogen during the process cycle. These panels were exposed to the air within the interior of the chamber as well as any air that entered the chamber via the autoclave's circulation system and vents.

The thermal cycling test matrix is shown in Table 2.3.1-1. Thermal cycling trials were conducted for the following conditions: (1) thermal cycling at the 280° and 380°F precure temperature in an inert atmosphere; (2) thermal cycling at the 280° and 380°F precure temperature in air; (3) thermal cycling at the 480° and 510°F postcure temperature in an inert atmosphere. (Thermal cycling trials were not conducted in air at the postcure temperatures because the results of previous ORNL studies[2] have already demonstrated that the RS-14 resin properties are degraded by the resin surface reactions caused by high temperature exposures to ambient atmosphere.)

Including the initial cure in the mold, the subject panels were given either three additional precure cycles or three additional postcure cycles (depending on its test designation), for a total of four precure or postcure cycles. Panels designated for multiple postcure cycles were precured only once during the initial cure in the mold. All subsequent thermal cycling was performed from room temperature directly to the postcure temperature. Panels designated for multiple precure cycles were

removed from the mold in a partially cured condition before being subjected to additional precure cycles. At the end of the last precure cycle, the panels were then ramped to the postcure temperature.

Table 2.3.1-1. Thermal cycling/air versus inert atmosphere cure matrix.

RS-14	RS-14A	280°F (3 hrs)		380°F (3 hrs)		480°F (4 hrs)	510°F (4 hrs)
		Air	N2	Air	N2	N2	N2
X	X		1 time			1 time	
	X	1 time				1 time	
	X	4 times				1 time	
X	X	1 time				4 times	
X	X				1 time	1 time	
X	X				4 times	1 time	
X					1 time		1 time
X				1 time			1 time
X					4 times		1 time
X				4 times			1 time
X					1 time		4 times

Tests: Tensile strength, modulus and elongation
DMA

All postcures were conducted in an inert (nitrogen environment). If the samples had been cycled at the precure temperature in nitrogen, they were postcured at an elevated temperature directly after the last thermal soak. If the samples had been cycled at the precure temperature in air, the autoclave was taken back to room temperature after the last thermal soak, purged with nitrogen, and then ramped to the elevated postcure temperature.

The dwell times (for cure and thermal cycling) at the process temperature were maintained at 3 hr for the precure segment and 4 hr at the postcure segment of the cure cycle. Ramp rates to precure and postcure temperature were 2°–3°F/min.

Between cycles, the resin panels were allowed to cool to room temperature in the autoclave and then removed for examination. Nominal 1 in. × 1 in. chips were cut from the panels after each thermal soak to document any changes in visual appearance. The panels were then returned to the autoclave for the next cycle.

2.3.2 Evaluation

After thermal cycling was completed, the resin panels were examined visually for changes in appearance, and tested for tensile properties, density and DMA. The results are summarized in the following sections.

2.3.2.1 Visual Appearance

Examination of the panel cycled four times to the 510°F postcure temperature in nitrogen (RX-4) showed significant darkening of the resin with each cure cycle. The darkening was not due to oxidation as a result of an imperfect nitrogen purge because the color change went all the way through the panel thickness as opposed to being only at the surface. The panels that were cycled four times to the 480°F postcure temperature in nitrogen (RX-25 and RX-32) also showed some darkening of the resin with each cure cycle but to a much lesser degree than the samples cycled to 510°F.

The implication of the color change with multiple postcure cycles is that a physical/chemical change occurs in the cyanate ester resin with prolonged exposure at elevated temperature. The fact that the samples cycled to 510°F darken significantly more than samples cycled to 480°F suggests that the threshold for change lies somewhere between these two temperature extremes.

The resin panel cycled four times to the 380°F precure temperature in air prior to postcure (RX-3) exhibited a slight darkening of the resin with each cycle. In this case, the color change was at the surface only and indicative of reaction of the cyanate ester resin with the ambient oxygen and/or humidity in the autoclave chamber. The panels that were cycled four times to the 380°F precure temperature in an inert (nitrogen) environment prior to postcure (RX-1, RX-21 and RX-28) showed no discoloration.

Examination of the resin panel cycled four times to the 280°F precure temperature in air prior to postcure (RX-30) also revealed no discoloration with thermal cycling. The conclusion is that the reaction of the surface resin with the ambient environment either does not occur or proceeds at a much slower rate at the lower temperature.

2.3.2.2 Tensile Properties

Tables 2.3.2.2-1 and 2.3.2.2-2 are, respectively, a compilation of the tensile data for RS-14 and RS-14A resin panels fabricated and tested as part of the thermal cycling study. Panels fabricated with comparable precure and postcure temperatures (but not thermally cycled) are included for comparison.

The data show no change in the tensile strength of RS-14 and/or RS-14A resin panels cycled four times to 510°F in nitrogen (RX-4); four times to 480°F in nitrogen (RX-25 and RX-32); and cycled four times to the 380°F precure temperature in nitrogen prior to postcure (RX-1, RX-21 and RX-28).

The tensile moduli of the RS-14 panels that were thermally cycled at either the precure temperature or postcure temperature tended to be slightly higher than their non-thermally cycled counterparts. The largest increase was for RS-14 panel RX-4 (four postcure cycles at 510°F) which had an average tensile modulus of 454 ksi. This compares with the tensile modulus range of 377 to 406 ksi measured for non-thermally cycled RS-14 resin. The average percent elongation at failure for panel RX-4 was also slightly lower and averaged 3.4% as opposed to 4% or higher for the non-thermally cycled panels. The increase in modulus with thermal cycling was not as apparent for the RS-14A resin panels.

The most significant finding was that the RS-14 panel cycled four times to the 380°F precure temperature in air prior to postcure (RX-3) had an average tensile strength of only 7,450 psi. This is only 60% of the tensile strength of the non-thermally cycled RS-14 and RS-14A panels. This reduction is attributed to degradation of the resin surface layer when exposed to air and humidity at the 380°F precure temperature. The damage is apparently irreversible and still evident after the sample is postcured in a nitrogen environment. It is believed that the degraded surface resin layer acts as a series of flaws to promote premature failure in the tensile specimen during testing. The RX-3 panel also had a slightly elevated average tensile modulus (437 ksi), suggesting the degraded surface resin has a significantly higher tensile modulus than the bulk resin.

Table 2.3.2.2-1. Effect of thermal cycling on RS-14 resin tensile properties.

Panel ID	Cure/Thermal History	No. of Specimens	Strength (psi)	Elongation (%)	Modulus** (ksi)
RX-22*	380°F; N2 // 480°F; N2	9	11,878 (4.4)	4.1 (8.3)	396 (2.9)
RX-21	4x380°F; N2 // 480°F; N2	10	12,072 (5.9)	4.1 (12.6)	413 (2.5)
RX-2*	380°F; N2 // 510°F; N2	13	12,255 (12.9)	5.1 (26.1)	406 (3.2)
RX-1*	4x380°F; N2 // 510°F; N2	3	11,914	4.1	418 (1.8)
RX-5*	380°F; Air // 510°F; N2	5	11,125 (6.8)	3.5 (10.7)	425 (0.9)
RX-3	4x380°F; Air // 510°F; N2	10	7,450 (9.0)	1.9 (11.4)	437 (4.3)
RX-4*	380°F; N2 // 4x510°F; N2	7	12,116 (8.3)	3.4 (12.4)	454 (1.8)
RX-24	280°F; N2 // 480°F; N2	10	12,264 (3.0)	4.8 (7.2)	377 (2.1)
RX-25	280°F; N2 // 4x480°F; N2	10	12,482 (7.1)	3.9 (13.4)	416 (2.2)

* Strength and elongation data exclude specimens with visible red spots at fracture surfaces
** Average of 9 or more specimens
( ) Number in parentheses is percent coefficient of variation

Table 2.3.2.2-2. Effect of thermal cycling on RS-14A resin tensile properties.

Panel ID	Cure/Thermal History	No. of Specimens	Strength (psi)	Elongation (%)	Modulus (ksi)
RX-29	380°F; N2 // 480°F; N2	9	12,122 (5.3)	4.6 (10.9)	377 (1.8)
RX-28	4x380°F; N2 // 480°F; N2	10	12,353 (5.2)	4.7 (12.2)	372 (3.4)
RX-33	280°F; N2 // 480°F; N2	10	12,820 (4.5)	5.5 (12.0)	372 (1.3)
RX-31	280°F; Air // 480°F; N2	10	13,001 (5.5)	5.2 (14.2)	382 (2.4)
RX-30	4x280°F; Air // 480°F; N2	10	12,271 (5.9)	4.4 (12.4)	391 (3.3)
RX-32	280°F; N2 // 4x480°F; N2	10	13,271 (3.4)	4.9 (9.0)	391 (2.4)

( ) Number in parentheses is percent coefficient of variation

The tensile strength, modulus and percent elongation of the RS-14A resin panel that was cycled four times to the 280°F precure temperature in air prior to postcure (RX-30) were not substantially different from those of the other panels. Surface resin degradation as a function of the cyanate ester resin reacting with air and humidity either does not occur at this low a temperature or occurs at too slow a rate to be significant for these exposure times.

2.3.2.3 Density

Tables 2.2.2.3-1 and 2.2.2.3-2 are, respectively, a compilation of all of the RS-14 and RS-14A neat resin densities. Density data are included for the resin panels cycled four times to 510°F in nitrogen (RX-4); four times to 480°F in nitrogen (RX-25 and RX-32); cycled four times to the 380°F precure temperature in air prior to postcure (RX-3); cycled four times to the 380°F precure temperature in nitrogen prior to postcure (RX-1, RX-21 and RX-28); and cycled four times to the 280°F precure temperature in air prior to postcure (RX-30).

The data show that thermal cycling for all of the above did not change the RS-14 and RS-14A resin density from its nominal value of 1.20 g/cm^3. It should be cautioned, however, that the ASTM D792 displacement method may not be a sufficiently sensitive test for measuring subtle density shifts associated with chemical/physical changes in the RS-14 and RS-14A resin.

2.3.2.4 DMA

Tables 2.2.2.4-1 and 2.2.2.4-2 are, respectively, a compilation of all of the RS-14 and RS-14A resin DMA results. DMA data are included for the resin panels cycled four times to 510°F in nitrogen (RX-4); four times to 480°F in nitrogen (RX-25 and RX-32); cycled four times to the 380°F precure temperature in air prior to postcure (RX-3); cycled four times to the 380°F precure temperature in nitrogen prior to postcure (RX-1, RX-21 and RX-28); and cycled four times to the 280°F precure temperature in air prior to postcure (RX-30).

Examination of the data shows that the additional time at the postcure temperature for the RS-14 and RS-14A resin panels cycled four times to 480° or 510°F in nitrogen did not raise the T_g of the resin. Indeed, the T_g for the RS-14 panels is at the lower end of the range of T_g values measured for this material. The shear modulus also increased slightly for panels that received

multiple postcure cycles. The largest increase was for panel RX-4 which was cycled four times to 510°F. Its shear modulus was 177 ksi versus the 150 to 165 ksi range that is typical for this material.

The most significant finding is that the T_g of the RS-14 panel cycled four times to the 380°F precure temperature in air prior to postcure (RX-3) has a T_g that is roughly 20°F lower than the range of T_g values measured for non-thermally cycled RS-14 resin. This reduction is attributed to degradation of the resin surface layer when contacted with air and humidity at the 380°F precure temperature. The degradation was irreversible and still apparent after the sample was postcured. A slightly higher shear modulus (170 ksi) was also measure for the RX-3 panel.

With the exception of the T_g calculated using the line-fit intersection method, the T_g of the RS-14A panel cycled four times to the 280°F precure temperature in air prior to postcure (RX-30) is comparable to the typical range of T_g values measured for this resin. This indicates that reaction of the surface resin with air and humidity is less of a factor at the lower precure temperature. A slightly higher shear modulus (159 ksi) was also measured for the RX-30 panel. This compares with the range of 150 to 152 ksi measured for the RS-14A panels that were not thermally cycled. This slightly higher value may not be significant, however, because 159 ksi is not substantially different from the shear moduli measured for the RS-14 resin.

Multiple precure cycles at 380°F in nitrogen prior to postcure did not substantially affect the T_g of the resin after postcure. The values of the RS-14 panels (RX-1 and RX-21) are slightly lower by ~5°F than the lower end of the range of T_g values measured for this material. The T_g values for the RS-14A resin panel (RX-28), however, was unaffected by the multiple precure cycles. The shear modulus values for all of these panels was similarly unchanged.

2.4 Moisture Preconditioning Trials

The objective of this work was to characterize the impact of moisture, or ambient humidity, on RS-14/RS-14A cured and uncured properties. These data make it possible to establish "thresholds" or limits at which RS-14/RS-14A resin properties are compromised by moisture exposure. This in turn, makes it possible to design an optimum process for handling and curing these resins and their composites. Emphasis was placed on characterizing the resin's moisture resistance at 175°F because this is a key process temperature for wet-winding with RS-14 and

RS-14A resin.

The moisture preconditioning trials were conducted in a Tenney Benchmaster Environmental Chamber. Two series of experiments were conducted with this equipment. The first set of experiments involved measuring the weight change of the resin with time in order to determine how long and at what moisture level the sample would reach a saturation (equilibrium) state. In the second (and larger) series of experiments, quantities of RS-14 and RS-14A resin were preconditioned and subsequently tested to characterize the effects of moisture exposure on the resin properties.

2.4.1 Equilibrium Weight Gain Measurement

In this series of experiments, ~10 to 11 g of resin was poured in a thin layer across the bottom of a 3.5 in. diameter glass petri dish. To prevent inadvertent moisture exposure due to condensation, all of the containers of RS-14 (or RS-14A) resin used in this study were allowed to warm to room temperature within a sealed plastic bag containing desiccant prior to being opened. After measuring the initial weights, the glass petri dishes were then placed inside the environmental chamber for exposure.

The intent of the thin resin layer in the petri dish was to maximize the surface area of the resin exposed to the humidity. These samples were not stirred because doing so may have introduced error in the weight measurement due to transfer of resin to the stirrer blade, resin slinging outside of the dish, etc. An empty glass petri dish was also placed near the resin samples during exposure to serve as a control and to determine if humidity condensing on the sides of the glass was a potential source of error in the weight measurement.

One set of three RS-14 resin samples (plus control) was exposed to 80% relative humidity at 120°F. The sample weights were measured at 24 hr intervals up to 96 hr total exposure and then again after 168, 192, and 216 hr (9 days) total exposure. By this time, relative weight change with time had decreased and the test was terminated. A second set of RS-14 resin samples was exposed to 80% relative humidity at 175°F and the sample weights were measured at 24 hr intervals up to 96 hr total exposure. Testing was terminated after 96 hr total exposure because the resin samples had solidified.

The weight gain with time data from the 120° and 175°F resin exposures at 80% relative humidity are summarized respectively in Tables 2.4.1-1 and 2.4.1-2. Figure 2.4.1-1 is a plot of average weight gain with time for both sets of data. There is good agreement between the measurements of the three individual samples comprising each set. The empty glass petri dish showed no appreciable weight change with time. Therefore, it can be concluded that the weight gains are due entirely to moisture absorption by the RS-14 resin. The average moisture gain for the samples tested at 175°F was 4.3 wt % before the resin solidified. The moisture absorption for the samples tested at 120°F was less and reached an average of 1.1% before the test was terminated. As shown in Figure 2.4.1-1, the most rapid moisture absorption at 120°F (~ 0.5%) occurred in the first 24 hr of exposure. Thereafter, moisture absorption was approximately linear with time.

In addition to measuring weight change with time, resin samples from this experiment were submitted at the conclusion of testing for DSC and FTIR analysis. The results of these analyses are presented in Sections 2.4.3.1.2 and 2.4.3.1.3, respectively.

2.4.2 Resin Preconditioning Procedure

The cans of RS-14 and RS-14A resin were removed from the refrigerator and allowed to warm to room temperature within a sealed plastic bag containing desiccant. Nominal 450 g (or 378 cc) samples were then poured in a 150 × 75 glass crystallizing dish.

The dish was placed inside the environmental chamber and a stirring attachment was positioned so that the blades were beneath the surface of the resin in the center of the dish. The stirring attachment was driven by a flexible coupling to a motor outside of the environmental chamber. After sample placement, the chamber door was closed and the humidity and temperature were adjusted to the exposure set points. The stirrer motor was turned on after the chamber reached the set point temperature and humidity level specified for the experiment. The sample was then stirred continuously for the test duration to maximize the resin surface area exposed to the humidity.

After the specified test time had elapsed, the stirrer motor was turned off and the crystallizing dish was removed from the chamber. The resin was transferred into labeled glass jars with Teflon-lined lids. Thereafter it was stored in a refrigerator until further testing could take place.

Table 2.4.1-1. RS-14 resin weight gain (80% RH @ 120°F).

	Pre-Exposed Sample Weight (gms)			
	1	2	3	4*
Gross Weight (gm)	41.2364	42.6671	44.2403	34.5835
Dish Weight (gm)	30.8906	32.5420	33.8875	34.5835
Resin Weight (gm)	10.3458	10.1251	10.3528	34.5835
Time	Post-Exposure Gross Weight (gms)			
	1	2	3	4*
~24 hours	41.2870	42.7160	44.2892	34.5829
~48 hours	41.2969	42.7272	44.2997	34.5829
~72 hours	41.3046	42.7346	44.3085	34.5824
~96 hours	41.3104	42.7407	44.3141	34.5824
~168 hours	41.3299	42.7608	44.3343	34.5830
~192 hours	41.3383	42.7693	44.3433	34.5828
~216 hours	41.3455	42.7763	44.3509	34.5827
Time	Weight Change (gms)			
	1	2	3	4*
~24 hours	0.0506	0.0489	0.0489	-0.0006
~48 hours	0.0605	0.0601	0.0594	-0.0006
~72 hours	0.0682	0.0675	0.0682	-0.0011
~96 hours	0.0740	0.0736	0.0738	-0.0011
~168 hours	0.0935	0.0937	0.0940	-0.0005
~192 hours	0.1019	0.1022	0.1030	-0.0007
~216 hours	0.1091	0.1092	0.1106	-0.0008
Time	% Weight Change			
	1	2	3	4*
~24 hours	0.49	0.48	0.47	0.00
~48 hours	0.58	0.59	0.57	0.00
~72 hours	0.66	0.67	0.66	0.00
~96 hours	0.72	0.73	0.71	0.00
~168 hours	0.90	0.93	0.91	0.00
~192 hours	0.98	1.01	0.99	0.00
~216 hours	1.05	1.08	1.07	0.00

*Empty glass petri dish used as a control

Table 2.4.1-2. RS-14 resin weight gain (80% RH @ 175°F).

	Pre-Exposed Sample Weight (gms)			
	1	2	3	4*
Gross Weight (gm	45.3825	46.4587	38.0061	34.5832
Dish Weight (gm)	35.1982	36.3307	27.8704	34.5832
Resin Weight (gm)	10.1843	10.1280	10.1357	34.5832
Time	Post-Exposure Gross Weight (gms)			
	1	2	3	4*
~24 hours	45.5860	46.6603	38.2043	34.5780
~48 hours	45.7211	46.7873	38.3358	34.5789
~72 hours	45.8275	46.8951	38.4371	34.5800
Time	Weight Change (gms)			
	1	2	3	4*
~24 hours	0.2035	0.2016	0.1982	-0.0052
~48 hours	0.3386	0.3286	0.3297	-0.0043
~72 hours	0.4450	0.4364	0.4310	-0.0032
Time	% Weight Change			
	1	2	3	4*
~24 hours	2.00	1.99	1.96	-0.02
~48 hours	3.32	3.24	3.25	-0.01
~72 hours	4.37	4.31	4.25	-0.01

*Empty glass petri dish used as a control

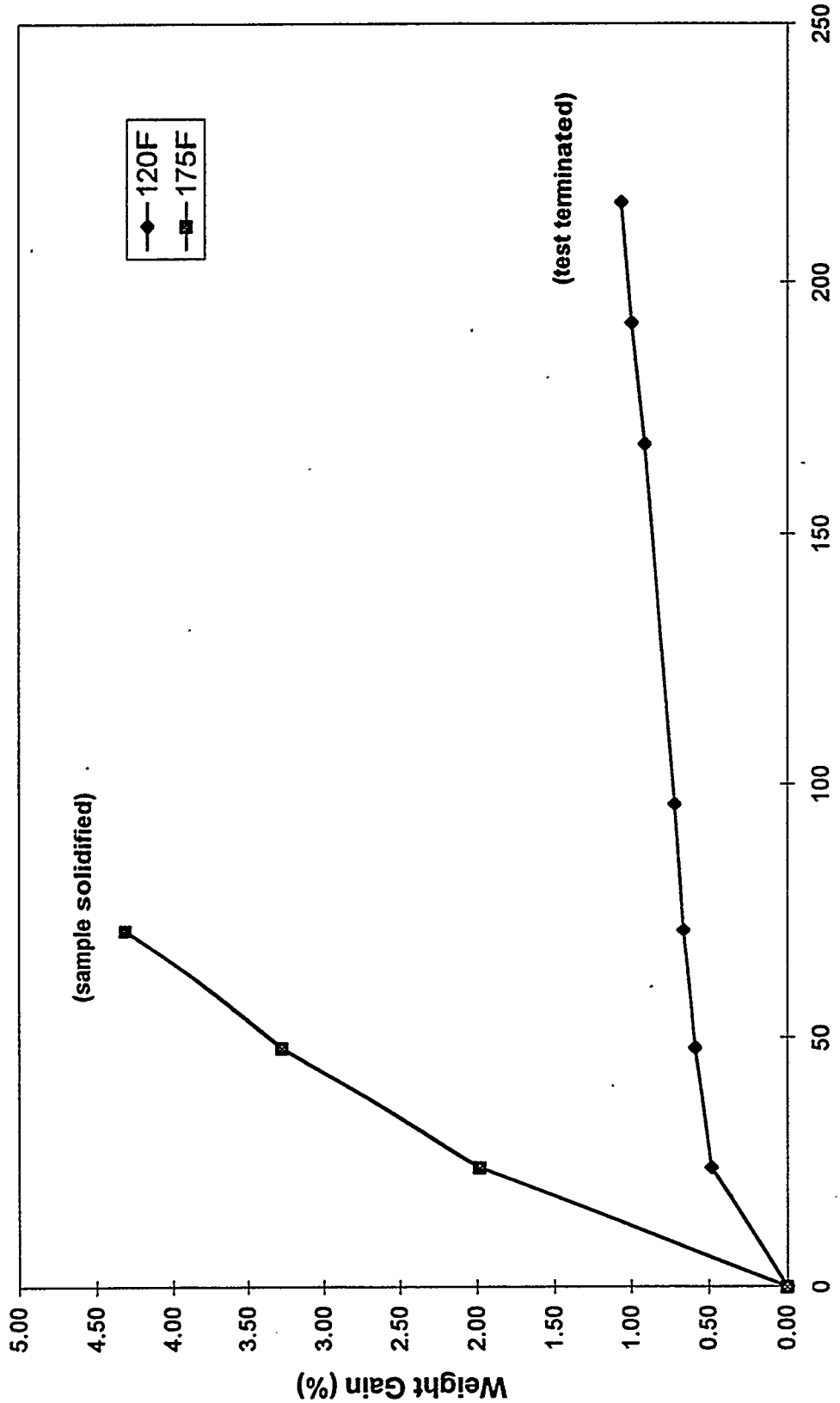

Figure 2.4.1-1. RS-14 neat resin weight gain (80% relative humidity).

Table 2.4.2-1 is a summary of the preconditioning matrix for the RS-14 and RS-14A resin samples. The evaluation and test results are presented in the following section.

Table 2.4.2-1. Resin preconditioning matrix (175°F).

Relative Humidity (%)	Time (hrs)	Resin System	
		RS-14	RS-14A
20	8	x	
30	8		x
40	2	x	
	4	x	x
	8	x	x
50	4		x
	8		x
60	2	x	
	4	x	x
	8	x	
70	4		x
80	2	x	
	4	x	
	8	x	

2.4.3 Preconditioned Resin Evaluation

The visual appearance of all of the preconditioned RS-14 and RS-14A resin was unchanged with the exception of the RS-14 resin sample which was preconditioned for 8 hr at 80% relative humidity. This sample had a higher viscosity and a "curdled" appearance, as if polymerization had initiated.

Each of the preconditioned resin samples was characterized for both uncured and cured resin properties. A portion of each sample was evaluated by Karl-Fischer, DSC, and Fourier transform infrared (FTIR) analyses. The remainder of the resin was cast into panels and cured. The cured panels were then further tested for tensile properties and by DMA. Comparison of the results was made with the test data from as-received (non-preconditioned) RS-14 and RS-14A resin that was generated from other parts of this subtask.

2.4.3.1 Uncured Resin Properties

The results of the Karl-Fischer, DSC and FTIR analyses performed on the preconditioned RS-14 and RS-14A resin are summarized, respectively, in Tables 2.4.3.1-1 and 2.4.3.1-2. Discussions of the results are provided in the following sections.

2.4.3.1.1 Karl-Fischer

The Karl-Fischer technique is a method for determining moisture content by titration and can be used to accurately measure moisture levels in the uncured resin. The Karl-Fischer data in Tables 2.4.3.1-1 and 2.4.3.1-2 show that the water content of the as-received RS-14 and RS-14A is very low and on the order of 0.01 to 0.02%. The RS-14 and RS-14A resin preconditioned for 8 hr at 175°F and at 20 and 30% relative humidity, respectively, are similarly low.

At 40% relative humidity, the water content increases significantly to above 0.1% for both the RS-14 and RS-14A resins. The increase is seen in samples with as little as 2 hr exposure. Preconditioning above 60% relative humidity yielded water contents between 0.3 to 0.45% for both resins. The highest water contents were for the RS-14 samples preconditioned at 80% relative humidity (>0.5%). The RS-14 resin sample that was preconditioned for 8 hr at 175°F and 80% relative humidity had a measured water content of 1.4%. This is also the sample that had a "curdled," thickened appearance after preconditioning.

The one anomaly was the sample of RS-14 resin that was preconditioned for 8 hr at 175°F and 40% relative humidity. It had measured water contents of only 0.03 and 0.02%. The Karl-Fischer analysis was repeated at a later date on a second sample from this resin batch and both results showed good agreement. It is not known why this sample absorbed less moisture during preconditioning. RS-14 resin samples preconditioned for 2 and 4 hr at the 40% relative humidity had significantly higher water contents, as did the RS-14A samples preconditioned for 4 and 8 hr under the same conditions.

Table 2.4.3.1-1. RS-14 resin moisture/temperature exposure trials.

Sample ID	Exposure			DSC				Karl Fischer Water (%)
	R. H. (%)	Temp. (°F)	Time (hours)	Onset (°F)	Tp (°F)	Delta H (J/gm)	Tg (°F)	
Control *	NA	NA	NA	316	369	-624	493	0.02/0.02
20808	20	175	8	315	369	-577	486	0.03
40802	40	175	2	315	367	-573	466	0.16
40804	40	175	4	316	368	-569	469	0.21/0.15
40808	40	175	8	315	367	-599	476	0.03/0.02
60802	60	175	2	312	366	-594	449	0.37
60804	60	175	4	309	364	-603	436	0.38/0.26
60808	60	175	8	304/305	358/358	-581/-573	395/398	0.45
80802	80	175	2	309	363	-599	433	0.50
80804	80	175	4	305	362	-601	413	0.52
80808	80	175	8	302	356	-611	372	1.42
8050216	80	120	216	299	361	-620	387	NA
808072**	80	175	72	265	331	-401	206	NA

DSC run: 2°C/min ramp to 265°C (510°F) and hold for 4 hours. Return to room temperature.
Rescan at 5°C/min for Tg.
* As-received
** Sample solidified

Table 2.4.3.1-2. RS-14A resin moisture/temperature exposure trials.

Sample ID	Exposure			DSC				Karl Fischer Water (%)
	R. H. (%)	Temp. (°F)	Time (hours)	Onset (°F)	Tp (°F)	Delta H (J/gm)	Tg (°F)	
Control *	NA	NA	NA	316/324	373/373	-570/-598	518/518	0.01
30808A	30	175	8	332/336	376/377	-571/-580	507	0.01
40804A	40	175	4	342/333	376/375	-583/-593	501	0.14
40808A	40	175	8	313/334	368/375	-581/-536	465	0.15
50804A	50	175	4	336/335	375/375	-534/-591	467	0.21/.28
50808A	50	175	8	329/320	373/372	-564/-543	455	0.16/.31
60804A	60	175	4	331/331	374/374	-590/-574	467	0.28
70804A	70	175	4	324/323	375/373	-580/-605	469	0.31

DSC run: 2°C/min ramp to 265°C (510°F) and hold for 4 hours. Return to room temperature.
Rescan at 5°C/min for Tg.
* As-received

2.4.3.1.2 DSC Analysis

DSC analyses were performed on the preconditioned resin and equilibrium weight gain samples using equipment and procedures described in Section 2.2.1. A nominal 10 mg weight of resin was sealed in an aluminum sample pan and placed in the DSC sample cell. The samples were ramped at 2°C/min from 25° to 265°C and held at that temperature for 4 hr to cure the resin. The onset temperature, peak temperature and delta H were determined from the enthalpy profile. The samples were cooled back to 25°C after cure and then ramped at 5°C/min from 25° to 300°C to obtain the T_g.

The DSC data in Tables 2.4.3.1-1 and 2.4.3.1-2 show a dramatic impact from moisture preconditioning on the RS-14 and RS-14A resin's ultimate T_g after cure. A slight reduction (~7°–11°F) is evident even with the 8 hr exposures at 175°F and 20 and 30% relative humidity (sample nos. 20808 and 30808A, respectively). The largest reduction in T_g occurs for exposures >40% relative humidity. As expected, the longer the exposure time at a given humidity level, the greater the reduction in T_g. After 4 hr of exposure at 175°F and 40% relative humidity (Sample No. 40808A), the RS-14A showed a nominal T_g reduction of 17°F; after 8 hr at 40% relative humidity (Sample No. 40808A), the reduction was over 50°F.

The DSC data in Tables 2.4.3.1-1 and 2.4.3.1-2 show no significant or consistent differences in the onset temperature, peak temperature and delta H values for the RS-14 and RS-14A samples preconditioned up to 80% relative humidity. This is true even for the RS-14 sample that was preconditioned for 8 hr at 80% relative humidity and 175°F (Sample No. 80808). Even though this sample had a curdled appearance, a higher viscosity and its ultimate T_g was reduced to 372°F, the DSC data show only a marginal (~5°F) reduction in the onset and peak temperatures and no change in the delta H value.

The enthalpy profile of the RS-14 equilibrium weight gain sample that was exposed for 216 hr (9 days) at 120°F and 80% humidity (Sample No. 8050216) also shows no effect from prolonged moisture exposure at this temperature. Weight gain data indicate that the resin absorbed

nominally 1.1 wt % moisture before the weight gain with time experiment was terminated. Its ultimate T_g was only 387°F. However, the delta H value, onset and peak temperatures of this sample are comparable to those of the control and other preconditioned specimens.

The enthalpy profile of the RS-14 equilibrium weight gain sample that was exposed for 72 hr at 175°F and 80% humidity (Sample No. 808072) is significantly different from the other samples. This resin solidified or gelled prior to termination of the weight gain with time experiment. Weight gain data showed that it absorbed nominally 4.3 wt % moisture during exposure and its T_g was only 206°F. The DSC data show that the measured delta H is only -401 J/gm as opposed to the nominal -570 to -620 J/g range measured for as-received RS-14 resin. Estimates are that the conversion (or cyanate consumption) resulting from the weight gain with time experiment was 30 to 35%. Residual moisture in the resin is believed to have catalyzed a polymerization reaction at a lower temperature. The onset and peak temperatures for this specimen are reduced by ~50° and 38°F, respectively.

The DSC enthalpy profile results for preconditioned RS-14 and RS-14A resin are comparable. The RS-14A has slightly higher (10° to 15°F) onset and peak temperatures than the RS-14. The RS-14A resin T_g is similarly reduced by moisture exposures with time and temperature. This indicates that removal of the zirconate coupling agent did not improve the cyanate ester resin's resistence to ambient humidity.

2.4.3.1.3 FTIR

The following paragraphs on cyanate ester chemistry and the cyclotrimerization process are provided as background information to better explain the FTIR results. The reaction of cyanate ester resins with moisture to produce a species called carbamates is also described.

Cyanate ester resins are bisphenol derivatives containing the ring-forming cyanate (-O-C≡N) functional group. The formation of polycyanurates through polycyclotrimerization of cyanate ester resins is described by Shimp. "Chemically, cyanate ester resins and their prepolymers (Figure 2.4.3.1.3-1) are esters of bisphenols and cyanic acid which cyclotrimerize to substituted triazine rings upon heating (Figure 2.4.3.1.3-2). Conversion, or curing, to thermoset plastics forms three-dimensional networks of oxygen-linked triazine rings and bisphenol units, correctly termed polycyanurates."[5]

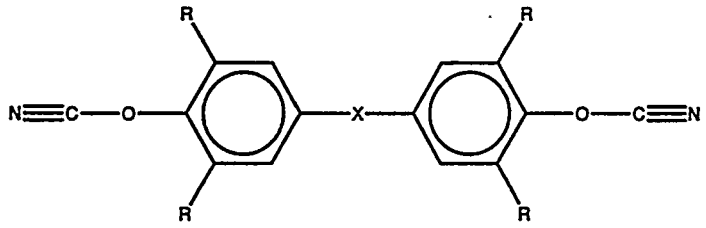

X - Bisphenol Linkage

R - Ring Substituent

Figure 2.4.3.1.3-1. Chemical structure model for dicyanate monomers.[5]

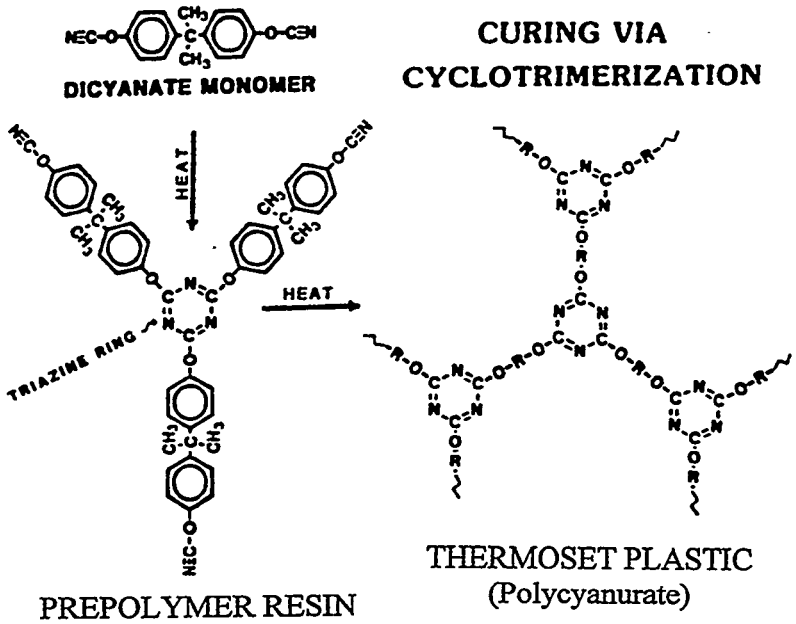

Figure 2.4.3.1.3-2. Homopolymerization of dicyanates.[5]

The cyclotrimerization process is further described by Bauer. "The formation of polycyanurates through polycyclotrimerization of cyanate esters is a typical step-growth network building process. Starting from low molecular weight monomers with at least two cyanate groups, the reacting system passes through a pregel state with a broad distribution of oligomers to reach the gelpoint at a certain value of the functional group's conversion. When nearly all of the functional groups have reacted, the system consists of "one giant macromolecule."[3]

Two key features of the reaction summarized by Bauer are that (1) a catalytically active species is formed during the process that gives the reaction an autocatalytic character, and (2) the reaction rate is very sensitive to small impurities of the monomer or the added catalyst. Without the intervention of a catalyst, the key product during cyclotrimerization of cyanates is an intermediate iminocarbonate that is formed by a reaction of a cyanate ester with a phenolic hydroxyl group. This phenol is usually left as an impurity from the cyanate synthesis.[6] In fact, no reaction takes place if completely purified cyanate esters are heated[7] and a small amount of impurities (e.g., H_2O/ArOH, metal ions) are needed to start the reaction.[3]

The formation of the iminocarbonate is shown in Figure 2.4.3.1.3-3, Scheme A. Bauer proposed the second step to be "a reaction of the iminocarbonate with two OCN groups to form a triazine ring. The abstracted phenolic group is then able to enter into Scheme A again (Scheme B)."[3] Scheme C is still another model of the second reaction step proposed by Alla.[8] Cyclotrimerization in the presence of a catalyst is also determined by the formation of an intermediate reactive species.

Reaction of the cyanate function with water (hydrolysis) leads to the production of a carbamate (Figure 2.4.3.1.3-4, Scheme A).[9,10] "Above 190°C (374°F), the carbamate function decomposes, giving rise to an amine and evolving CO_2. Finally, the resulting amine can react with another cyanate group leading to a linear junction (Scheme B)."[10]

The significance of carbamate formation to cyanate ester resin and composite properties are two-fold. The evolution of CO_2 gas at elevated temperatures can lead to bubbles and voids in resin and composite samples. Excessive bubbles can even lead to delamination in composite specimens. The second consequence is that the amine resulting from carbamate decomposition can interrupt

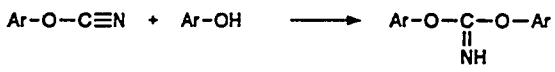

Scheme A

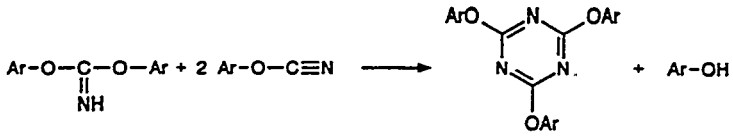

Scheme B

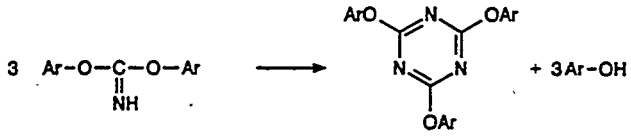

Scheme C

Figure 2.4.3.1.3-3. Intermediate steps in cyclotrimerization reaction.[3,8]

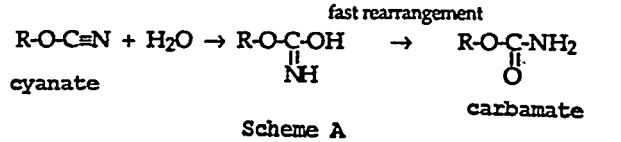

Scheme A

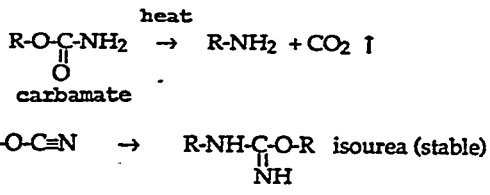

Scheme B

Figure 2.4.3.1.3-4. Mechanisms of carbamate formation and decomposition.[9,10]

the triazine ring formation process by reacting with available cyanate groups. The resulting linear species may have less desirable properties than the triazine ring structure, impacting the material's ultimate performance.

The FTIR analyses were performed by YLA Incorporated using a Perkin Elmer Spectrum 1000 FTIR spectrophotometer with a Zinc Selenide sample trough. For all analyses, the sample compartment was purged with nitrogen and a minimum of 16 scans were used to collect sample and/or background data between 650 to 4000 cm^{-1}.

The scans of the RS-14 and RS-14A samples are compiled in Appendix A.1 and are the results of the sample scans after subtraction of the background baseline. Reference scans of the RS-14 resin and its two major constituents (XU71787.07L from the Dow Chemical Company and AroCy L-10 from Ciba Geigy have been provided by YLA and are included in Appendix A.2 for comparison.

Selected peak heights from the scans were normalized with respect to the CH stretch band at 2945 cm^{-1}. The results for the RS-14 and RS-14A resin samples are tabulated, respectively, in Tables 2.4.3.1.3-1 and 2.4.3.1.3-2. Figures 2.4.3.1.3-5 and 2.4.3.1.3-6 are bar chart presentations of the data. The peak height ratios selected for examination, and their significance, are summarized below.

1750 cm^{-1} – Carbonyl Group

Low quantities of carbonyl functionality are present in un-conditioned RS-14 and RS-14A resin. The source is believed to be the elastomeric toughening agent from the Dow XU71787.07L resin constituent and/or residual solvents from the cyanate ester manufacturing process. However, an elevated carbonyl level can also be indicative of carbamate formation.

The RS-14 results show that the 1750 cm^{-1} peak height ratio of the as-received control sample (No. RS-14C) is 0.396. The 1750 cm^{-1} peak height ratio increases with increasing time and humidity exposures, suggesting that carbamate formation has occurred in the resin samples. The data show carbamate formation for the RS-14 resin exposed to as little as 20% relative humidity for

Table 2.4.3.1.3-1. RS-14 – FTIR peak heights normalized to CH stretch band.*

Sample	1336	1373	1750	2263	3374	1578
RS-14C	0.382	0.584	0.396	1.495	0.2475	0.4059
20808	0.4215	0.6765	0.4411	1.5	0.2647	0.4313
40802	0.3737	0.4444	0.4444	1.5556	0.2424	0.3636
40804	0.40196	0.4706	0.5	1.549	0.2647	0.3725
40808	0.4327	0.673	0.4423	1.49	0.2788	0.4423
60802	0.404	0.4545	0.505	1.5758	0.2727	0.3737
60804	0.4412	0.4902	0.5588	1.505	0.3039	0.3823
60608	0.666	0.7333	0.8095	1.447	0.419	0.4952
80802	0.4135	0.4615	0.5192	1.5385	0.2788	0.375
80804	0.4646	0.505	0.606	1.5454	0.3131	0.3838
80808	0.7087	0.7475	0.8543	1.427	0.466	0.5048
808072	2	1.87	1.636	0.9636	0.7272	0.8727
8050216	0.6907	0.6391	0.8865	1.4948	0.4639	0.4639

Wavelength	Group
1336	Iminocarbonate
1373	Cyanurate ether
1578	Triazine
1750	Carbonyl (Carbamate)
2263	Cyanate
3374	NH or OH Stretch

*Provided by YLA, Incorporated.

Example of sample numbering scheme: Sample 20808 made of RS-14 was exposed to 20% relative humidity at ~80° C (175° F) for 8 hr.

Table 2.4.3.1.3-2. RS-14A – FTIR peak heights normalized to CH stretch band.*

Sample	1336	1373	1750	2263	3374	1578
RS-14A	0.2333	0.3444	0.2	1.655	0.1222	0.3222
30808A	0.382	0.55056	0.4606	1.6067	0.2247	0.382
40804A	0.3636	0.4659	0.4431	1.7045	0.2159	0.3522
40808A	0.4888	0.5666	0.6222	1.611	0.2888	0.3333
50804A	0.4444	0.4777	0.6	1.5777	0.2666	0.3666
50808A	0.5494	0.6	0.6703	1.5934	0.3296	0.4066
60804A	0.5168	0.5056	0.6854	1.6067	0.3033	0.382
70804A	0.5165	0.4835	0.7033	1.6153	0.31568	0.3846

Wavelength	Group
1336	Iminocarbonate
1373	Cyanurate ether
1578	Triazine
1750	Carbonyl (Carbamate)
2263	Cyanate
3374	NH or OH Stretch

*Provided by YLA, Incorporated.

Example of sample numbering scheme: Sample 50804A made of RS-14A was exposed to 50% relative humidity at ~80° C (175° F) for 4 hr.

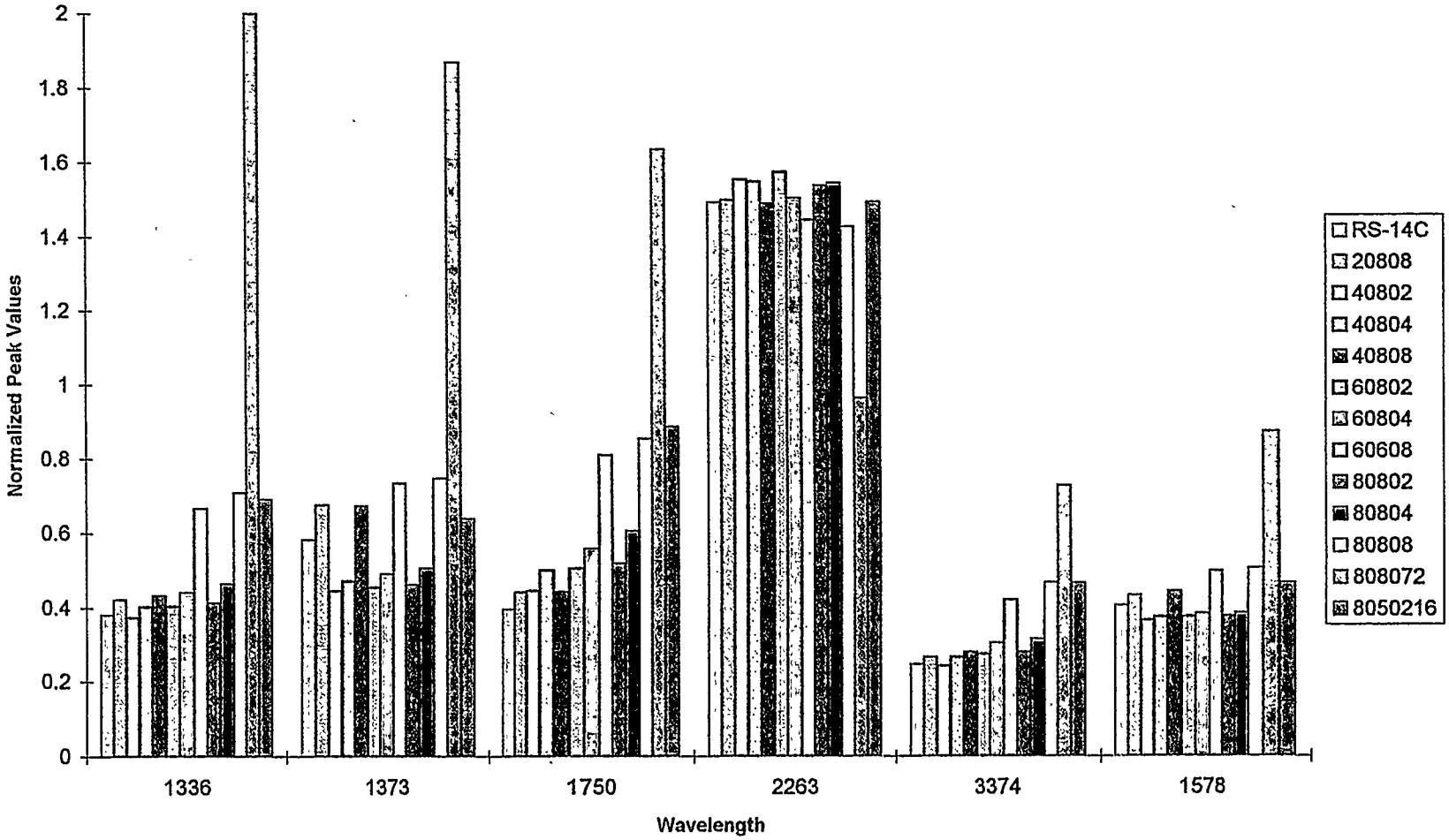

Sample	1336	1373	1750	2263	3374	1578
RS-14C	0.382	0.584	0.396	1.495	0.2475	0.4059
20808	0.4215	0.6785	0.4411	1.5	0.2647	0.4313
40802	0.3737	0.4444	0.4444	1.5556	0.2424	0.3636
40804	0.40196	0.4706	0.5	1.549	0.2647	0.3725
40808	0.4327	0.673	0.4423	1.49	0.2788	0.4423
60802	0.404	0.4545	0.505	1.5758	0.2727	0.3737
60804	0.4412	0.4902	0.5588	1.505	0.3039	0.3823
60608	0.666	0.7333	0.8095	1.447	0.419	0.4952
80802	0.4135	0.4615	0.5192	1.5385	0.2788	0.375
80804	0.4646	0.505	0.606	1.5454	0.3131	0.3838
80808	0.7087	0.7475	0.8543	1.427	0.466	0.5048
808072	2	1.87	1.636	0.9636	0.7272	0.8727
8050216	0.6907	0.6391	0.8865	1.4948	0.4639	0.4639

Provided by YLA, Incorporated.

Example of sample numbering scheme: Sample 20808 made of RS-14 was exposed to 20% relative humidity at~80°C (175°F) for 8 h.

Figure 2.4.3.1.3-5. RS-14 - FTIR analysis peak heights normalized to CH stretch band.

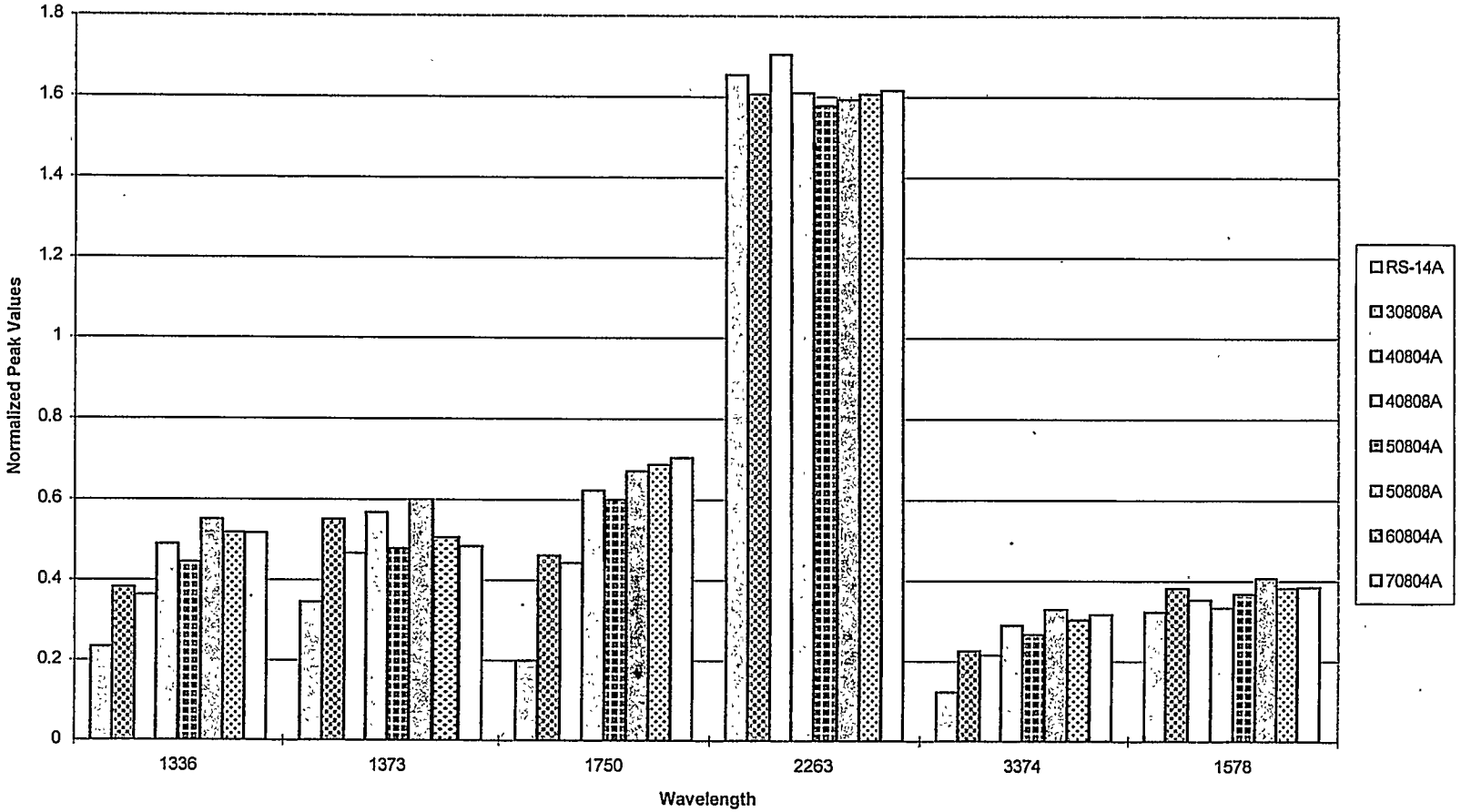

Sample	1336	1373	1750	2263	3374	1578
RS-14A	0.2333	0.3444	0.2	1.655	0.1222	0.3222
30808A	0.382	0.55056	0.4606	1.6067	0.2247	0.382
40804A	0.3636	0.4659	0.4431	1.7045	0.2159	0.3522
40808A	0.4888	0.5666	0.6222	1.611	0.2888	0.3333
50804A	0.4444	0.4777	0.6	1.5777	0.2666	0.3666
50808A	0.5494	0.6	0.6703	1.5934	0.3296	0.4066
60804A	0.5168	0.5056	0.6854	1.6067	0.3033	0.382
70804A	0.5165	0.4835	0.7033	1.6153	0.31568	0.3846

Provided by YLA, Incorporated.

Example of sample numbering scheme: Sample 50804A made of RS-14A was exposed to 50% relative humidity at~80°C (175°F) for 4 h.

Figure 2.4.3.1.3-6. RS-14A - FTIR analysis peak heights normalized to CH stretch band.

8 hr at 175°F (Sample No. 20808/0.441) which is about the same magnitude as the resin exposed to 2 hr at 40% relative humidity (Sample No. 40802/0.444). With the exception of the sample exposed 8 hr at 40% relative humidity (explained earlier as exhibiting anomalous behavior), the 1750 cm^{-1} peak height ratio increases dramatically above 0.5 for exposures above 4 hr at 40% relative humidity or humidity levels >40%. The highest 1750 cm^{-1} peak height ratio measured was 1.636 for the equilibrium weight gain sample (Sample No. 808072) which solidified after 72 hr at 80% relative humidity and 175°F.

The RS-14A results differ from those of the RS-14 resin in that the 1750 cm^{-1} peak height ratio of the RS-14A control sample is only 0.2. It is not known whether the higher 1750 cm^{-1} peak height ratio (0.396) of the RS-14 resin control is due to normal batch-to-batch variability or due to moisture contamination of the resin during its manufacture. Data provided by YLA indicate that the 1750 cm^{-1} peak height ratio of as-blended batches of RS-14 and RS-14A resin can range between 0.18 to 0.36. [YLA's data on this particular RS-14A lot (Reference No. FB5K176) prior to shipment actually yielded a peak height range of 0.36.]

The RS-14 resin lot was also 17 months older than the RS-14A resin lot and this may be a contributing factor. If the higher 1750 cm^{-1} peak height ratio does reflect a higher amount of carbamate formation in the as-received RS-14 resin, this could explain why it has an apparently lower T_g than the RS-14A resin lot.

The 1750 cm^{-1} peak height ratio of the RS-14A resin increases significantly in two steps with increasing time and humidity exposures. The RS-14A 1750 cm^{-1} peak height ratio increases sharply over 0.2 for exposures of 8 hr at 175°F and 30% relative humidity (Sample No. 30308A/0.461) and 4 hr at 40% relative humidity (Sample No. 40804A/0.443). At this point, the 1750 cm^{-1} data of the RS-14A resin is slightly higher than that of the as-received RS-14 control sample (0.396) and comparable to RS-14 resin that has been exposed up to 2 hr at 175°F and 40% relative humidity (0.44).

The next significant increase occurs at exposures >8 hr at 175°F and 40% relative humidity (Sample No. 40808A/0.622). Above this level, and for similar time and humidity exposures, the 1750 cm^{-1} peak height ratios of the RS-14A resin are comparable to, or greater, than that of the

RS-14 resin, indicating that removal of the zirconate coupling agent has not improved its resistance to carbamate formation.

1336 cm^{-1} – Iminocarbonate Group

As described earlier, the iminocarbonate group appears as a precursor to triazine ring formation. However, this peak also correlates with the intermediate species that is the precursor to carbamate formation.

The 1336 cm^{-1} peak height ratio of the RS-14 control resin is 0.382. The pattern of 1336 cm^{-1} peak height ratio change with increasing time and humidity exposure is more erratic than that of the 1750 cm^{-1} peak height ratio data. The most significant increase is for the resin exposures to 8 hr at 175°F and 60% (Sample No. 60808/0.666) and 80% (Sample No. 80808/0.709) relative humidity. The highest 1336 cm^{-1} peak height ratio was 2 and was for the Sample No. 808072 equilibrium weight gain sample that solidified after 72 hr at 175°F and 80% relative humidity.

The 1336 cm^{-1} peak height ratio of the RS-14A control resin is 0.233 and (comparable to the 1750 cm^{-1} peak height ratio results) lower than that of the RS-14 control sample. The RS-14A 1336 cm^{-1} peak height ratios increase steadily with increased time and humidity exposure. After 8 hr at 175°F and 30% relative humidity (Sample No. 30808A), the RS-14A peak height ratio (0.382) is comparable to that of the RS-14 control sample. At exposures >8 hr at 40% relative humidity, the RS-14A has equivalent or higher 1336 cm^{-1} peak height ratios than similarly exposed RS-14 resin samples.

3374 cm^{-1} – NH (or OH) Stretch Band

The band at 3374 cm^{-1} is sometimes examined for N-H (amine) functionality which is one of the byproducts of carbamate decomposition. The band can also signify the O-H bond, such as that found in phenols or water. The preconditioned resin samples were maintained at or below ambient temperature so it is not likely that significant carbamate decomposition would have occurred. It is theorized, instead, that this band is primarily the result of residual phenols in the cyanate ester resin and/or moisture absorbed by the resin during preconditioning.

The 3374 cm^{-1} peak height ratio of the RS-14 control is 0.247. The 3374 cm^{-1} peak height ratio changes only slightly at the lower humidity and time exposures. At exposures of 8 hr at 175°F and 60 and 80% relative humidity, it increases to 0.4 and higher.

The 3374 cm^{-1} peak height ratio of the RS-14A control is 0.122 and less than that of the RS-14 control sample. The 3374 cm^{-1} peak height ratio of the RS-14A resin increases steadily with increasing time and humidity exposures in a pattern that is similar to the 1336 cm^{-1} peak height ratio results. The RS-14A 3374 cm^{-1} peak height ratio increases sharply over 0.122 for exposures of 8 hr at 175°F and 30% relative humidity (Sample No. 30308A/0.225) and 4 hr at 40% relative humidity (Sample No. 40804A/0.216). At this point, the 3374 cm^{-1} peak height ratio of the RS-14A resin is slightly less than the as-received RS-14 control sample (0.247). Above these levels, and for similar time and humidity exposures, the peak height ratios of the RS-14A resin are comparable to those of the RS-14 resin samples.

1373 cm^{-1} – Cyanurate Ether

The cyanurate ether group is produced in conjunction with triazine ring formation. Its presence, therefore, is an indicator that resin cure is occurring.

Excluding the control, the 1373 cm^{-1} peak height ratios for the RS-14 samples increase significantly from the 0.44 to 0.50 range to >0.67 for the long-term (8 hr or greater) exposures at 175°F. The change with humidity level is less evident than the increase with time suggesting that the lengthy exposures at elevated temperature are initiating the polymerization. It is not known why the 1373 cm^{-1} peak height ratio for the as-received RS-14 control is 0.58 unless this particular resin sample had partially polymerized during storage.

The 1373 cm^{-1} peak height ratio data for the RS-14A resin samples show a definite pattern of increasing peak height ratio with time of exposure. The 1373 cm^{-1} peak height ratio of the RS-14A control sample is 0.344, which is lower than that of the RS-14 control resin sample. The 1373 cm^{-1} peak height ratios of the RS-14A resin samples with 4 hr exposures at 175°F are all between 0.47 to 0.50; the 8 hr exposures yielded peak height ratios between 0.55 to 0.60. This pattern was independent of humidity exposure, again suggesting that it is the prolonged exposure to 175°F that is promoting resin polymerization.

1578 cm^{-1} – Triazine Group

The triazine group appears as cyclotrimerization proceeds, i.e., as the cyanate ester resin cures. The 1578 cm^{-1} peak height ratio data for the RS-14 resin follows the same pattern as that of the 1373 cm^{-1} peak height ratio data. With the exception of the RS-14 control, the highest peak height ratios are for those samples with prolonged (8 hr) exposures at 175°F suggesting that some triazine ring formation has occurred. Similar to the 1373 cm^{-1} peak height ratio results, the 1578 cm^{-1} peak height ratio of the RS-14 control is slightly elevated. The peak height ratio data for the RS-14A resin follow a similar pattern to that of the RS-14 resin data and are comparable in value at the higher exposure times.

2263 cm^{-1} – Cyanate Group

The cyanate group is consumed as the cyclotrimerization reaction proceeds. A low(er) cyanate group peak indicates that the cyanate ester resin has been partially converted or has lost some of its functionality due to competing (less desirable) reactions.

The 2263 cm^{-1} peak height ratio of the RS-14 control sample is 1.495. The cyanate functionality is comparable to or higher than all of the preconditioned RS-14 resins with the exception of the samples exposed 8 hr at 175°F and 60% (Sample No. 60808/1.447) and 80% (Sample No. 80808/1.427) relative humidity. The lowest 2263 cm^{-1} peak height ratio measured was 0.964 for the equilibrium weight gain (Sample No. 808072) which solidified after 72 hr at 175°F and 80% relative humidity. The low value indicates that the resin lost significant cyanate functionality either from carbamate formation and/or polymerization.

The 2263 cm^{-1} peak height ratio of the RS-14A control sample is 1.655 and is higher than that of the RS-14 control sample. There is no discernable pattern with humidity level or exposure time in the RS-14A 2263 cm^{-1} peak height ratio data. With the exception of the sample exposed to 4 hr at 175°F and 40% relative humidity (Sample No. 40804A/1.705), the 2263 cm^{-1} peak height ratios of all of the preconditioned RS-14A resin samples dropped slightly from that of the control to between 1.578 to 1.615. These values are higher than their RS-14 resin counterparts but otherwise show no other changes with humidity level or exposure time.

2.4.3.2 Cast Panel Properties

The results of the tensile tests and DMA analyses performed on the preconditioned RS-14 and RS-14A resin are summarized, respectively, in Tables 2.4.3.2-1 and 2.4.3.2-2. Details of the resin panel fabrications, as well as the test results are provided in the following sections.

2.4.3.2.1 Panel Fabrication

Resin panels were cast and cured from the preconditioned RS-14 and RS-14A resin per the procedure described in Section 2.2.2.1 (Panel Fabrication). The cure cycle was a 3 hr precure at 280°F followed by a 4 hr postcure at 480°F and was conducted in a nitrogen atmosphere. This cure cycle was selected because the lower precure and postcure temperatures gave marginally higher tensile strength values in the RS-14 and RS-14A resin property-versus-cure cycle study (Section 2.2). The 480°F postcure temperature was also less likely to discolor (darken) the resin than the 510°F postcure temperature.

The first set of resin panels in this study were cast and cured with the RS-14 resin samples that had been preconditioned 8 hr at 175°F and 20, 40, 60, and 80% relative humidity. During the resin evacuation process, it was observed that the RS-14 samples that had been preconditioned for 8 hr at 60 and 80% relative humidity took over 15 min to remove volatiles compared to the nominal 4 min required to debulk the samples preconditioned at 20 and 40% relative humidity. After cure, the panels from the resin preconditioned at 60 and 80% relative humidity were full of large bubbles while the panels cast from the resin preconditioned at 20 and 40% relative humidity were reasonably void free.

The voids are attributed to moisture that permeated the resin and later reacted with the RS-14 to produce carbamates. These carbamates later decomposed into CO_2 gas at the postcure temperature, producing the large bubbles.

Table 2.4.3.2-1. RS-14 resin moisture/temperature exposure trials.

Sample ID	Exposure			DMA				Tensile Properties		
	R. H. (%)	Temp. (°F)	Time (hrs)	Tg (F°) G' Line-Fit	Tg (F°) G" Peak	Tg (F°) T. Delta Peak	G' @ 82°F (ksi)	Strength (psi)	Elongation (%)	Modulus (ksi)
RX-6/Control *	NA	NA	NA	485	487	524	159	13,023	5.8	395
								(3.5)	(12.3)	(2.9)
RX-11/20808	20	175	8	485	490	527	160	12,366	4.8	403
								(7.0)	(15.9)	(4.7)
RX-15/40802	40	175	2	469	480	517	160	13,256	5.9	389
								(6.8)	(20.0)	(2.4)
RX-16/40804	40	175	4	459	471	507	162	12,997	5.3	393
								(5.1)	(16.9)	(2.6)
RX-12/40808	40	175	8	479	487	515	157	13,113	5.5	409
								(3.7)	(12.5)	(2.7)
RX-17/60802	60	175	2	452	462	499	162	12,669	4.8	401
								(8.2)	(19.0)	(3.4)
RX-18/60804**	60	175	4	440	443	489	163	12,175	4.4	405
								(13.1)	(27.5)	(3.9)
RX-13/60808	60	175	8	402	416	444	173	(Panel contained extensive bubbles/voids)		
RX-19/80802	80	175	2	456	462	499	167	12,615	4.9	394
								(9.6)	(25.8)	(2.9)
RX-20/80804	80	175	4	448	452	498	162	12,871	5.0	407
								(9.4)	(25.9)	(2.2)
RX-14/80808	80	175	8	391	397	434	178	(Panel contained extensive bubbles/voids)		

Panels cured 3 hrs @ 280°F and 4 hrs @ 480°F
Number of tensile specimens: 8-10
( ) Number in parentheses is percent coefficient of variation
* As-received
** Some bubbles/voids visible in panel and at fracture surfaces of tensile specimens.

Table 2.4.3.2-2. RS-14A resin moisture/temperature exposure trails.

Sample ID	Exposure			DMA				Tensile Properties		
	R. H. (%)	Temp. (°F)	Time (hrs)	Tg (F°) G' Line-Fit	Tg (F°) G" Peak	Tg (F°) T. Delta Peak	G' @ 82°F (ksi)	Strength (psi)	Elongation (%)	Modulus (ksi)
RX-33/Control*	NA	NA	NA	504	515	542	152	12,820 (4.5)	5.5 (12.0)	372 (1.3)
RX-41/30808A	30	175	8	499	506	533	152	12,842 (6.5)	5.2 (21.7)	387 (1.7)
RX-34/40804A	40	175	4	497	506	533	159	12,536 (6.1)	5.1 (19.7)	385 (2.0)
RX-38/40808A**	40	175	8	477	487	516	159	12,987 (12.1)	5.2 (24.5)	400 (1.7)
RX-36/50804A	50	175	4	484	497	515	153	13,206 (2.4)	5.3 (10.6)	396 (1.4)
RX-37/50808A**	50	175	8	461	469	497	162	12,814 (9.4)	5.1 (28.7)	402 (1.5)
RX-39/60804A***	60	175	4	464	478	497	162	13,523 (3.1)	5.1 (9.4)	413 (2.3)
RX-40/70804A	70	175	4	460	469	497	167	(Excessive cracks and bubbles in panel)		

Panels cured 3 hrs @ 280°F and 4 hrs @ 480°F
Number of tensile specimens: 10
( ) Number in parentheses is percent coefficient of variation
* As-received
** Panel cracked in mold
*** Some bubbles/voids visible in panel

The second set of resin panels were cast and cured from the RS-14 resin samples that had been preconditioned 2 and 4 hr at 175°F and 20, 40, 60, and 80% relative humidity. An experiment was performed to determine if the moisture had chemically reacted with the RS-14 resin during the preconditioning step, or if it was still in its free (unreacted) form. These resin samples were evacuated longer until volatile escape was no longer apparent. The resin samples preconditioned at 40, 60, and 80% relative humidity took, respectively, 15, 20, and 30 min to debulk prior to being cast into panels.

At the same time, samples from the RS-14 resin preconditioned for 8 hr at 175°F and 60% relative humidity and 2 and 4 hr at 80% relative humidity were evacuated to remove all volatiles and submitted for Karl-Fisher analysis. The results are summarized in Table 2.4.3.2.1-1 and show that the free (chemically uncombined) moisture entrapped in the RS-14 resin can be removed by evacuation so that the water content is essentially the same as the as-received resin.

Table 2.4.3.2.1-1. RS-14 resin evacuated versus non-evacuated samples.

Sample ID	Exposure			Karl Fischer (% Water)	
	R. H. (%)	Temp. (°F)	Time (hours)	Non-evacuated	Evacuated
Control *	NA	NA	NA	.02/.02	NA
60808	60	175	8	0.45	0.02
80802	80	175	2	0.50	0.02
80804	80	175	4	0.52	0.02

*** As-received**

All of the panels cast in the second set of preconditioned RS-14 resin were relatively void free with the exception of one panel. This panel had a few visible bubbles in one location and was prepared from the resin preconditioned 4 hr at 60% relative humidity.

The third set of resin panels were cast and cured with the RS-14A resin samples that had been preconditioned 4 and/or 8 hr at 175°F and 30, 40, 50, and 70% relative humidity. In this set of panels, the debulking time was established as the time required to remove air from non-preconditioned resin (5–10 min) and all of the preconditioned resin samples were evacuated accordingly.

It turned out that 5–10 min evacuation time was sufficient to remove most of the apparent volatiles in this set of preconditioned RS-14A resin samples. However, there was sufficient RS-14A resin degradation from the moisture preconditioning that the panel cast from resin exposed 4 hr at 70% relative humidity had excessive bubbles and cracked in the mold. The panel cast from resin preconditioned 4 hr at 60% relative humidity had a few bubbles but did not crack. The panels cast from resin preconditioned 8 hr at 40 and 50% relative humidity had no visible bubbles but also cracked in the mold. The cracking phenomena had not been encountered during the fabrication of preconditioned RS-14 resin panels. It is attributed to moisture effecting the RS-14A resin's physical and chemical properties during cure because it occurred with those samples with the highest and longest humidity exposures.

2.4.3.2.2 Tensile Properties

The data compiled in Tables 2.4.3.2-1 and 2.4.3.2-2 show that the tensile properties of preconditioned RS-14 and RS-14A resin are remarkably insensitive to moisture exposure with time and temperature. With the exception of the panels molded from RS-14 resin that was preconditioned for 8 hr at 175°F and 60 and 80% relative humidity (RX-13 and RX-14) and RS-14A resin that was preconditioned for 4 hr at 175°F and 70% relative humidity (RX-40) that contained too many bubbles to test, all of the tensile data is very good. The tensile strengths for all exposures range between 12 to >13 ksi for both resins systems. The average elongations at failure are similarly high and range between 4.8 to 5.9%. The tensile moduli are typical for RS-14 and RS-14A (372 to 413 ksi).

Even the panels that developed bubbles and voids during cure and/or cracked in the mold (panel nos. RX-18, RX-37, RX-38, and RX-39) had excellent tensile properties in the sections remaining that were large enough to test. These data suggest that exposure of the RS-14 and

RS-14A resin to moisture does not necessarily degrade its mechanical (tensile) properties.

2.4.3.2.3 DMA

The RS-14 and RS-14A panels molded from preconditioned resin were tested by DMA using the equipment and procedures described in Section 2.2.2.4. The results summarized in Tables 2.4.3.2-1 and 2.4.3.2-2 mirror the DSC data (Section 2.4.3.1.2) in that they show a dramatic reduction in the RS-14 and RS-14A resin's ultimate T_g from exposure to moisture.

Significant reductions in T_g begin with exposures of as little as 2 hr at 175°F and 40% relative humidity for the RS-14 resin and >4 hr at 40% relative humidity for the RS-14A resin. The T_g reductions in these cases are >15°F. As expected, the longer the exposure time at a given humidity level, the greater the reduction in T_g. After 4 hr exposure at 175°F and 40% relative humidity, the RS-14A showed a nominal T_g reduction of 7°F; after 8 hr, the reduction was over 27°F. Rachetting the humidity level to 50% for 4 and 8 hr exposures produced T_g reductions of 20° and 43°F, respectively, in the RS-14A resin.

Increasing time and humidity exposures tended to raise the shear modulus of panels cast and cured from preconditioned RS-14 and RS-14A resin. This effect was observed in the RS-14 panels that had been cast from resin exposed to 8 hr at 175°F and 60 and 80% relative humidity (RX-13 and RX-14) and from the RS-14A panel cast from resin that had been exposed to 4 hr at 175°F and 70% relative humidity (RX-40). All three panels had extensive bubbling and/or cracks making tensile testing difficult. The shear modulus from these panels were respectively 173, 178, and 167 ksi. This compares with the 152- to 163-ksi range of the control and other preconditioned specimens.

2.4.4 Summary of Results

The combination of results from the moisture preconditioning study indicate that the most significant effect from exposure to ambient humidity is depression of the resin T_g after postcure. Resin tensile properties are largely unaffected, provided that excessive bubbles or voids are not produced in the resin panels during postcure as a result of carbamate decomposition.

The FTIR analyses of preconditioned RS-14A resin indicates that the cyanate ester resin is susceptible to moisture at the 175°F temperature for exposure levels as low as 8 hr at 30% relative

humidity. Slight depressions of the RS-14 and RS-14A resin T_g (measured by DSC and DMA) were also observed after 8 hr exposures at 20 and 30% relative humidity. More significant T_g reductions were encountered at exposures >4 hr at 40% relative humidity for the RS-14A resin system and at exposures >2 hr at 40% relative humidity for the RS-14 resin.

A comparison of the FTIR results for the RS-14A and RS-14 preconditioned resin samples suggest that the RS-14 resin used in this study was either slightly pre-polymerized and/or contaminated with moisture. The RS-14A resin showed a greater sensitivity to moisture at low humidity levels than the RS-14 resin, indicating that these changes occur very rapidly in fresh resin. At higher humidity exposures, the behavior of RS-14A and RS-14 resin essentially became equivalent.

2.4.5 Recommendations

Based on the aforementioned results, practical humidity exposure limits for the RS-14 and RS-14A resins at 175°F are recommended to be 8 hr maximum at 30% relative humidity or 4 hr maximum at 40% relative humidity. With respect to the ORNL wet-filament-winding process for RS-14/RS-14A resin, the resin is routinely maintained at these temperatures in the vicinity of the resin wet-out pot and the mandrel.

The resin wet-out pot is a particularly vulnerable part of the wet-filament-winding operation because a large surface area of heated (175°F) cyanate ester resin is continuously exposed to the ambient environment for long periods of time. In addition, there is a constant mixing of the resin with the air due to the fiber being pulled through the resin pot at high speeds around a partially submerged pulley. Excess resin picked up by the fiber is continuously squeegeed by two nip rollers and this resin falls back into the pot, producing further mixing of the ambient environment with the resin.

The susceptibility of the cyanate ester resin to degradation as a result of contact with ambient humidity indicates that the resin pot should be maintained in as dry an environment as possible. A plexiglass box housing (Figure 2.4.5-1) was therefore fabricated to isolate the pot from the surrounding air.

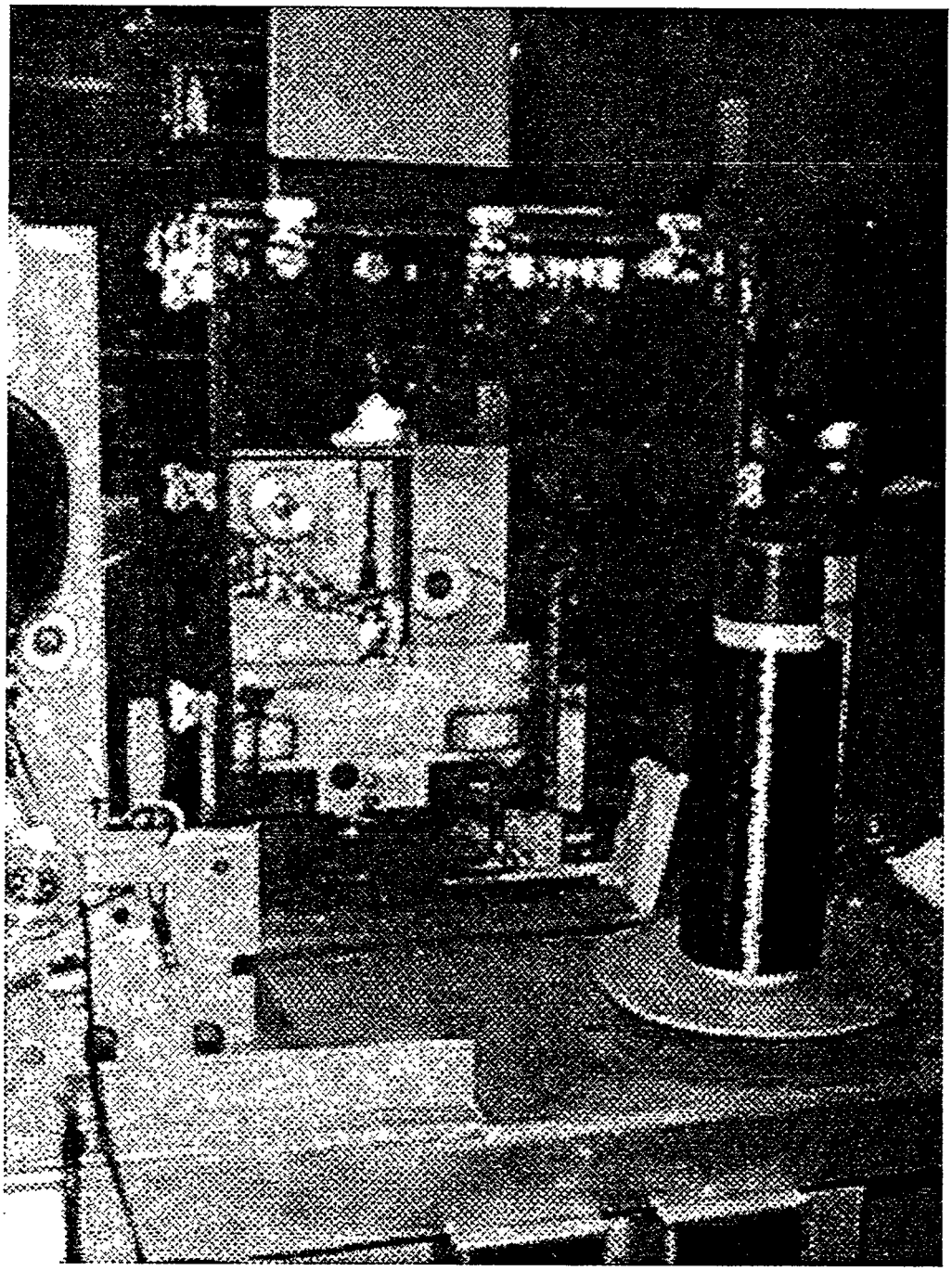

Figure 2.4.5-1. Resin pot with inert atmosphere enclosure.

During operation, the plexiglass box is continuously purged with a slightly positive pressure of nitrogen gas to maintain an inert (dry) atmosphere blanket around the resin. A small opening in the side of the box allows the fiber to pass through for resin impregnation in the pot. The fiber then passes out of the box through another opening to the brake system for tensioning and then continues on to the mandrel. Measurements made with an oxygen deficiency monitor and humidity gages indicate that the box is effective at reducing the humidity level in the vicinity of the resin pot by 90%.

Resin humidity exposure at the mandrel is considered to be less significant than at the wet-out pot because the time from which the impregnated fiber is laid down to the moment at which it is covered by the next layer is estimated to be only 10 to 15 min, depending on the length of the part and the number of compaction passes conducted.

2.5 Oven-Aged Resin Properties

This activity was performed to study the effects of thermal aging on RS-14 resin and composite properties. There were two objective for this study: (1) to determine whether the RS-14 resin is subject to physical aging caused by prolonged exposures to elevated temperatures below its T_g, and (2) to determine the impact to RS-14 resin properties from long term elevated temperature exposures to ambient air.

2.5.1 Discussion of Physical Aging

Physical aging as applied to polymers describes the reduction of free volume with time and temperature for amorphous, or "glassy" (non-crystalline) materials. A discussion of physical aging and its implications to thick composite hardware are provided below.

A simple model for a polymeric material is that of a network of chains that are tangled together. The polymer chains may be linear or they may have some functional (chemical) groups attached along the backbone at various locations similar to the branches on a tree. In a thermoplastic material (such as polyethylene or nylon), the chains are not interconnected and are free to slide freely past one another when undergoing deformation. In a thermoset material (for example, epoxy and cyanate ester resins) the chains are connected to one another at a various locations by chemical

bonds, or crosslinks, and chain mobility is inhibited unless sufficient force is applied to break the bonds. For both classes of materials, the free volume can be thought of as the "holes" or spaces in between the chains and functional groups.

The free volume state of a polymer affects the ability of the individual polymer chains and segments to deform under load. If a chain segment is pushed, it must be able to "slide" into an adjacent hole or space if deformation is to occur.[11] A large free volume provides lots of space for polymer segmental motion to take place. A small free volume is more difficult to deform. For this reason, some of the properties affected by a polymer's free volume state are its toughness and creep resistance.

The free volume of the polymer network is a function of the chemistry of the polymer, the temperature and the polymer's thermal history. Below the glass transition temperature (T_g), segmental mobility is limited. The polymer segments do not have sufficient energy to move past one another and the material is a "glass." Applied stress results in local bond distortions that can be more or less recovered when the stress is removed. Above the T_g, the polymer segments have sufficient energy to rearrange themselves to relieve an externally applied stress. The material is then in a "rubbery" state.[11]

The T_g can also be characterized as the inflection point in the specific volume (volume per unit mass) versus temperature curve for a polymer. Below the T_g, the specific volume of a polymer increases as the temperature increases due to the normal coefficient of expansion for the material. At the T_g, the coefficient of expansion increases sharply. This greater increase in volume with temperature above the T_g represents the addition of free volume for segmental motion.[11]

The chains of a polymer network will strive to reach an "equilibrium" state or conformation that is defined by the temperature, polymer chemistry and thermodynamics. The equilibrium state therefore defines the final free volume state of the polymer, as well as its ultimate properties.

The free volume state of a polymer can be "erased" by heating the polymer above its T_g. If the polymer is allowed to cool slowly, the polymer chains will have sufficient time and thermal energy to rearrange themselves as closely as possible into an equilibrium conformation. Heating above the T_g followed by rapid cooling ("quenching"), however, will freeze or lock in the maximum

amount of free volume for the material because the polymer chains will have insufficient thermal energy for segmental motion.

A polymer that has been quenched, or is otherwise in a nonequilibrium condition, will continue molecular rearrangement as it strives toward equilibrium, but at a much slower rate. Below a specific temperature, the glassy state mobility is too small to allow any changes in free volume. At higher temperature, however, thermal energy accelerates the process. The most rapid rearrangement will occur at temperatures close to, but just below the T_g. The process whereby a polymer is heated to a temperature below its T_g to increase the rate at which if approaches equilibrium is called "annealing" or "sub-T_g annealing."

Physical aging, therefore, describes the phenomena whereby a polymer undergoes free volume reduction with time and temperature as it strives toward equilibrium.[11,12] The effects of free volume reduction can be significant because of the material property changes that accompany it. These include increases in densification, modulus increase and embrittlement as well as changes to its optical and dielectric properties.[11,12]

Cyanate ester resins have the unique property that after gelation, free volume increases with conversion (cyclotrimerization).[13] At maximum conversion, or cure, the free volume for the resin is greatest. This is why cyanate ester resins experience lower shrinkage associated with cure. The relatively high toughness for a 250°C T_g resin is also attributed to the high free volume and the low cross link density associated with the triazine ring structure.[14]

The susceptibility of the RS-14 and RS-14A cyanate ester resin to physical aging is not yet known. The high free volume associated with cured cyanate ester resins suggests that the potential for free volume reduction (and material property change) with time and temperature may be significant. The physical aging of cyanate ester resins and the affect on creep and mechanical properties have been studied and reported in the literature.[15-20]

The impact of physical aging on thick hoop-wound composite hardware could be significant. Embrittlement of the matrix material in high fiber fraction composite rings may increase their susceptibility to failure under shear and transverse tensile loads. Thick composite rings may already have some radial residual tensile stresses as a result of the fabrication process. Physical aging of the matrix can exacerbate these stresses by causing resin shrinkage and embrittlement, resulting in radial

cracking. On the other hand, free volume reduction may also retard the creep process in composite rings.

An alternate point of view is that it may be desirable to "precondition" or "heat treat" thick composite hardware in order to accelerate the physical aging process. The result would be to expedite bringing the cyanate ester resin polymer to its thermodynamic equilibrium state. For preconditioned composite material, physical and mechanical properties should be less susceptible to change during long-term use. Radial and transverse creep deformation of hoop-wound rings under load should similarly be reduced. In another application, preconditioning composite rings prior to the assembly of compressively preloaded nested rings assemblies could reduce the loss of preload associated with polymer relaxation at elevated temperature.

2.5.2 Panel Preparation

This activity was initiated during an earlier study when the effects of air on resin properties were not yet characterized. The control and test panels prepared for this study were therefore precured and postcured in air. Both panels were cast and cured using the same batch of RS-14 resin (Reference No. FB3K702). The resin was poured into molds and precured for 4 hr at 380°F. After precure, the partially cured panels were returned to room temperature and removed from the molds. The panels were laid flat on a metal plate and postcured for 4 hr at 510°F. The surfaces of both panels had a dark brownish-black color indicating some surface reaction occurred during the elevated temperature postcure cycle. This dark layer was estimated to be 0.001 to 0.002 in. thick and could be easily removed by lightly sanding the panel, thereby revealing the tan colored RS-14 resin beneath.

One of the panels (GL-13) was laid flat on a metal plate and placed in an air-circulating oven. The panel was aged one year at 275°F in air and then removed from the oven. The other panel (GL-12) was designated as a control and was stored under ambient conditions.

2.5.3 Evaluation

After the oven-aging exposure was completed, both the test and the control panels were examined visually, by density and tensile property measurements and by DMA. The following are the results of this investigation.

2.5.3.1 Visual Examination

Visual examination of the two panels showed that the oven-aged RS-14 panel was a dark black color. Sections cut from this panel showed that there was a nominal 0.008 to 0.009 in. thickness of blackened resin on both sides of the panel. (Apparently laying the panel flat on a metal sheet did not prevent the ambient air and humidity from reacting with the bottom surface layer.) The black layer was brittle and flaked easily when cut with a grinding wheel.

As expected, the control panel was visually unchanged after one year at ambient conditions. Figure 2.5.3.1-1 shows a cross section from both the oven-aged and control panels. The black surface layer denoting cyanate ester resin degradation after elevated exposures to hot oven air is substantially thicker on the faces of the oven-aged panel. What is also interesting is that this layer increased in thickness with time. This indicates that this layer must be permeable to the atmosphere because it did not block/prevent further reaction from occurring. Theoretically this means that eventually the entire thickness of the panel could deteriorate with sufficient time and temperature in air.

2.5.3.2 Tensile Properties

Table 2.5.3.2-1 is a summary of the tensile and density data for the oven-aged and control test panels. The tensile data for the control panel are typical for RS-14 resin that has been postcured in an air environment. The nominal 0.001 to 0.002 in. layer of reacted resin on the specimen surface acts a series of flaws that promote premature tensile failure. The average tensile strength is only 9,375 psi as opposed to 12,000 to 13,000 psi for RS-14 resin that is cured in an inert atmosphere. In addition, most of the failures occur in the grip rather than the gagelength.

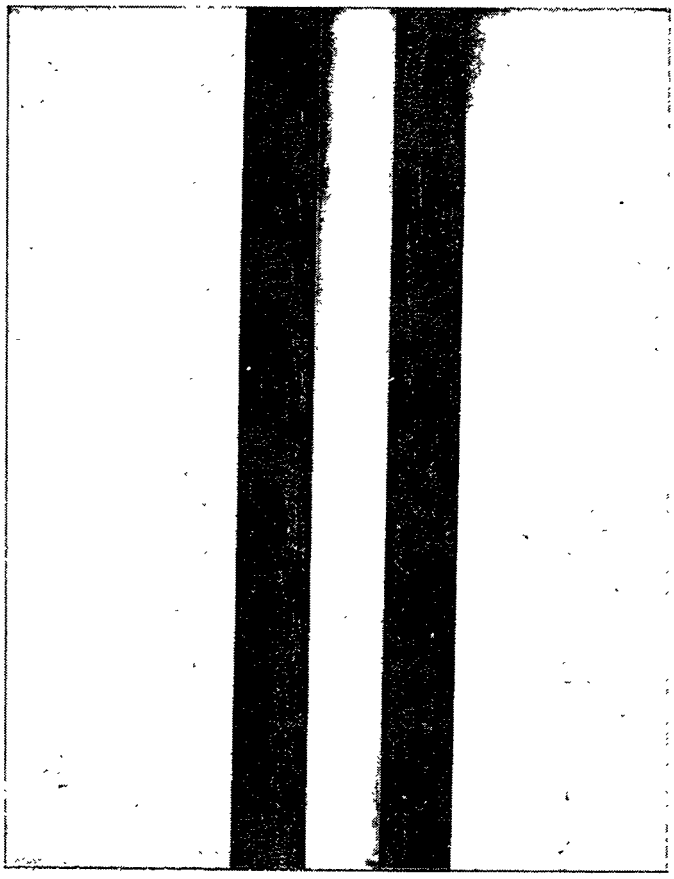

(3X)

Figure 2.5.3.1-1. Cross sections of oven-aged (left)and control (right) RS-14 panels. Oven-aged panel has thick, black reacted resin layer on both sides.

Table 2.5.3.2-1. RS-14 resin panel properties (oven-aged versus control).

Sample ID	Description	Density (g/cm3)	Tensile Strength (psi)	Tensile Elongation (%)	Tensile Modulus (ksi)	Failure Location
GL-12	Control; stored 1 year @ amb. temp. in air	1.2070				
# 1			9,974	2.9	416	grip
# 2			9,438	2.7	417	gagelength
# 3			9,696	2.8	398	grip
# 4			8,804	2.4	420	grip
# 5			8,672	2.5	396	gagelength
# 6			9,666	2.8	403	grip
			AVG: 9,375	**AVG: 2.7**	**AVG: 408**	
GL-13	Oven-aged; 1 year @ 275°F in air	1.2213				
# 1			3,725	0.9	464	gagelength
# 2			3,813	0.9	473	gagelength
# 3			3,780	0.8	507	gagelength
# 4			3,774	0.9	467	gagelength
			AVG: 3,773	**AVG: 0.9**	**AVG: 477**	
GL-13S	GL-13; surface reacted layer removed by sanding	1.2051				
# 1			8,138	2.1	431	grip
# 2			7,060	1.8	413	grip
			AVG: 7,599	**AVG: 2.0**	**AVG: 422**	

Note 1: Panels GL-12 and GL-13 precured for 4 hrs @ 380°F in air, returned to ambient ambient temperature and demolded. Panels then postcured for 4 hrs @ 510°F in air.

The reason for the high number of grip failures is that the reacted resin layer at the surface tends to be thicker in this region than in the gagelength. This occurs because the reacted layer thickness tends to be thicker near the perimeter of the panels on one side as opposed to the center. When the panels are postcured, they are laid flat on a metal sheet. Air contact with the bottom face is limited because the air must permeate under the panel from around the edges. The center of the panel faces tend to make better contact with the metal sheet and are therefore less exposed. Dogbone tensile specimens are usually cut from the panel in an orientation that tends to put the thicker reacted layer from the panel perimeter in the specimen grip region and the less reacted regions in the gage length. It is this thicker reacted resin layer in the grip region which causes the specimen to fail in the grip rather than the gagelength.

The average tensile strength of the oven-aged specimens is substantially lower and only 3,773 psi. During testing, cracking sounds were heard during the loading of the specimen. Failures for all specimens in this set were in the grip rather than the gagelength.

Figures 2.5.3.2-1 and 2.5.3.2-2 are photographs of the fracture surfaces for the control and oven-aged tensile specimens. The striations and texture of the control specimens denote some ductility prior to failure. The oven-aged specimens, by contrast, are smooth as glass. The thick reacted resin layer on the surfaces is believed to have initiated a brittle fracture mode.

The reacted resin layer was hand sanded from the surfaces of two of the oven-aged tensile specimens. The resulting specimens (GL-13S) were a light tan color, typical for RS-14 resin that has been cured in an inert atmosphere. Removal of the reacted resin layer increased the tensile strengths of the GL-13S specimens substantially (8,138 and 7,060 psi) to the same range as that of the controls. Failure was in the grip, primarily because these regions were not as efficiently sanded and had some reacted resin layer remaining.

The average tensile modulus for the oven-aged specimens (477 ksi) was substantially higher than that of the control specimens (408 ksi). Removal of the reacted surface resin layers by sanding brought the oven-aged specimen modulus down to 431 and 413 ksi for the two specimens. Based on the fraction of wall thickness of the reacted surface resin layer, a rule-of-mixtures calculation indicates that the modulus of the reacted resin layer material is on the order of 815 ksi.

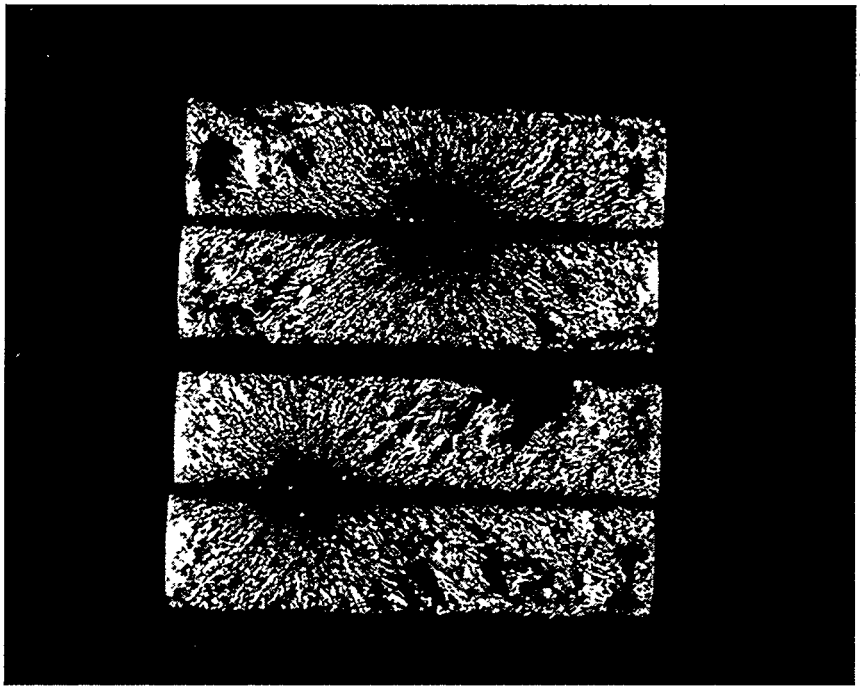

(5X)

Figure 2.5.3.2-1. Fracture surface showing ductile failure mode of control RS-14 tensile specimen.

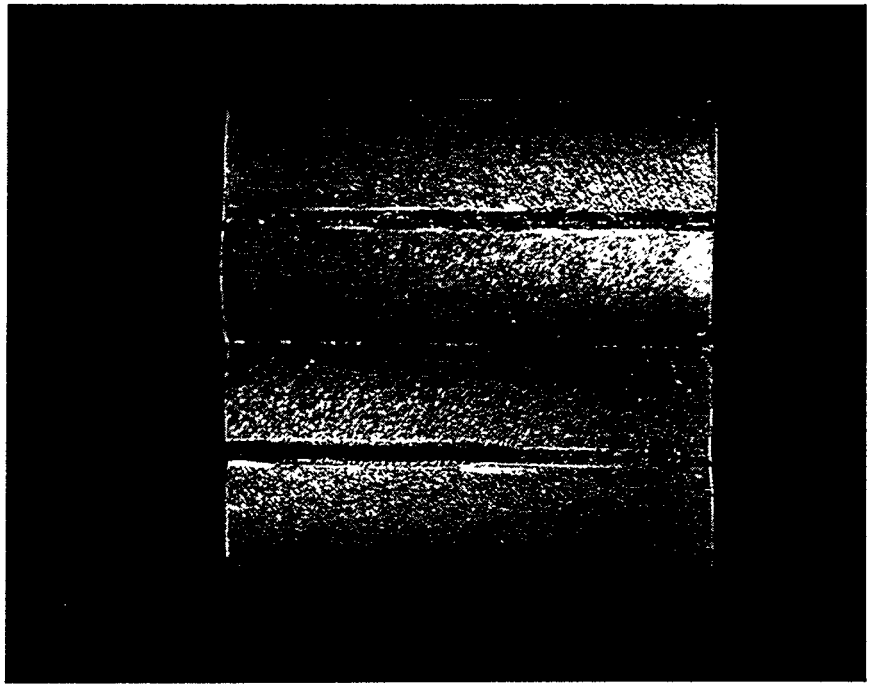

(5X)

Figure 2.5.3.2-2. Fracture surface showing brittle failure mode of oven-aged RS-14 tensile specimen.

These data indicates that the reacted surface resin layer was a major factor causing the increased tensile modulus and reduced tensile strength. Evidence of resin physical aging is inconclusive. Removal of the reacted surface resin layer from the GL-13S tensile specimens should have provided specimens of cyanate ester resin that were physically aged. However, the samples size (two specimens) was too small to determine if the tensile properties were significantly different than those of the control. The data for both sample sets were also biased by the presence of at least some residual reacted resin at the surface.

2.5.3.3 Density

The density data in Table 2.5.3.2-1 show that the oven-aged panel had a significantly higher density (1.22 g/cm^3) than the control panel (1.20 g/cm^3). Removal of the reacted surface resin layers on sample GL-13 by sanding (GL-13S) brought the resin density back to its nominal 1.20 g/cm^3 value.

This indicates that the reacted surface resin layer was the primary factor causing the increased density value. Based on the fraction of wall thickness of the reacted surface resin layer, a rule-of-mixtures calculation indicates that the density of this reacted resin layer is on the order of 1.34 g/cm^3.

Evidence of physical aging of the RS-14 resin was not found by this investigation. Removal of the reacted surface resin layer from the GL-13S tensile specimens should have provided specimens of cyanate ester resin that were physically aged but there was no measurable difference in the density of these specimens and the control.

2.5.3.4 DMA

Table 2.5.3.4-1 is a summary of the DMA results for the oven-aged and control test panels. Typically a physical aging phenomena causes densification of the polymer chains thereby increasing the T_g and modulus of the material. DMA permits measurement of both properties.

DMA was performed using a Rheometrics Dynamic Spectrometer and the procedure described in Section 2.2.2.4. A temperature sweep was performed from 30° to 300°C to obtain the shear modulus and T_g of the specimens. Each sample was then cooled back to ambient temperature and retested. The intent was to determine if heating the cyanate ester past its T_g would "erase" its

Table 2.5.3.4-1. DMA of oven-aged and control RS-14 resin panels.

Sample ID	Description	G' @ 82°F	Tg (°F)		
			G' Line-Fit	G" Peak	Tan Delta Peak
GL-12	Control; stored 1 year @ amb. temp. in air				
# 1		166	468	491	509
#1R		185	463	482	508
# 2		148	471	500	508
# 2R		166	461	491	509
GL-13	Oven-aged; 1 year @ 275°F in air				
# 1*		NA	460	484	511
#1R		159	453	485	512
# 2*		167	463	491	509
GL-13S	GL-13; surface reacted layer removed by sanding				
# 1		162	481	499	527
# 1R		168	470	492	518
# 2		169	484	500	518
# 2R		168	475	492	518

Note 1: Panels GL-12 and GL-13 precured for 4 hrs @ 380°F in air, returned to ambient ambient temperature and demolded. Panels then postcured for 4 hrs @ 510°F in air.
Note 2: R denotes a retest of the same sample.

* Sample surface decomposed and bubbled.

prior thermal history. "Quenching" or cooling the sample rapidly back to room temperature would in theory lock in a high free volume state with low(er) T_g and shear modulus values.

The DMA results for the two control specimens are typical for RS-14 resin that has been postcured in an air environment. The T_gs (459° and 458°F, calculated by the G' line-fit method) are ~30°F lower than for panels that have been cured in an inert atmosphere. (The lower T_g is believed to be due to resin degradation arising from contact of the cyanate ester resin with air and humidity at the elevated postcure temperature). The shear moduli for these specimens are also slightly elevated (167 and 172 ksi).

Retesting the two control specimens yielded T_g values that were nominally 10°F lower than the initial test values. The shear moduli were also reduced. These phenomena may be indicative of additional free volume in the specimens resulting from heating the specimens past their T_g followed by rapid cooling.

An alternative explanation for the reduced T_g values is that the DMA testing was conducted in an air environment. Testing from 25° to 300°C lasts ~2.5 hr. The samples may be experiencing some additional degradation of the surface resin which could account for the low(er) T_g data. The results of the thermal cycling trials (Section 2.3) have demonstrated that panels given multiple high temperature exposures in air experienced a slight reduction in the T_g value. However, the thermally cycled panels in that study also experienced an increase in modulus. The lower modulus of the retested DMA specimens is consistent with an increase in free volume.

The oven-aged specimens had significantly lower T_g values (448° and 440°F calculated by the G' line-fit method) and higher shear moduli (209 and 204 ksi) than the control specimens indicating the greater extent of reaction with the oven environment during the thermal aging experiment. These specimens could not be retested because the reacted surface resin layer decomposed and bubbled during the heat up to elevated temperature.

Figure 2.5.3.4-1 is a photograph of a control and oven-aged specimen after one cycle of DMA testing. The control specimen surface darkened slightly from the elevated temperature exposure to air during the DMA test but it did not decompose.

Shimp has proposed a mechanism to explain the deterioration of the oven-aged specimen.[17,21] During cyclotrimerization, and as cross link density increases, some cyanate groups become isolated

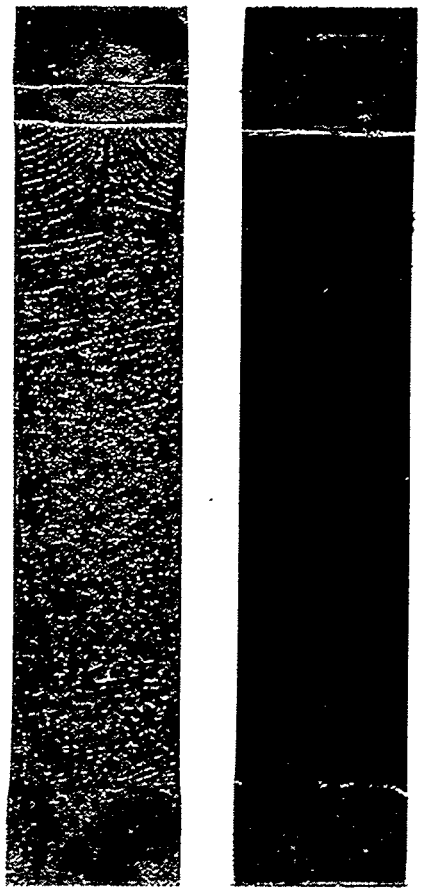

(1.8X)

Figure 2.5.3.4-1. Oven-aged (left) and control (right) RS-14 DMA specimens after one cycle to 300°C. Surface of oven-aged specimen has decomposed and blistered.

and unable to enter (react) into the triazine ring structure. These sterically isolated cyanate end groups later react with moisture, forming an intermediary, unstable carbamate.[17] At elevated temperatures, the carbamate decomposes to form an amine end group and CO_2.

It is speculated that the darkening of the oven-aged (and control) resin panel surfaces is due to the reaction of unreacted cyanate end groups with moisture in the oven. This reaction continued at the surface of the oven-aged resin panel at 275°F for one year, producing the thick scale on the surface. This scale is believed to be a combination of amine and carbamate groups.[17,21] When the oven-aged specimen was tested by DMA, the elevated temperature decomposed the carbamates,

evolving CO_2. The gas evolved at temperatures near the T_g deforms the plasticized matrix and collects in pockets, creating the "bubbled" appearance.

Removal of the reacted surface resin layer from the GL-13S tensile specimens should have provided specimens of cyanate ester resin that were physically aged. The initial T_gs of the two GL-13S specimens are slightly higher (462° and 464°F) than control specimens. Similar to the control specimens, the data from retesting the specimens showed a slight (~5° to 10°F) reduction in T_g.

Removal of the brittle outer coating also brought the shear modulus values for the both specimens down to 157 ksi which is typical for RS-14 resin that has been cured in an inert atmosphere. Based on the fraction of wall thickness of the reacted surface resin layer, a rule-of-mixtures calculation indicates that the shear modulus of the reacted resin layer material is on the order of 500 ksi. Similar to the control specimens, the retested specimens had slightly lower shear moduli (152 and 151 ksi).

2.5.4 Summary and Recommendations

The results of this study indicate that RS-14 resin is subject to chemical degradation when heated to elevated temperatures in air. Unreacted (free) cyanate groups are hypothesized to react with ambient moisture to produce carbamates and amines according to one mechanism proposed by Shimp.[21] The result is a brittle, black material on the outside surface that has a significantly lower T_g, higher modulus and higher density. This reacted resin layer has a significantly low(er) ductility and promotes premature failure in tensile specimens. Heating the resin past its T_g causes the reacted surface resin to decompose into at least one gaseous product which produces severe blistering and bubbles beneath the surface. This gas is believed to be CO_2 which is a known by-product from the decomposition of carbamates.

The growth of the reacted surface resin layer in the oven-aged resin panel suggests that the layer is porous and permeable to the ambient environment. The implication is that the reaction can continue to progress deeper into the cyanate ester resin substrate with time. Achieving a higher percentage of cyanate ester resin conversion could minimize this reaction by reducing the number of cyanate groups free to react with moisture. However, it is probably not

feasible to achieve 100% conversion in all resin and composite samples. Therefore, it is recommended that RS-14 (and RS-14A) cyanate ester resins and their composite be maintained in either a vacuum or inert environment when exposed for prolonged periods to elevated temperatures.

Evidence of physical aging is inconclusive from this study because of complications introduced by the reacted resin layer. Removal of this layer by sanding should have provided samples of physically aged cyanate ester resin without chemical degradation. Testing of this material showed no change in density and the tensile data is insufficient to determine if the modulus increased significantly with time at temperature. However, the DMA data for these specimens (and the controls), do show a slight reduction in the modulus and T_g after the specimens are heated above their T_g values and then rapidly cooled. These phenomena are consistent for polymeric materials that have been physically aged.

It is recommended that the long-term physical aging behavior of RS-14/RS-14A resin be studied further to determine the effects on such resin and composite properties as creep resistance, modulus and density. The test specimens should be cured in an inert atmosphere and to the maximum level of cyanate group conversion to prevent surface degradation due to contact with air and moisture. All elevated temperature testing should be conducted in an inert atmosphere as well to prevent chemical degradation of the surface. Doing this will make it possible to study the effects of physical aging on RS-14 and RS-14A resin separately from the effects of chemical degradation.

3. COMPOSITE PROCESS TRIALS

The purpose of the Composite Process Trials subtask was to conduct process optimization trials for T1000G/RS-14 composite. The focus of these studies was to investigate the impact to composite properties from performing cure cycles in an inert environment. Process trials were conducted with the intent of selecting an optimum cure schedule for fabricating thick stage-cured T1000G/RS-14 composite. An added objective was to evaluate the recently introduced RS-14A resin formulation for wet-filament-winding and compare its composite properties with those of the original RS-14 resin.

3.1 Description of Wet-Filament-Winding Method

The wet-filament-winding method was selected for fabrication of the composite rings and cylinders used in these studies because of inherent advantages it offers over alternate composite manufacturing methods. Figure 3.1-1 is a schematic of the wet-filament-winding process. The dry carbon fiber bundle (tow) is unreeled from spools and drawn through a wet-out pot where it is impregnated with resin. Tension is applied to the fiber via a suitable brake system and the tow is guided by pulleys, rollers, combs, etc., up to and through the winding machine feedeye and onto the mandrel. Process control points include the wet-out pot, the tensioning system, the winding machine pay-out, and the mandrel.

The advantages of wet-filament-winding are that it permits instantaneous and in-situ ply-by-ply consolidation *during* the lay up of the composite. Resin bleed-out is almost immediate with the application of each layer. These process characteristics lead to reduced fiber wrinkling and voids in thick constructions, particularly when compared to composites made via the prepreg lay up fabrication method in which resin bleed-out and ply consolidation occur after the total thickness has been laid up.

Another advantage is that higher fiber fractions are achievable using the wet-filament-winding method. ORNL has experience fabricating hoopwound carbon fiber composites with fiber fractions on the order of 78–80 vol %. Typical fiber fractions for parts made from prepreg

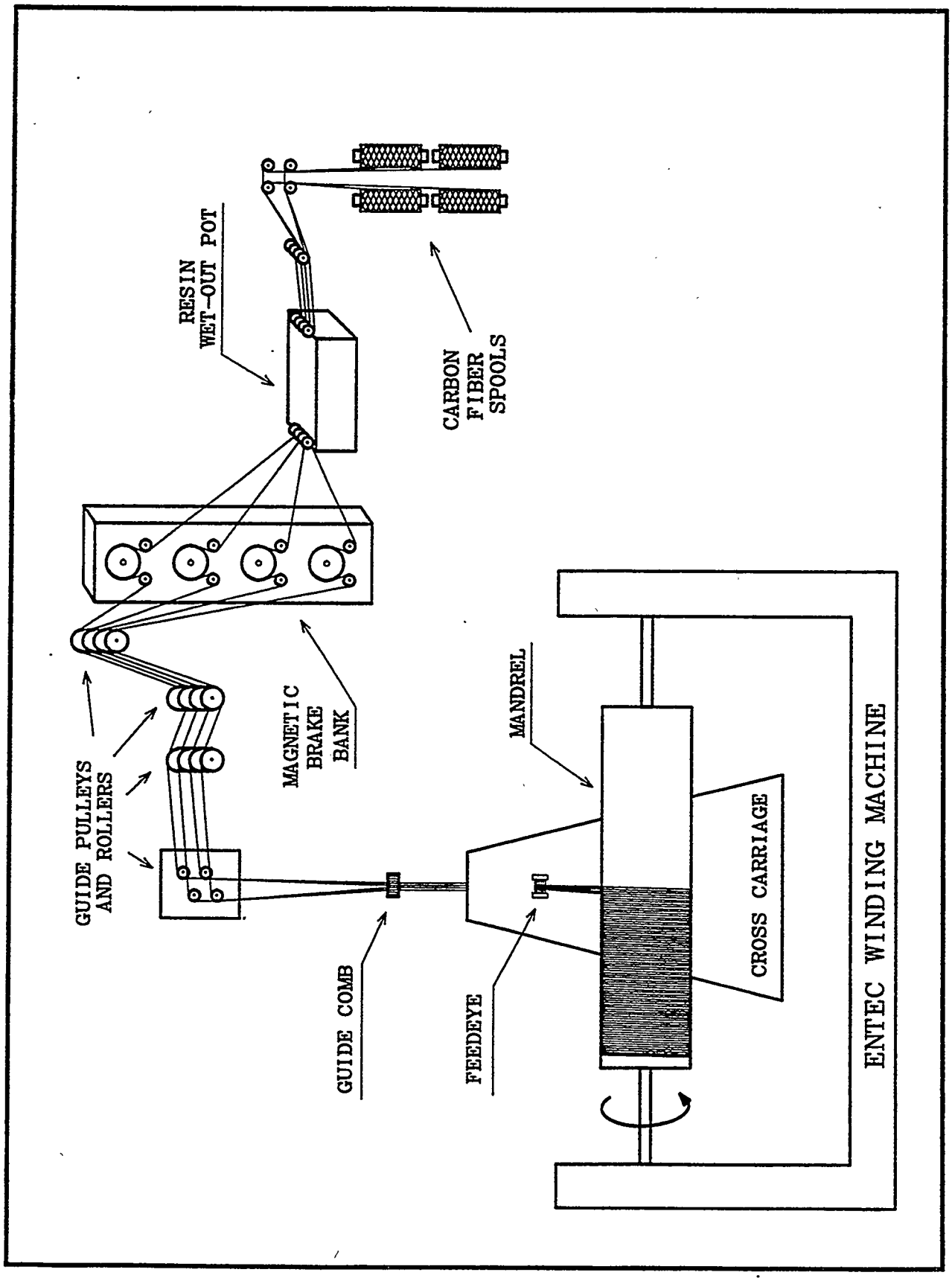

Figure 3.1-1. Schematic of winding operation.

lay ups are on the order of 60–63 vol %. High fiber content composite rings and cylinders can be important in some applications because they have a higher hoop strength and modulus as well as a reduced tendency toward transverse and radial resin viscoelastic creep.

3.2 Mandrel Description

The mandrel used to conduct the composite process trials was designed and constructed to provide capability to wet-wind thick hoop reinforced carbon fiber/cyanate ester resin composites for these studies. A summary of the mandrel design and features is provided in this section.

The mandrel body consists of a 1.25 in.-thick cylindrical shell made of 4340 steel that has been heat treated to obtain a 300–330 Brinell hardness. The shell was fabricated with a nominal 24 in. OD so that it could be used to wet-wind composite specimens compatible with existing ORNL split-D (NOL) test fixtures. The overall length of the mandrel shell is 19 in. The OD was flash chromed to prevent rusting and protect the surface. The shell concentricity after machining met or exceeded the 0.0005 in. tolerance specified by the design.

The cylindrical shell is supported between steel end plates. The shafts for chucking the mandrel into the winding machine are 4 in. OD × 5/8 in. wall thickness steel tubing that are welded to the end plates.

The mandrel is internally heated with an array of eight radiant heaters that are focused on the shell ID and that are mounted at equal distances around the center assembly. The heaters are wired through a slip ring so the mandrel surface temperature can be heated and controlled while the mandrel is rotated in the winding machine. Heater output is adjusted by a variac potentiometer to provide a specific mandrel temperature. Temperature control can be maintained nominally within ±5°F of a set point during winding.

A set of nominal 1/8 in. diameter × 1 in. deep holes were drilled into both side faces of the mandrel just below the OD surface for the insertion of thermocouple probes so that accurate temperature measurements of the mandrel shell can be made. As part of this study, temperature measurements were made periodically during the process by stopping the mandrel and inserting a thermocouple probe into the hole(s) to check the OD surface temperature.

3.3 Wet-Winding Parameters

The composite process trials were conducted by wet-filament-winding nominal 1/8 in. wall thickness hoop-wound cylinders on the internally heated mandrel. The fiber reinforcement was T1000G from Lot No. 615022. Depending on the fabrication, the resin was either RS-14 (Reference No. FB3K702) or RS-14A (Reference No. FB5K176).

Figure 3.3-1 is a photograph of the Entec winding machine used to fabricate the cylinders and Figure 3.3-2 shows the cart containing the fiber spool, resin wet-out pot and fiber tensioning system. Figure 3.3-3 is a view of the internally heated steel mandrel chucked into the winding machine prior to composite lay down. A view of the mandrel after winding several layers of composite is in Figure 3.3-4.

The wet-winding parameters used to fabricate the cylinders were developed in previous ORNL studies.[1,2] The pot temperature was maintained between 175° and 180°F to provide a nominal resin impregnation viscosity of 50–100 cps. All intermediate contact points between the wet-out pot and the mandrel were heated with infrared heat lamps to maintain a reduced viscosity and to keep the pulleys and contact points free of resin and fuzz buildup.

The T1000G fiber was wound with 12-lb tension throughout the fabrications. Weighted stainless steel rollers were run over the hoopwound composite during winding to provide further compaction of the fiber layer by squeezing out additional resin and air. Every layer (except the first ID layer) was compacted during winding, and an additional two compaction passes were applied after every five-layer winding increment. During compaction, the excess resin was skimmed lightly from the surface with the lip of a hand-held polyethylene cup.

The mandrel's internal heaters were used to maintain the mandrel surface temperature and the composite surface temperature between 170° and 180°F for the duration of the fabrication. An external strip heater helped maintain the composite surface temperature at these temperatures as the composite thickness increased. The composite OD surface resin content was adjusted to be slightly resin rich.

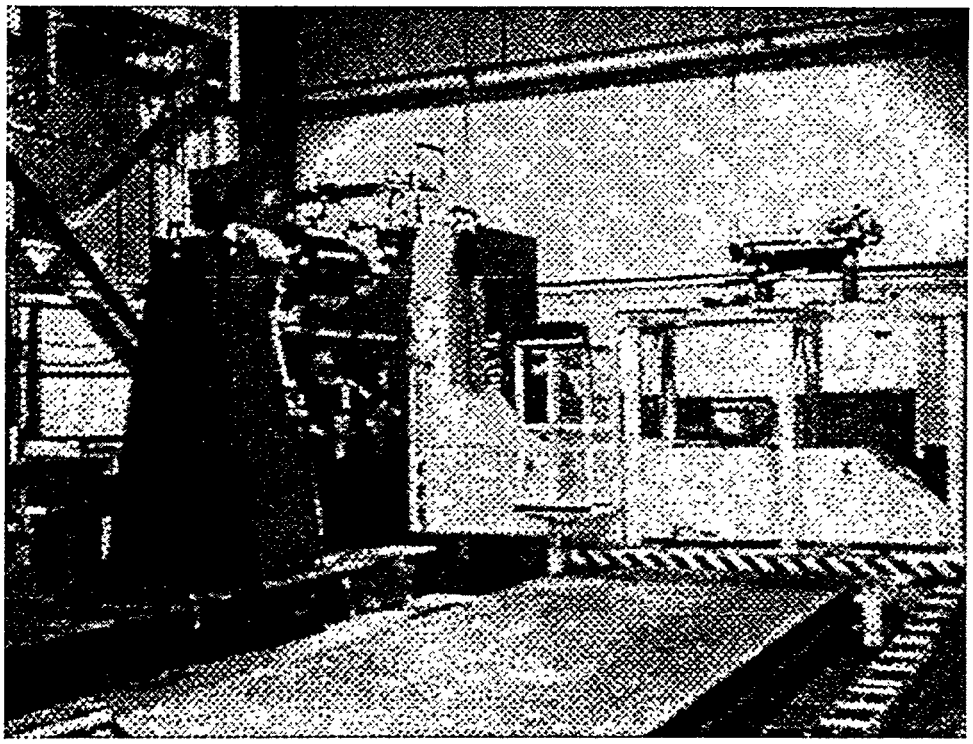

Figure 3.3.1. EnTec 4-axis computer controlled filament winding machine.

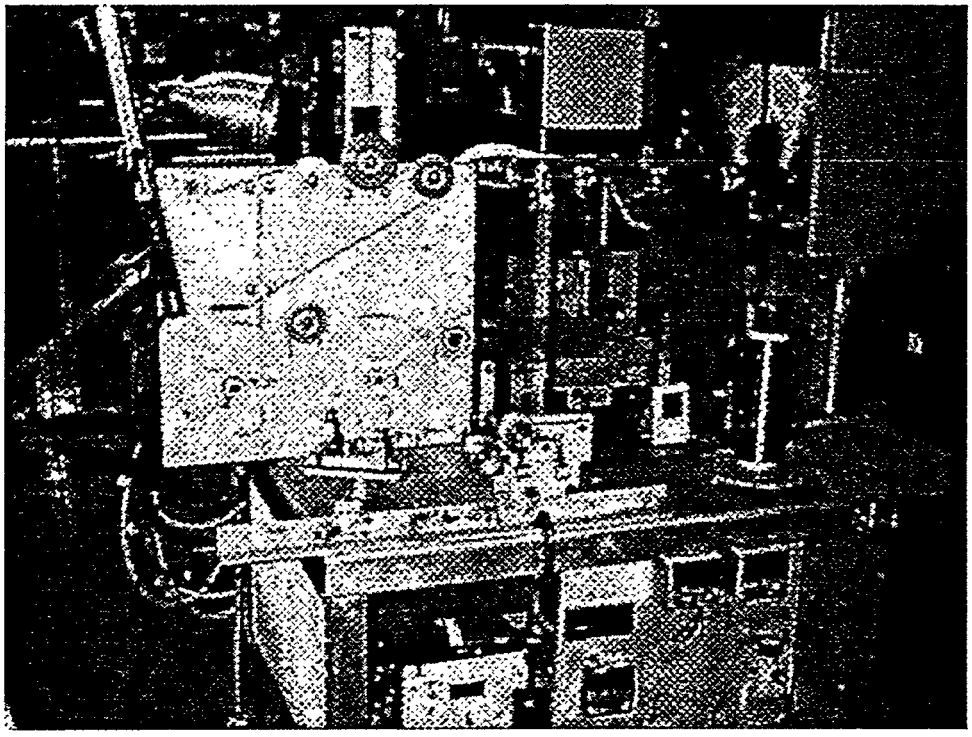

Figure 3.3-2. Filament-winding cart with spool, resin pot, and fiber tensioning system.

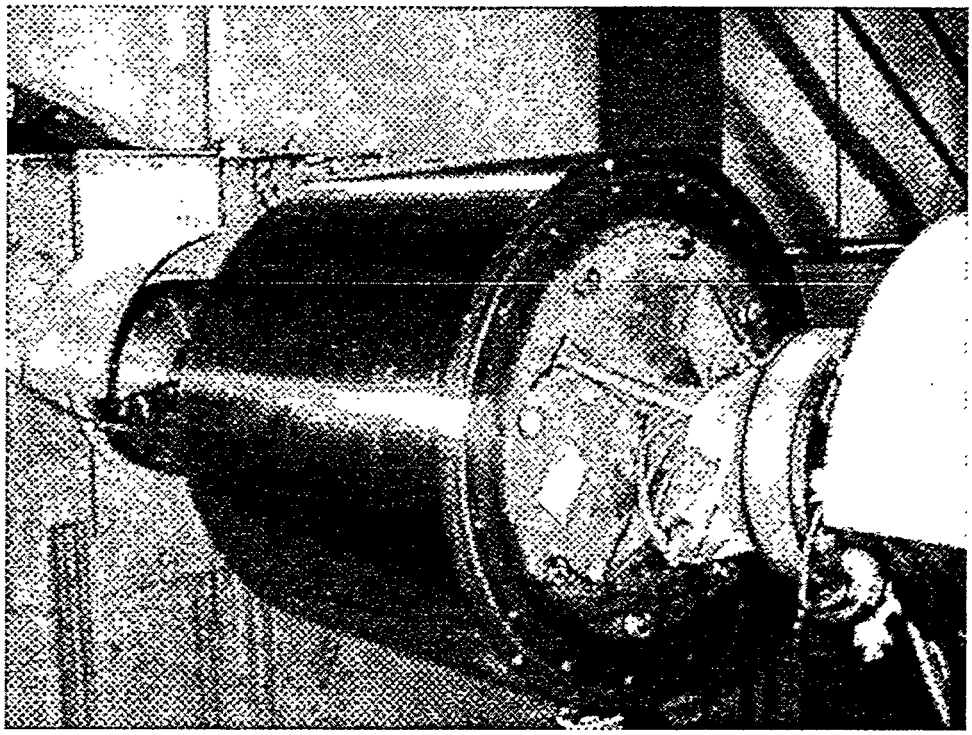

Figure 3.3-3. 24 in. OD internally heated steel mandrel.

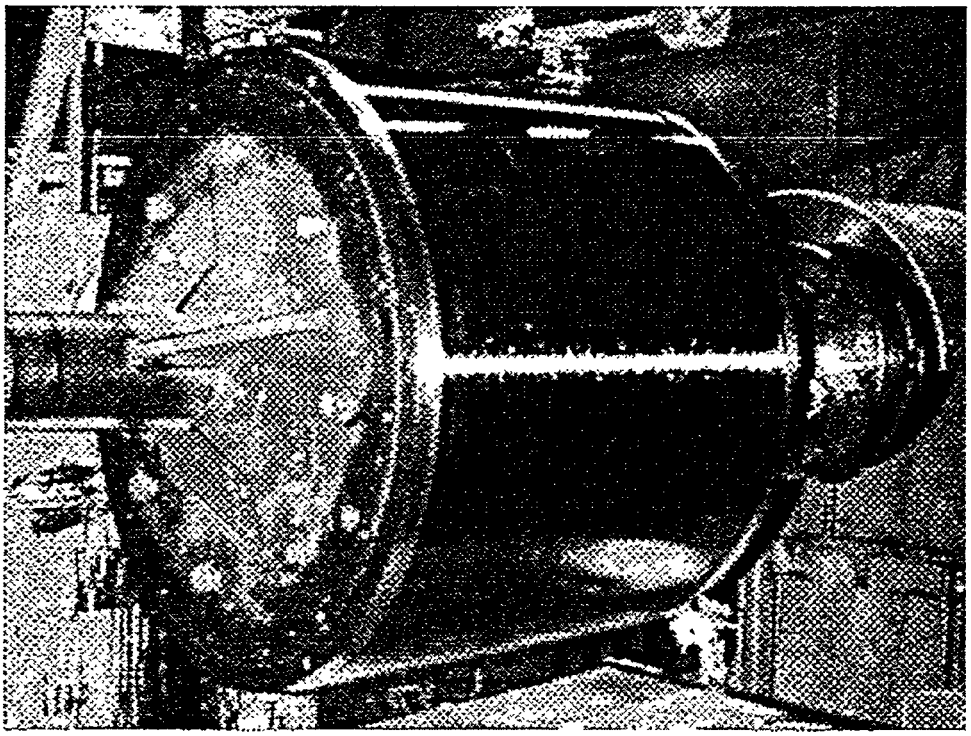

Figure 3.3-4. T1000G/RS-14 filament-winding operation.

When winding was completed, the mandrel was transferred immediately from the Entec winding machine to the rotisserie cart and prepared for cure. The rotisserie cart is a cure stand that was modified with bearings to allow the mandrel to be turned inside the oven during the precure portion of the cure cycle. With wet-filament-wound composites it is important that immediately after winding the mandrel be kept turning until the resin can gel or "set up" to prevent sag and deformation. The rotisserie cart allows one of the mandrel's shafts to protrude through a hole in the back panel of the oven. A drive clamp and chain connect the shaft to a variable speed motor mounted on the floor outside the oven which rotates the composite for as long as necessary. A view of the mandrel and composite resting in the rotisserie cart is shown in Figure 3.3-5.

3.4 ORNL Cure Process Modifications

The key difference between process trials conducted as part of this study versus previous work conducted by ORNL is that all curing was conducted in an inert (N_2) environment. This accomplishment required some additional equipment and procedures to the existing oven-cure process. Figure 3.4-1 is a schematic highlighting the process developed by ORNL to cure composite in an inert atmosphere.

As is, the oven is a convection oven that circulates air through a bank of heaters and into the oven chamber. Fans draw fresh air into the oven and over the heaters during operation and some air exits through the door seals and up through the stack. It was therefore not feasible to purge the oven chamber with nitrogen gas and maintain an inert environment.

A three-piece aluminum sheet metal canopy or cover was therefore constructed to go over the mandrel. The canopy consists of a front panel, back panel and a curved top panel which tie together with screws. It resembles a children's pup tent when fully assembled (Figure 3.4-2).

The canopy attaches to a baseplate on the rotisserie cart and has a snug-fitting hole in the back panel. The mandrel shaft passes through this hole for attachment to the motor that rotates the composite during cure. The canopy isolates the mandrel and composite from the circulating oven air. This makes it possible to bleed nitrogen through ports in the canopy wall to provide a nitrogen blanket around the mandrel.

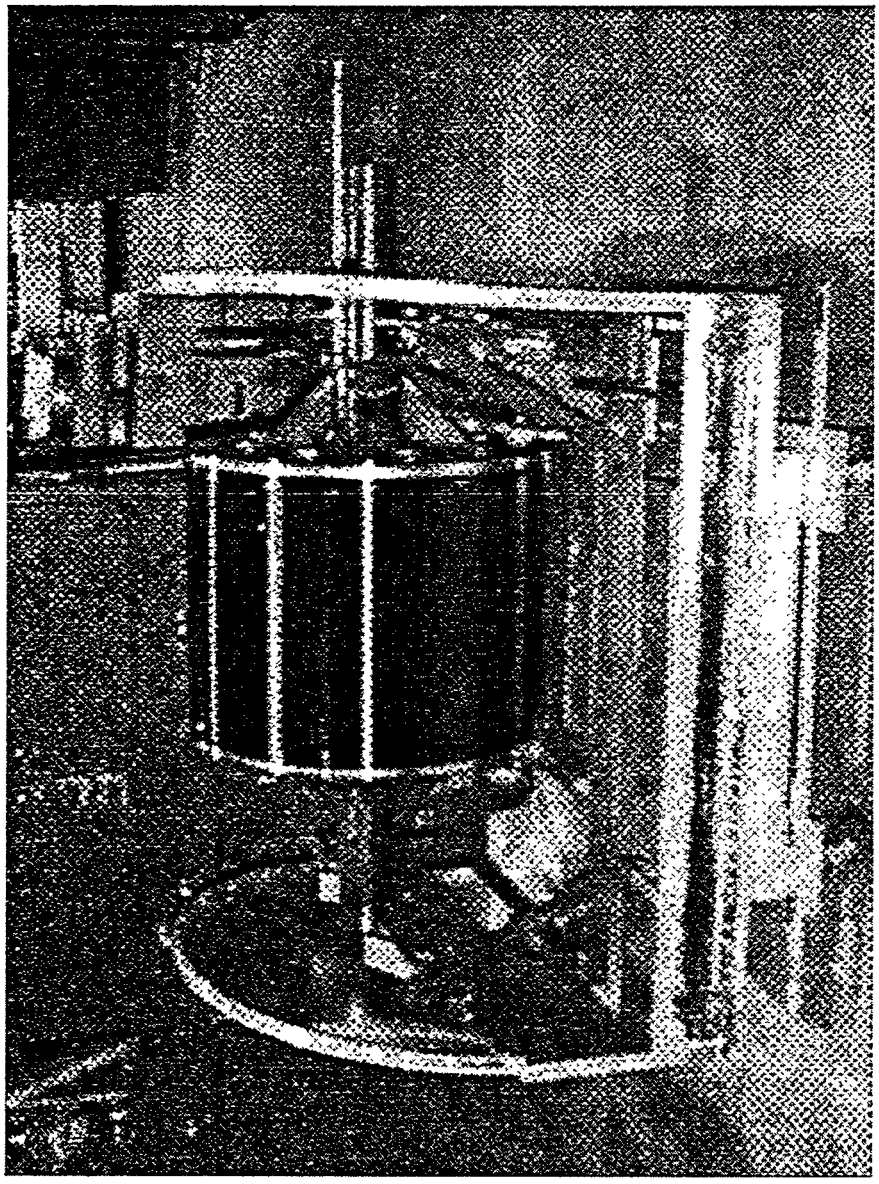

Figure 3.3-5. Mandrel in rotisserie cart.

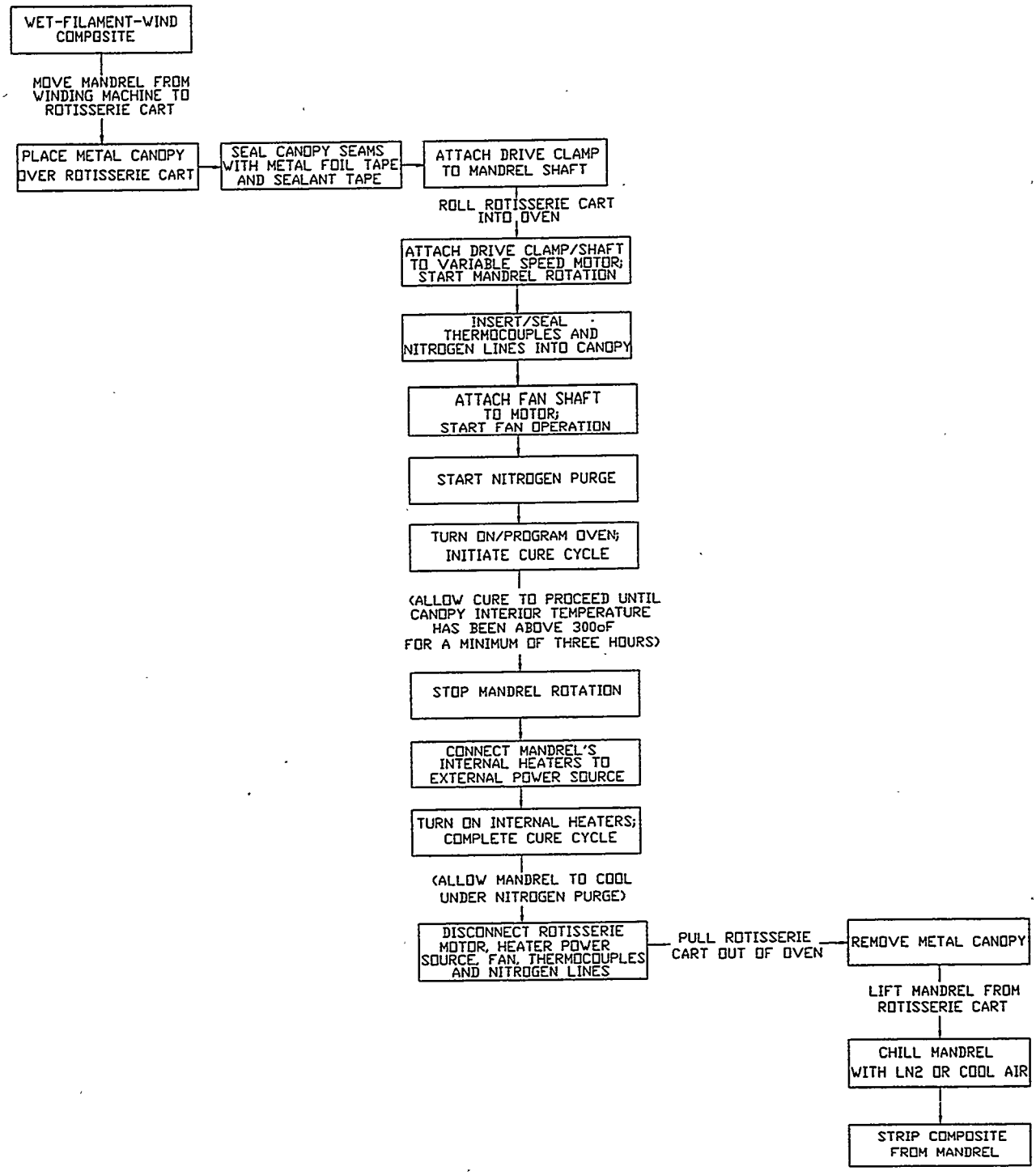

Figure 3.4-1. ORNL composite cure process.

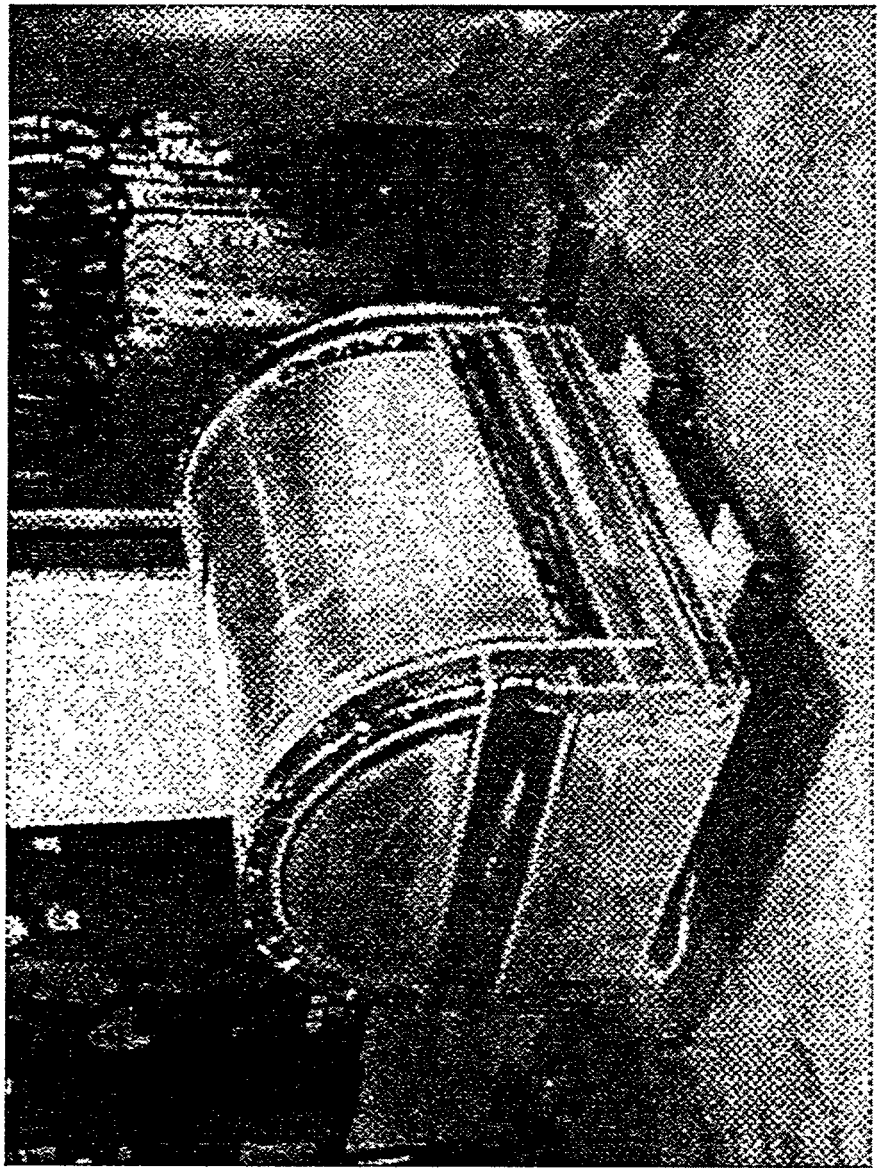

Figure 3.4-2. Metal canopy over mandrel/cart.

A manifold was constructed to provide the capability to bleed nitrogen from either a compressed nitrogen cylinder (220 ft^3 capacity) or from a liquid nitrogen cylinder (~4460 ft^3 capacity). The liquid nitrogen cylinder was the preferred nitrogen source because it could last through a 10–13 hr process cycle without having to be changed. Copper tubing was used to convey the nitrogen from the cylinders to the canopy interior.

The oxygen level under the canopy was monitored using a Bacharach Oxor II analyzer. This model draws a sample for analysis via a small pump. This makes it possible to obtain samples remotely through a tube from the interior of the canopy to the analyzer outside the oven. A sufficiently long tube was used so that the sample would cool before it reached the analyzer, making it possible to monitor oxygen levels continuously through the entire cure cycle.

The seams of the canopy were sealed using a combination of 6 in. wide pressure sensitive aluminum foil tape and 600°F sealant tape (sold for sealing the vacuum bags used to cure prepreg laminates at elevated temperatures). Initially the seams were sealed using the sealant tape only but it was difficult to apply the tape (which has a putty-like consistency and is only 1/2 in. wide) so that all gaps and openings were filled. In addition, there was the potential that the tape would stretch away from the walls during cure due to thermal expansion and warping of the cover. One process trial (cylinder SR-0029) experienced seal failure and the oxygen level rose to 8–10% at the postcure temperature. This process trial had to be repeated.

The sealing method was improved in subsequent process trials by first covering the seams with the aluminum foil tape. The aluminum foil is impermeable and the 6 in. width made it simpler to straddle the screws and gaps, ensuring that the entire seam was covered. The edges of the foil tape were then sealed with the 600°F sealant tape to reinforce the seal and to prevent the foil edges from curling up at the elevated postcure temperatures. This sealing method proved satisfactory, making it possible to maintain oxygen levels below 2% during cure.

Initial tests with the sheet metal canopy showed that the lack of convective air flow within the canopy makes it more difficult to bring the mandrel to elevated temperature. Heating the mandrel involves first raising the temperature of the oven, allowing the outside of the canopy to heat up and in turn warm the (nitrogen) environment within. This in turn eventually raises the temperature of the mandrel.

To expedite the cure cycle, several process improvements were made. Additional coils of copper tubing were added to the line used to convey the nitrogen gas from the cylinders to the canopy interior. The copper coils were located outside of the canopy but inside the oven. They therefore functioned as a heat exchanger to prewarm the nitrogen gas before it entered the canopy. The purpose was to avoid flooding the interior with cold nitrogen, thereby making it more difficult to bring the composite to the cure temperature. Tests showed that it was possible to prewarm the nitrogen to ~500°F using this method.

A metal fan was installed within the sheet metal enclosure to improve the circulation of the nitrogen gas. The fan blades are attached to a shaft which passes through small holes in the back panel of the canopy and the oven. The shaft is attached to a small variable speed motor which operates the fan. Testing showed that operation of the fan reduced the time required to heat the mandrel and minimized thermal gradients within the interior of the canopy.

The last process modification was to wire the mandrel's internal heaters so that they could be turned on during the cure cycle. Ordinarily, the mandrel interior would be the last location to come to temperature because it is shielded from the warmer air by the mandrel's thick steel shell. It thus acts as a heat sink which retards the rate at which the mandrel surface temperature can be raised. Focusing heat on the mandrel ID eliminates this cold spot so that the mandrel shell can get to temperature more rapidly.

The mandrel shafts were not long enough to permit using the slip ring and so rotation of the mandrel had to be stopped before the heaters could be connected to the power source. Therefore the internal heaters were only used after sufficient time and temperature had elapsed to ensure that the cyanate ester resin had gelled. The procedure was to wait until the interior of the canopy had reached 300°F or higher for a minimum of 3 hr before turning off the rotisserie and connecting the mandrel's internal heaters.

Another procedure was to heat the canopy interior to a higher temperature than the designated set point temperature specified by the cure cycle. The temperature overshoot was maintained for a short period in order to accelerate the rate at which the mandrel temperature increased. The maximum difference between the canopy interior temperature and the designated set point temperature for the precure portion of the cure cycle was 40°F or less. After the mandrel

temperature reached the designated set point temperature, oven power was reduced to bring the canopy air temperature down to the same set point. For postcure, the maximum permissible overshoot temperature for the canopy interior was 520°F.

3.5 Composite Properties with Cure Cycle

Selected cure cycles were studied in Section 2 (RS-14/RS-14A Resin Optimization Study) to evaluate their impact on cured resin properties. In this section, these cure cycles form the basis for studying the effect of cure temperature and thermal cycling on ultimate properties of T1000G/RS-14 or RS-14A composite.

Table 3.5-1 is the composite process trials matrix conducted for T1000G/RS-14 and RS-14A composite. In summary, the cycles involve a variation of (1) a 280°F precure step followed by a 500°F postcure step, (2) a 380°F precure step followed by a 500°F postcure step, and (3) no precure step and the composite is ramped directly to the 500°F postcure temperature.

The 500°F ultimate postcure temperature was selected for these trials as a compromise between the 480° and 510°F temperatures used to postcure the neat resin. There is less precision associated with the cure of the composite due to the thermal lag during heatup associated with the heavy steel mandrel and thermal gradients under the metal canopy. The difference between the temperature set point and the actual process temperature is estimated to be ±10°F. A cure cycle with a 480°F set point might inadvertently undercure the composite if the temperature drifts below; a 510°F set point may lead to over curing and cyanate ester resin degradation as experienced with some of the RS-14 resin panels evaluated in Section 2. The 500°F set point provides some margin of safety as the temperature should not drift substantially out of the range of 490°–510°F.

The aforementioned cure cycles comprise the core processes under consideration to fabricate thick hoopwound T1000G/RS-14 or RS-14A composite cylinders. Currently, thick cylinders are wound and stage-cured by ORNL over a period of several days. The term "stage" refers to the fraction of total wall thickness that is wound and cured in one day. The stage thickness is partially a function of the resin pot life or the time beyond which the resin viscosity in the wet-out pot and coating the pulleys becomes too thick to wet-wind and the winding operation must be terminated for cleanup.

Table 3.5-1. Composite process trials matrix.

Process Trial	Resin		280°F			380°F			500°F		
	RS-14	RS-14A	Ramp	Hold	Cycle	Ramp	Hold	Cycle	Ramp	Hold	Cycle
# 1	x	x	2°/min	3	0				2°/min	4	0
# 2	x	x	2°/min	3	3 times				2°/min	4	0
# 1-PST	x		2°/min	3	0				2°/min	4	3 times
# 3		x				2°/min	3	0	2°/min	4	0
# 4		x				2°/min	3	3 times	2°/min	4	0
# 3-PST		x				2°/min	3	0	2°/min	4	3 times
# 5	x	x							2°/min	4	0
# 5-PST	x	x							2°/min	4	3 times

Cure cycles will be performed under nitrogen blanket, unless otherwise specified.

Tests: NOL strength and modulus
SBS strength
Transverse flexure (concave up and down)
Composition

It is also theorized that the winding and cure of multiple stages can reduce the residual stresses in thick composites below those resulting from winding and curing the composite in one step. Residual stresses can arise after resin gelation has occurred and when the deformation of a composite layer during the cure process is restricted because the layer is confined by the presence of other layers above and below. Stage curing can reduce these residual stresses because the individual stage is free to deform without confinement from the outermost composite layers.

The last factor to consider is that stage curing provides for a gradual and controlled release of the exothermic heat liberated during the cyclotrimerization process. Heat transfer mechanisms in thick composite parts are limited to radiation outward from the composite OD to the oven or by conduction into the mandrel. It is speculated that if there is no mechanism for providing a gradual dissipation of the chemical heat of reaction, that the interior of a thick composite could overheat (exotherm), resulting in a deterioration of the composite's properties.

There are two methods for stage curing thick cylinders. One involves precuring each stage to a specific degree of cyanate ester conversion, or cure, dictated by the precure temperature and waiting until the last stage has been wound and precured to postcure the entire cylinder thickness at once. The second option is to bring each stage to the postcure temperature directly after it is wound. In both scenarios, the underlying stages receives some combination of multiple precure and postcure cycles. Attendant with these additional cures are the interaction of the mandrel on the composite ID as it expands during the heat up part of the cycle or shrinks away during cooling.

The baseline process used in previous ORNL[23] thick cylinder fabrications has been to precure each stage at 380°F and postcure the entire thickness after the last stage has been wound and cured. Process trials were therefore conducted to investigate the effect of single and multiple 380°F precure cycles on the composite's ultimate properties.

The 280°F precure temperature is near the minimum temperature at which gelation occurs in the RS-14 and RS-14A resin. Precuring each stage at this temperature offers the advantage that the low(er) degree of cyanate ester conversion, or cross linking, will permit the resin to deform more freely (or "flow") at the postcure temperature than a composite precured at 380°F. It is theorized that this resin relaxation can relieve internal stresses in the composite and yield a thick composite with low(er) residual stresses.

The concern with precuring each stage at 280°F, however, is that the low cyanate ester conversion also lowers the resin strength. When the material cools below its estimated T_g for that degree of conversion (~280°F), it will be relatively brittle. Experience with 280°F-precured resin panels confirms that the resin is weak. As the mandrel cools, the composite may develop small flaws or microcracks due to the relaxation of residual stresses in the hoop-wound composite. This damage might not be erased when the composite is ultimately taken to the postcure temperature, resulting in permanent flaws in the composite. Process trials were therefore conducted to verify that composite ultimate properties were not affected by single and multiple thermal cycles to the 280°F precure temperature.

Process trials were also performed to determine the effect on composite ultimate properties from a cure cycle with no precure step. Eliminating the precure step and ramping the composite directly to the postcure temperature shortens the time the mandrel is in the oven and might be preferred in production. Alternatively, the precure step can be important because it provides time for resin gelation to occur and for a gradual liberation of the exothermic heat of reaction associated with cure.

Finally, process trials were conducted to determine the impact of multiple elevated temperature postcure cycles on composite ultimate properties. There are two reasons why this information is important. The first is that there is a logic for postcuring individual stages rather than waiting to postcure the final thickness. During postcure, the mandrel (and any previously cured stages) expand against the ID of the composite layer at elevated temperature, causing a radial "thinning" of the composite layer. Some of this thinning is irreversible: that is the composite undergoes permanent, inelastic radial deformations as a result of postcuring on a metal mandrel. Residual stresses can arise when the thinning process of individual layers in a thick part is restricted because the layer is confined by the presence of the layers above or below.

Postcuring the composite off the mandrel would eliminate this problem but experience[2] has shown that precured composite rings that are not supported by a tool will soften and delaminate at the postcure temperature as internal compressive stress are relieved. The alternative is to postcure the individual stages so that they are free to undergo the radial thinning process gradually and unrestricted by outer composite layers.

The second reason to investigate the effect of multiple postcure cycles on cured composite properties is for the case that a polycyanate-based adhesive or edge coating is selected for assembling composite hardware. It is probable then that the composite would have to be taken back to elevated temperature to fully cure the coating or adhesive. In order for this to be a viable option, it must be demonstrated that additional postcure cycles do not harm the composite.

3.5.1 Procedures

All process trials summarized in Table 3.5-1 were conducted with the fabrication and cure procedures described in Sections 3.3 and 3.4, respectively. The time at the cure temperature was 3 hr for the precure portion of the cure cycle and 4 hr for postcure. Heatup rates were nominally 1°F/min. All cure cycles were conducted in an inert (nitrogen) atmosphere.

All thermal cycling was conducted with the cylinder supported on the mandrel. Cylinders receiving multiple precure cycles were wound and then ramped to the precure temperature. The mandrel was allowed to cool back to ambient temperature and then ramped again to the precure temperature. This process was repeated until the cylinder had received a total of four cycles to the precure temperature. The mandrel was then ramped to 500°F to postcure the cylinder.

Cylinders receiving multiple postcure cycles were obtained by winding and curing a standard process trial cylinder twice as long. After postcure, the cylinder was removed from the mandrel and cut in half. One half of the cylinder was set aside to serve as a control as well as to provide information on the effect of the cure schedule on ultimate properties. The second half of the cylinder was placed back on the mandrel and ramped directly to the 500°F postcure temperature for a second thermal cycle. This cylinder was then cycled two additional times between ambient temperature and 500°F for a total of four thermal cycles to the postcure temperature.

3.5.2 Cylinder Evaluation

The composite cylinders were cut into specimens and tested for composition, hoop tensile strength and modulus, interlaminar shear strength and transverse flexural strength. The data for the T1000G/RS-14 and T1000G/RS-14A composite cylinders are summarized in Tables 3.5.2-1 and 3.5.2-2, respectively.

Table 3.5.2-1. T1000G/RS-14 composite process trial results.

Cylinder Number	SR-0029*	SR-0029*PST	SR-0030	SR-0033	SR-0032	SR-0032PST
Precure Cycle	280°F; N2	280°F; N2	4 x 280°F; N2	280°F; N2	None	None
Postcure Cycle	500°F; N2	4 x 500°F; N2	500°F; N2	500°F; N2	500°F; N2	4 x 500°F; N2
Ring Tensile						
Strength (ksi)	652.8	621.9	661.5	619.3	621.8	621.4
	(6.1)	(5.3)	(2.4)	(4.6)	(5.4)	(6.7)
Modulus (Msi)	32.8	33.2	32.7	32.7	32.7	32.1
	(1.0)	(1.0)	(1.7)	(0.7)	(1.0)	(1.2)
SBS Strength (psi)	9,369	9,183	8,066	9,652	9,187	8,986
	(5.6)	(7.4)	(4.3)	(5.4)	(5.0)	(4.9)
Transverse Flex. Strength						
Concave Up (psi)	10,729	8,956	9,999	10,797	11,555	11,010
	(6.7)	(9.2)	(9.0)	(6.0)	(8.6)	(3.8)
Concave Down (psi)	7,214	6,740	7,623	6,832	7,813	7,863
	(11.5)	(8.2)	(7.5)	(7.6)	(8.6)	(4.7)
Composition						
Density (gm/cm3)	1.6624	1.6624	1.6569	1.6575	1.6546	1.6546
Volume % Fiber	78.9	78.9	78.3	78.4	78.1	78.1
Volume % Resin	20.8	20.8	21.3	21.1	21.3	21.3
Volume % Voids	0.3	0.3	0.4	0.5	0.6	0.6

( ) Number in parentheses is percent coefficient of variation

* Seal failure caused oxygen level to rise to 8-10% level during first postcure; composite was noticably blacker than other cylinders.
Number of specimens: ring tensile (8-11); SBS strength (10-11); transverse flex. strength (10-11 each concave up and concave down)

Table 3.5.2-2. T1000G/RS-14A composite process trial results.

Cylinder Number	SR-0034	SR-0037	SR-0034PST	SR-0036	SR-0038	SR-0035	SR-0035PST
Precure Cycle	380°F; N2	4 x 380°F; N2	380°F; N2	280°F; N2	4 x 280°F; N2	None	None
Postcure Cycle	500°F; N2	500°F; N2	4 x 500°F; N2	500°F; N2	500°F; N2	500°F; N2	4 x 500°F; N2
Ring Tensile							
Strength (ksi)	634.7 (7.1)	673.1 (4.3)	623.9 (3.8)	641.3 (5.4)	639.5 (5.6)	656.2 (3.6)	645.3 (4.8)
Modulus (Msi)	32.7 (0.9)	33.0 (2.3)	33.0 (1.6)	33.3 (1.6)	32.9 (0.8)	33.2 (0.9)	33.2 (1.7)
SBS Strength (psi)	9,748 (5.1)	9,526 (5.7)	9,526 (5.5)	8,685 (4.6)	9,427 (4.7)	9,689 (4.2)	10,027 (5.3)
Transverse Flex. Strength							
Concave Up (psi)	11,652 (5.7)	10,733 (7.0)	11,875 (5.3)	10,392 (3.4)	10,356 (8.9)	11,445 (5.7)	10,600 (8.1)
Concave Down (psi)	6,789 (7.0)	6,837 (14.6)	7,241 (12.7)	7,396 (5.3)	7,330 (9.7)	8,487 (9.1)	7,885 (11.6)
Composition							
Density (gm/cm3)	1.6648	1.6658	1.6648	1.6611	1.6646	1.6663	1.6663
Volume % Fiber	79.2	79.0	79.2	78.6	78.7	79.5	79.5
Volume % Resin	20.6	21.0	20.6	21.2	21.4	20.3	20.3
Volume % Voids	0.2	0.0	0.2	0.2	-0.1	0.2	0.2

( ) Number in parentheses is percent coefficient of variation

Number of specimens: ring tensile (8-11); SBS strength (10-11); transverse flex. strength (10-11 each concave up and concave down)

3.5.2.1 Composition

Composition is calculated from the measured density of the composite (obtained via ASTM D792) and weight percent fiber and resin contents (determined from digestion of the composite in nitric acid). The volume percent fiber, resin, and void contents are then calculated using these data, the measured neat resin density, and the vendor-supplied T1000G fiber density.

The data in Table 3.5.2-1 show that all of the T1000G/RS-14 composite cylinders have approximately the same composition. The composite densities are on the order of 1.66 g/cm^3, and the fiber contents range between 78.1 to 78.9 volume percent. These fiber contents are comparable to the levels obtained in T1000G/RS-14 composite in previous ORNL studies.[1,2] This is to be expected because these cylinders were wet-wound using the same process parameters. The void levels are low and <0.6 vol %. These, too, are comparable to previous results.

The data in Table 3.5.2-2 show that all of the T1000G/RS-14A composite cylinders have compositions that are comparable to those of the T1000G/RS-14 composite cylinders. The composite densities are also on the order of 1.66 g/cm^3, and the fiber contents range between 78.6 to 79.5 vol %. The void levels are similarly low and <0.2 vol %.

These results indicate that removal of the zirconate coupling agent from the cyanate ester resin has not affected the ability of the RS-14A to wet out the T1000G carbon tow. They also demonstrate that RS-14A yields carbon fiber compositions equivalent to those of RS-14 resin when wet-wound using the same process parameters.

3.5.2.2 Photomicrographs

Samples taken from the SR-0034PST, SR-0037 and SR-0038 process trial cylinders were mounted and polished for examination under an optical microscope. Figures 3.5.2.2-1 through 3.5.2.2-3 are photomicrographs taken of selected areas that are representative of these specimens.

All three cylinders were wet-wound using the RS-14A resin system. The photomicrographs show that these cylinders have a high fiber loading and are essentially free of voids. The photomicrographs taken at 1000x also show that despite the high fiber packing, the T1000G

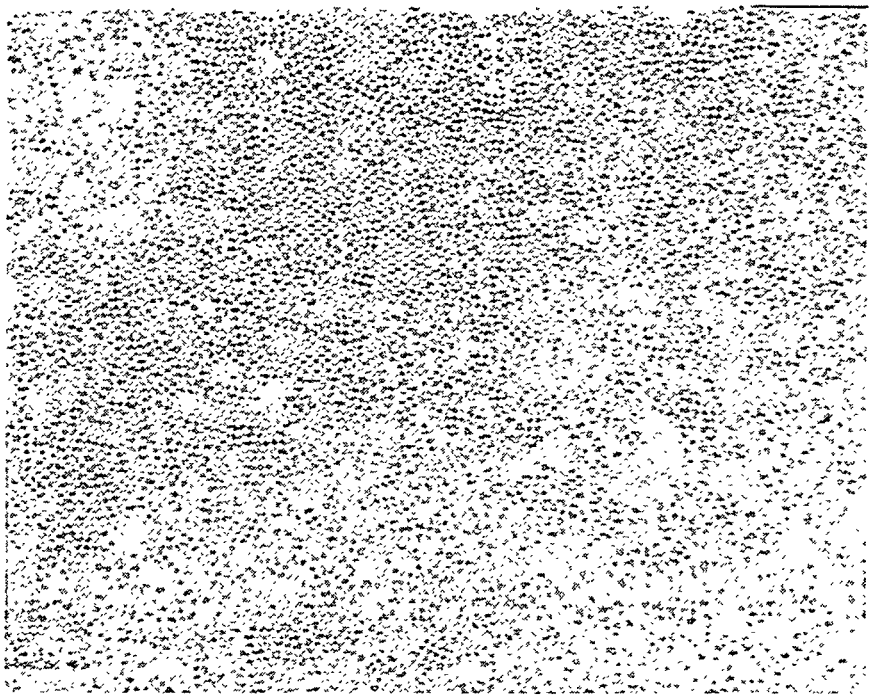

(a) 200X

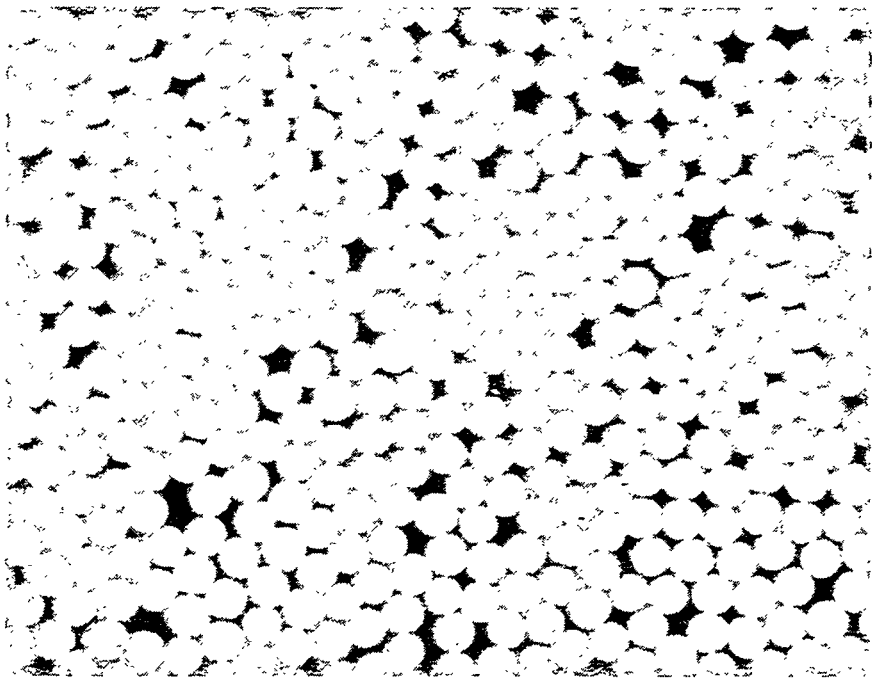

(b) 1000X

Figure 3.5.2.2-1. Photomicrograph of SR-0034PST composite cylinder.

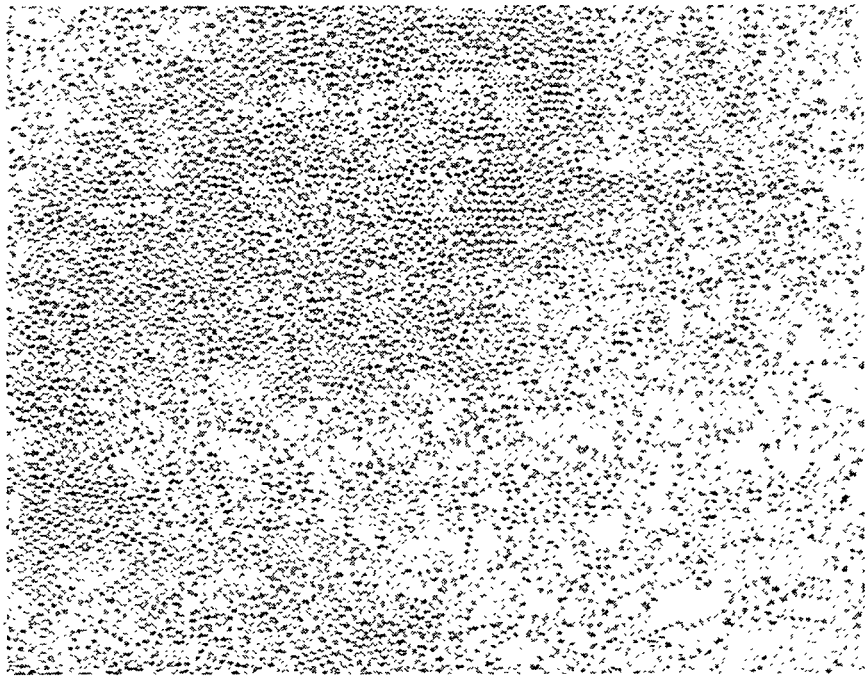

(a) 200X

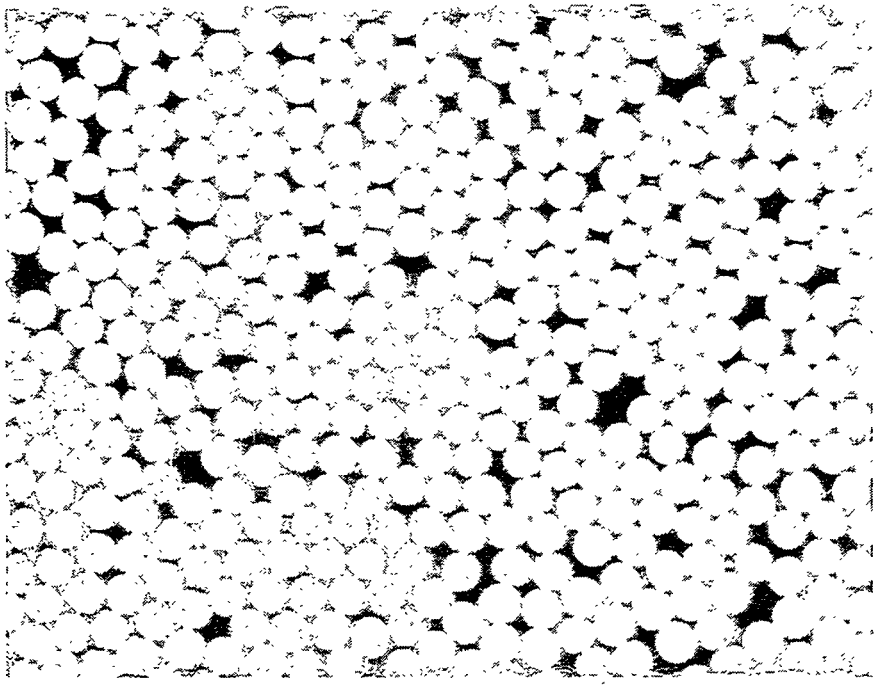

(b) 1000X

Figure 3.5.2.2-2. Photomicrograph of SR-0037 composite cylinder.

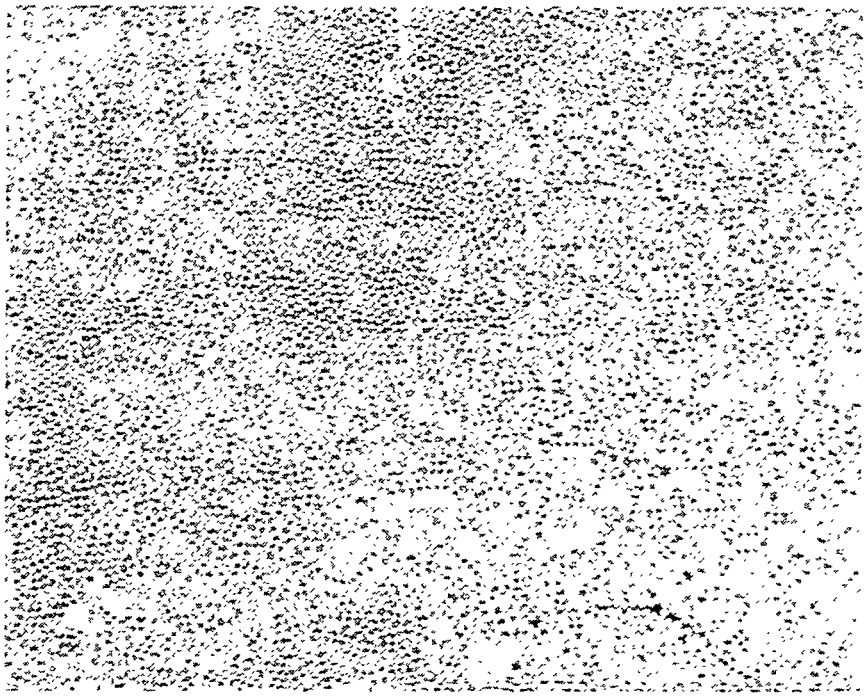

(a) 200X

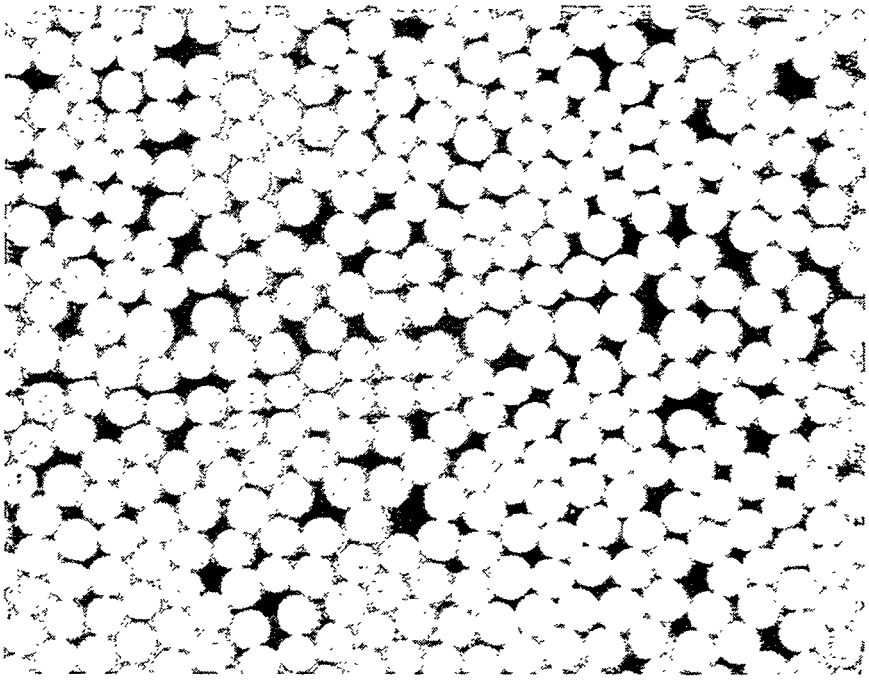

(b) 1000X

Figure 3.5.2.2-3. Photomicrograph of SR-0038 composite cylinder.

filaments in the tow bundle are uniformly coated with the RS-14A resin. These confirm the composition results and indicate that the RS-14A resin can effectively impregnate the T1000G carbon fiber bundle in the wet-winding process.

The samples prepared from the SR-0034PST and SR-0038 process trials were also examined for evidence of microcracking or other degradation due to thermal cycling. The SR-0034PST cylinder was precured at 380°F and then cycled four times to the 500°F postcure temperature; the SR-0038 cylinder was cycled four times to the 280°F precure temperature prior to postcure at 500°F. Evidence of microcracking and/or other damage were not visible in these specimens.

3.5.2.3 Ring Tensile

The ring tensile test uses a nominal 1/4 in. wide × 1/8 in.-thick ring specimen that is loaded in hoop tension by a split-D (NOL) fixture mounted in an oil-driven Tinius Olsen test machine. The specimen geometry and test method are similar to what is specified in the ASTM standard test method D2290, but the 24 in. ring diameter is larger in this application.

The composite ring is placed on the outer diameters of the split-Ds, and a tensile load is applied by pulling the Ds apart with a clevis/pin type loading mechanism. The split-D fixtures are solid steel plates that are nominally 1 in. thick. Friction between the composite ring and the Ds during loading is reduced by lining the inner diameter of the composite ring with Teflon tape prior to installation. The specimens are loaded to failure and the break load is recorded. The break loads, in conjunction with the cross-sectional area, are used to calculate the apparent hoop tensile strength for the composite.

An extensometer is used to measure deflection at the opening of the Ds. The load-deflection curve is plotted to ~6000 microstrain, and then the extensometer is removed to prevent it from getting damaged when the ring fails. The measured load and deflection are then used to calculate the composite hoop (fiber direction) modulus in the initial 1000–6000 microstrain range.

The data summarized in Tables 3.5.2-1 and 3.5.2-2 show that the ring or hoop tensile modulus for all of the process trial cylinders ranges between 32.1 to 33.3 Msi. There is good agreement between the hoop modulus values of all of the cylinders. This is to be expected based on the fact that the hoop tensile modulus is dominated by the modulus of the carbon fiber and that the

cylinders were fabricated with virtually the same fiber compositions. Similarly, the hoop modulus values for the cylinders fabricated with RS-14A resin are equivalent to those fabricated with RS-14 resin.

The ring tensile strength data in Tables 3.5.2-1 and 3.5.2-2 are, on average, comparable to the highest ring tensile strengths measured at ORNL.[2] However, high(er) average tensile strengths with lower data scatter were achieved more frequently in this study. The difference is attributed to conducting the cure cycles in an inert atmosphere. It is believed that doing so minimizes potential resin degradation at the composite cylinder OD due to reaction of the cyanate ester resin with moisture and air at elevated temperatures.

The ring tensile strengths for all of the process trials range between 619.3 ksi (SR-0033) and 673.1 ksi (SR-0037). The 673.1 ksi average tensile strength for the SR-0037 cylinder is the highest tensile strength measured by ORNL to-date for a set of carbon fiber composite rings. This set had three rings that broke with individual hoop tensile strengths that measured over 700 ksi. These measured hoop strengths are considered conservative and may actually be lower than the true material strength of the cylinder because of additional bending stresses the split-D fixtures impose on the ring during loading. The true hoop tensile strength of the material may be as great as 1.25 times the average measured strength based on split-D test stress analysis results.

The Statistical Analysis Program for MIL-HDBK-17 (STAT17), Rev. 3.1, November 4, 1992, was used to analyze batch-to-batch variability for the cylinders that were cured using different cure schedules (but not thermally cycled). STAT17 found no statistical difference in the tensile strengths data for cylinders SR-0029, SR-0032, SR-0034, SR-0035 and SR-0036.

This indicates that the tensile strength data are equivalent for cylinders cured with (1) a 280°F precure step (SR-0029 and SR-0036), (2) a 380°F precure step (SR-0034), or by (3) omitting the precure step and ramping directly to the postcure temperature (SR-0032 and SR-0035). These results also indicate equivalence of the tensile strength data for cylinders fabricated with RS-14A (SR-0034, SR-0035 and SR-0036) and RS-14 (SR-0029 and SR-0032) resin.

One anomaly is that STAT17 also determined that the tensile strength data for cylinder SR–0033 was statistically lower than that of the aforementioned cylinders. The SR-0033 cylinder was fabricated with RS-14 resin and was cured with a 280°F precure step prior to postcure.

Although found to be statistically lower, its tensile strength (619.3 ksi with a 4.6% coefficient of variation) is only 2.5 ksi lower than that of the next lowest average in the set (621.8 ksi with a 5.4% coefficient of variation for cylinder SR-0032). The 280°F precure step was used in the processing of cylinders SR-0029 and SR-0036, which had substantially higher tensile strengths (652.8 and 641.3 ksi, respectively). The low(er) tensile strength of cylinder SR-0033 is therefore considered to be a statistical aberration and the result of other factors (fiber strength, machining flaws, etc.) as opposed to the cure cycle itself.

Another interesting result is from cylinder SR-0029 which experienced a slight seal failure in the metal canopy that caused the oxygen level to rise to the 8 to 10% level during postcure. Evidence of the seal failure was visible at the cylinder OD which was noticeable blacker than the brownish-tint usually observed with cylinders postcured in nitrogen. However, the tensile strength of the SR-0029 cylinder (652.8 ksi with a 6.1% coefficient of variation) was one of the higher averages measured in this set of process trials. Apparently this low level of oxygen contamination during cure was not sufficient to degrade the composite's tensile strength.

STAT17 was also used to analyze for differences in tensile strengths of cylinders which were thermally cycled at either (1) the precure temperature prior to postcure, or (2) at the postcure temperature. STAT17 found no differences between the ring tensile strength data for thermally cycled cylinders and their control (non-thermally cycled) counterparts for the cases of (1) four precure cycles to 280°F followed by postcure (SR-0030 and SR-0038 compared with control cylinder SR-0036) and (2) four postcure cycles (SR-0029PST compared with SR-0029; SR-0032 compared with SR-0032PST; SR-0034 compared with SR-0034PST and SR-0035 compared with SR-0035PST).

STAT17 did find that the tensile strength data for cylinder SR-0037 (673.1 ksi) was statistically *higher* than its non-cycled counterpart, SR-0034 (634.7 ksi). The SR-0037 cylinder received four precure cycles to 380°F prior to postcure and had the highest recorded tensile strength for this study. The reason for the higher tensile strength is unknown but it indicates that cycling at the 380°F precure temperature prior to postcure does not degrade ring tensile strength.

Another observation is that the largest reduction in average tensile strength (4.7%) was measured for the SR-0029PST cylinder which was cycled four times to the 500°F postcure

temperature. As described earlier, the cylinder OD blackened during its first postcure cycle due to a seal failure in the canopy that allowed the oxygen level to climb to the 8 to 10% level. It is known that the SR-0029PST section underwent no additional reaction with air because it was cycled simultaneously on the mandrel with the SR-0034PST cylinder. The SR-0034PST cylinder OD turned a dark brown but did not blacken, indicating that oxygen was not present during these additional thermal cycles to the postcure temperature. Although the SR-0029 cylinder (from which the material for the SR-0029PST process trial is obtained) had an excellent tensile strength (652.8 ksi), this initial surface degradation from the first postcure cycle may have contributed to the reduced tensile strength (621.9 ksi) of the thermally cycled SR-0029PST section. However, as mentioned earlier, STAT17 found no statistical difference between the tensile strength data for the SR-0029 and SR-0029PST process trials.

The fiber strength translation is obtained by dividing the measured ring tensile strength by the product of the fiber strength and the fiber fraction in the composite, i.e.,

$$\text{fiber strength translation} = \frac{\text{ring tensile strength} \times 100}{\text{T1000G strength} \times \text{volume fiber fraction}}$$

It is therefore a measure of the efficiency of the carbon fiber in transferring its tensile strength to the composite. The fiber strength translations were calculated using the 954 ksi lot tensile strength average obtained for Lot No. 615022 in a previous study.[2]

Based on this method, the highest fiber strength translations achieved were 89% for the SR–0037 and SR-0030 cylinders. This strength translation is in the proximity of strength translations obtained for high-fiber fraction carbon fiber composites wet-wound with epoxy resins.

The very low data scatter (2.4% coefficient of variation) of the SR-0030 cylinder ring tensile data also suggest that this cylinder has a minimum of flaws. Therefore, its strength (661.5 ksi) and the strength of the SR-0037 cylinder (673.1 ksi) are probably as close to the maximum that can be achieved for this lot of T1000G carbon fiber and the RS-14/RS-14A resin with these process conditions.

3.5.2.4 Interlaminar Shear

The interlaminar shear test uses a curved short beam shear specimen geometry based on the ASTM D2344 standard test method with the fiber direction being parallel to the beam axis. The specimens are machined from a partial circumferential length of 1/4 in. wide × 1/8 in.- thick ring specimen, similar to what is used for the ring tensile test. The circumferential length of the short beam shear specimen is 3/4 in. Testing is accomplished with a nominal 4:1 span-to-depth ratio. The specimens are loaded to failure, and the break load is recorded. The apparent interlaminar shear strength is calculated from the break load and the specimen geometry.

The interlaminar strength data in Tables 3.5.2-1 and 3.5.2-2 are, on average, comparable to the strengths measured in previous ORNL studies.[1,2] Curing the composite in an inert atmosphere is not expected to affect the interlaminar shear strength because failure is not associated with the composite OD but is instead at the mid-plane of the specimen wall thickness. The interlaminar shear strengths for all of the process trials range between 8,066 psi (SR-0030) and 10,027 psi (SR-0035PST).

STAT17 was used to analyze batch-to-batch variability for the cylinders that were cured using different cure schedules (but not thermally cycled). STAT17 found no statistical difference in the tensile strengths data for cylinders SR-0029, SR-0032, SR-0033, SR-0034, and SR-0035.

This indicates that the interlaminar shear strength data are equivalent for cylinders cured with (1) a 280°F precure step (SR-0029 and SR-0033), (2) a 380°F precure step (SR-0034), or by (3) omitting the precure step and ramping directly to the postcure temperature (SR-0032 and SR–0035). These results also indicate equivalence of the tensile strength data for cylinders fabricated with RS-14A (SR-0034 and SR-0035) and RS-14 (SR-0029, SR-0032, and SR-0033) resin.

One anomaly is that STAT17 also determined that the interlaminar shear strength data for cylinder SR-0036 was statistically lower than that of the aforementioned cylinders. The SR-0036 cylinder was fabricated with RS-14 resin and was cured with a 280°F precure step prior to postcure. Its interlaminar shear strength (8,685 psi) is significantly lower than the 9,200- to 9700-psi range of the other cylinders. The 280°F precure step was used in the processing of cylinders SR-0029 and

SR-0033, which had substantially higher shear strengths (9,369 and 9,652 psi, respectively). The reason for the low(er) interlaminar shear strength for cylinder SR-0036 is presently unknown but may be due to other factors (fiber sizing level, machining flaws, etc) as opposed to the cure cycle itself.

STAT17 was also used to analyze for differences in the interlaminar shear strengths of cylinders which were thermally cycled at either (1) the precure temperature prior to postcure, or (2) at the postcure temperature. STAT17 found no differences between the shear strength data for thermally cycled cylinders and their control (non-thermally cycled) counterparts for the cases of (1) four precure cycles to 380°F followed by postcure (SR-0037 compared with control cylinder SR–0034) and (2) four postcure cycles (SR-0029PST compared with SR-0029; SR-0032 compared with SR-0032PST; SR-0034 compared with SR-0034PST; and SR-0035 compared with SR–0035PST). In fact, the highest interlaminar shear strength measured (10,027 psi) in this study was for cylinder SR-0035PST which was cured at 500°F (no precure step) and then given three additional thermal cycles to the 500°F postcure temperature.

STAT17 did find that the interlaminar shear strength data for cylinder SR-0030 (8,066 psi) was statistically lower than its non-cycled counterparts, SR-0029 (9,369 psi) and SR-0033 (9,652 psi). The SR-0030 cylinder received four precure cycles to 280°F prior to postcure and had one of the highest recorded tensile strengths (661.5 ksi) for this study. The SR-0038 cylinder also received four precure cycles to 280°F prior to postcure but had a significantly higher shear strength (9,427 psi).

These data are inconsistent, but the two process trials with the lowest shear strengths (SR–0030 and SR-0036) were both cured using a 280°F precure step. The low(er) shear strength of the SR-0030 cylinder may be the result of damage incurred to the composite by thermally cycling undercured composite on the mandrel.

3.5.2.5 Transverse Flexure

The transverse flexure test uses a 1/4 in. wide × 4 in.-long beam specimen that is loaded in 4-point bending in the rz-plane. The specimens are machined from a partial circumferential length of a 4 in. wide × 1/8 in.-thick composite band. The axis of the beam (z-axis) is parallel to the axis

of the ring geometry and transverse to the direction of the hoop fibers in the composite cylinder.

The tests are conducted both with the concave surface (or ID) of the ring radius of curvature being on the compression side of the beam ("concave up") and on the tension side of the beam ("concave down"). All of the tests used the 4-point loading configuration with a support length to depth (L/d) ratio of 24, where the beam depth corresponds to the composite ring thickness. The distance between support points was 3 in., and the distance between loading points was 2 in. The overall beam length is 4 in. and the width is 1/4 in. The specimens are tested to failure and the break load is recorded. The break load is used to calculate the composite transverse flexural strength in accordance with ASTM D790 standard test method.

The "concave up" test configuration places the portion of the beam corresponding to the cylinder OD in tension. It is sensitive to the outermost OD layers of the composite and the surface resin layer thickness. The "concave down" test configuration places the cylinder ID in tension and is sensitive to the innermost ID layers of the composite. Because the ID composite layers tend to be more compacted, with a higher fiber content, and have a minimal surface resin layer, the transverse tensile strength of these layers is expected to be lower than for the layers at the OD. For this reason, the concave up transverse flexural strengths are nearly twice the value of the concave down strengths.

Both the concave up and concave down transverse flexural strengths are subject to high data scatter because of their sensitivity to surface resin layer thickness and machining flaws. Correlation of the data with process cycle is therefore difficult for these same reasons. Observations from this study are summarized in the following paragraphs.

Concave Up

The concave up transverse flexural strength data in Tables 3.5.2-1 and 3.5.2-2 are, on average, comparable to the low(er) range of strengths measured in previous ORNL studies.[1,2] In this work, it was not unusual to obtain strength values of 12,000 to 14,000 psi. These composites were postcured in an air environment and the OD surface resin had a blackened appearance. It is speculated that this blackened outer resin layer had a somewhat higher modulus than comparable resin cured in an inert atmosphere. Since the outer surface resin is loaded in tension in the concave

up transverse flexural test, this blackened surface resin layer may have an artificially high impact on the transverse flexural strength values and biased the data upwards.

Excluding the data from cylinders that were thermally cycled, the concave up transverse flexural strengths for this set of process trials range between 10,392 psi (SR-0036) and 11,652 psi (SR-0034). STAT17 was used to analyze batch-to-batch variability for the cylinders that were cured using different cure schedules. There is a slight correlation that shows that the cylinders cured with a 280°F precure step (SR-0029, SR-0033, and SR-0036) prior to postcure have significantly lower concave up transverse flexural strengths than do cylinders cured without a precure step (SR-0032 and SR-0035) or with a 380°F precure step (SR-0034). A possible explanation for this is that gelling the resin at the lower precure temperature affects the amount of resin bleed out to the surface (probably reducing it) which may then affect the concave up transverse flexural strength.

The available data do not indicate any differences in the concave up transverse flexural strengths between cylinders wet-wound with RS-14A and RS-14 resin. The highest (and lowest) transverse flexural strengths for both sets of cylinders are comparable.

Another result is that cylinder SR-0029 (which experienced a slight seal failure in the metal canopy which caused the oxygen level to rise to the 8 to 10% level during postcure) does not have a significantly lower (or higher) concave up transverse flexural strength (10,729 psi). Apparently this low level of oxygen contamination during cure was not sufficient to affect the composite's flexural strength.

STAT17 was also used to analyze for differences in the concave up transverse flexural strengths of cylinders which were thermally cycled at either (1) the precure temperature prior to postcure, or (2) at the postcure temperature. STAT17 found no differences in the concave up transverse flexural strength data for thermally cycled cylinders and their control (non-thermally cycled) counterparts for the case of four precure cycles to 280°F followed by postcure (SR-0030 and SR-0038 compared with control cylinders SR-0029, SR-0033, and SR-0036).

STAT17 did find that the concave up transverse flexural strengths were statistically lower for the cylinders that received (1) four precure cycles to 380°F followed by postcure (SR-0037 compared with control cylinder SR-0034) and (2) four postcure cycles (SR-0029PST compared with SR-0029; SR-0032 compared with SR-0032PST; and SR-0035 compared with SR-0035PST). In

the majority of these cases, however the concave up transverse flexural strengths for the thermally cycled cylinders are still >10,600 psi. In one of the trials, the concave up transverse flexural strength of a cylinder cycled four times to 500°F (SR-0034PST) was the highest value recorded in this study (11,875 psi) and was statistically equivalent to its non-cycled counterpart (SR-0034).

The greatest reduction (16.5%) with thermal cycling to the 500°F postcure temperature was measured for cylinder SR-0029PST. In this case, it is speculated that the blackened surface layer (resulting from reaction of the cyanate ester resin with some air at elevated temperature during postcure) may have been weakened by the additional temperature exposures and incurred damage either from the thermal cycles on the mandrel and/or the specimen machining operation.

Concave Down

The concave down transverse flexural strength data in Tables 3.5.2-1 and 3.5.2-2 are, for the most part, comparable to the strengths measured previously at ORNL.[1,2] In the concave down configuration, the composite ID surface is loaded in tension and is the initiation site for failure. Curing the composite in an inert atmosphere is not expected to affect these strengths appreciably because the ID is already reasonably protected from the oven environment by the mandrel and the outer layers of composite.

The concave down transverse flexural strengths for all of the process trials range between 6,740 psi (SR-0029PST) and 8,487 psi (SR-0035). STAT17 was used to analyze batch-to-batch variability for the cylinders that were cured using different cure schedules (but not thermally cycled) but was unsuccessful at determining equivalence for these cylinders. The implication is that the data scatter is too high to determine batch-to-batch differences in concave down transverse flexural strength for cylinders cured using different cure cycles, or between cylinders wet-wound with RS–14A and RS–14 resin. A review of the data suggest, however, that there is enough overlap in the data that these properties are *probably* equivalent.

STAT17 was also used to analyze for differences in the concave down transverse flexural strengths of cylinders which were thermally cycled at either (1) the precure temperature prior to postcure, or (2) at the postcure temperature. In these cases, STAT17 found no differences between the concave down transverse flexural strength data for thermally cycled cylinders and their control

(non-thermally cycled) counterparts for the cases of (1) four precure cycles to 280°F followed by postcure (SR-0030 and SR-0038 compared with control cylinders SR-0029 and SR-0036); (2) four precure cycles to 380°F followed by postcure (SR-0037 compared with control cylinder SR-0034); and (3) four postcure cycles (SR-0029PST compared with SR-0029; SR-0032 compared with SR–0032PST; SR-0034 compared with SR-0034PST; and SR-0035 compared with SR-0035PST).

3.5.2.6 Composite DMA Measurements

The purpose of this activity was to determine if the cyanate ester resin in the T1000G/RS–14A composite was fully cured and, by inference, reached its maximum mechanical and thermal properties. Measuring the T_g from a composite specimen by DMA is a relatively simple method to evaluate the degree of cure.

Figures 3.5.2.6-1 and 3.5.2.6-2 are the DMA results, respectively, for specimens cut from the SR-0034PST and SR-0037 composite cylinders. Both cylinders were wet-wound with T1000G fiber and RS-14A resin as part of the thermal cycling study. The SR-0037 cylinder received four precure cycles at 380°F prior to postcure at 500°F. The SR-0034PST cylinder was precured at 380°F and then received four postcure cycles at 500°F.

The composite DMA specimens were tested in the torsion rectangular test mode using a Rheometrics Dynamic Spectrometer. The torsion rectangular specimens were cut from sections of the cylinder so that the hoop fibers were perpendicular (90 degrees) to the axis of the beam. The longitudinal axis of the specimens was parallel to the cylinder's axial direction. These specimens have a slight curvature because the front and back faces correspond to the OD and ID surfaces of the 24 in. diameter cylinder. However, this curvature is minimal and does not affect the T_g measurement.

The samples were tested with a fixed frequency of 6.28 rad/sec and a commanded strain of 0.03%. A temperature sweep was performed from 30° to 350°C with a heat up rate of 2°C/min. Data were taken at 2°C intervals with a 25-sec soak time at each test temperature prior to taking the measurement. The data recorded for each test temperature include G', G" and tan delta.

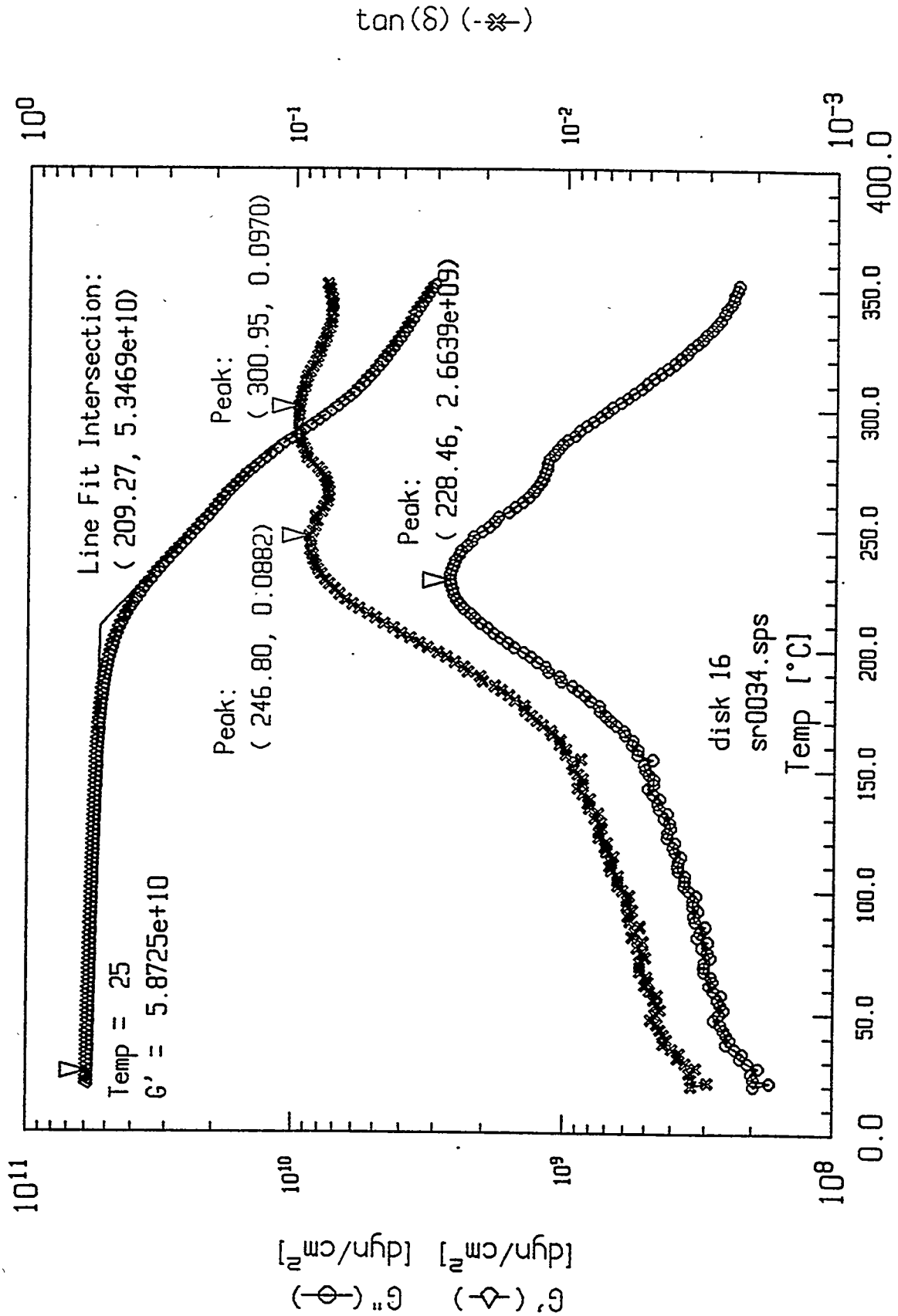

Figure 3.5.2.6-1. DMA plots for SR-0034PST.

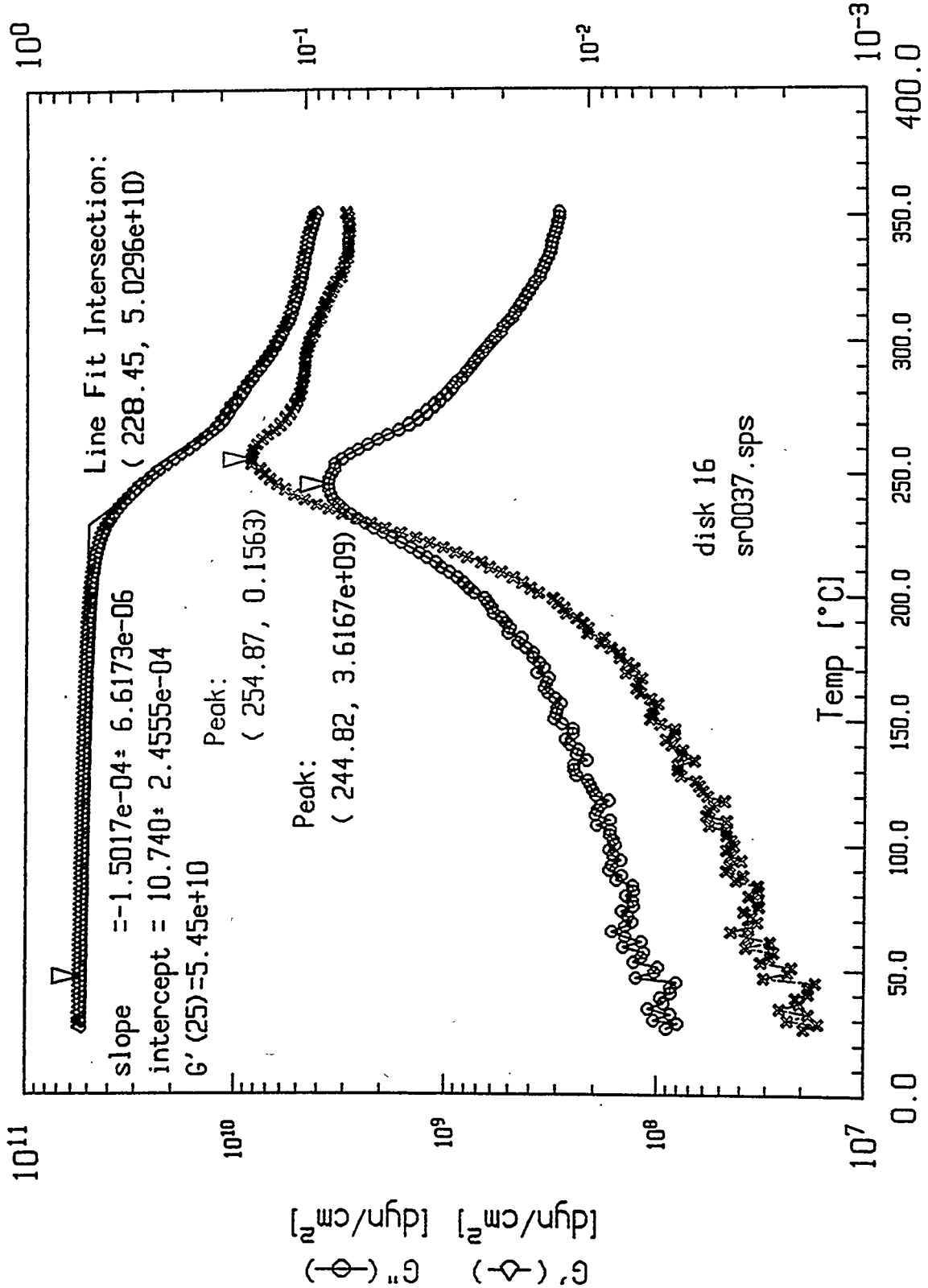

Figure 3.5.2.6-2. DMA plots for SR-0037.

The T_g data for the SR-0034PST and SR-0037 cylinders are summarized in Table 3.5.2.6-1 along with data from a neat RS-14A resin panel (RX-33) that was measured as part of the RS-14/ RS-14A Resin Optimization Study (Section 2). The data show that the T_g data for the composite are significantly lower than for the neat RS-14A panel.

Table 3.5.2.6-1. Comparison of RS-14A and T1000G/RS-14A DMA.

Specimen I.D.	Source	T_g (°F) G' Line-Fit	G" Peak	Tan Delta Peak
SR-0037	Composite cylinder	443	472	491
SR-0034PST	Composite cylinder	409	443	476
RX-33	Resin panel	504	515	542

It is interesting that the mechanical property data for these cylinders (Table 3.5.2-2) are reasonably high. Cylinder SR-0037 had the highest average ring tensile strength (673.1 ksi) of all of the process trials and a reasonably high interlaminar shear strength (9,526 psi). Yet, the T_g (G' line-fit intersection method) is only 228°C (442°F). The SR-0034PST cylinder which had a cumulative time of 16 hr at the 500°F postcure temperature actually had a *lower* T_g of 209°C (408°F) suggesting that the additional postcure cycles degraded the T_g of the composite.

Another interesting feature is that G" curves of both cylinders show a slight second peak in the vicinity 280° to 300°C which suggests an additional phenomena in this regime occurs. The second peak may signify further resin reaction at the higher temperature or a polymer relaxation mode. The precise source of this second peak is unknown at present.

The DMA results from the RS-14 and RS-14A thermal cycling trials (Tables 2.2.2.4-1 and 2.2.2.4-2, respectively) do not show a significant reduction in resin T_g associated with additional time at the postcure temperature, provided that the sample is maintained in an inert environment. It is speculated therefore that either (1) the carbon fiber sizing, or (2) moisture associated with the carbon fiber and/or its sizing may be responsible for the reduced T_g values in the composite. The sizing quantity is small and is 0.7 wt % of the carbon fiber according to Toray's lot certification data. However, the factors associated with the carbon fiber interface might be expected to play a larger

role in these higher fiber fraction (78–80 vol %) composite cylinders than for composite laminates made from prepreg (60–63 vol %).

The data in Tables 2.4.3.2-1 and 2.4.3.2-2 show that the tensile properties of panels cast from RS-14 and RS-14A resin that have been exposed to high humidity are relatively unaffected. Therefore, exposure to moisture during cure may not necessarily degrade the composite's mechanical properties.

The DSC and DMA data in Tables 2.4.3.1-2 and 2.4.3.2-2 show that in order to achieve comparable reductions in the neat RS-14A resin, cumulative humidity exposures >8 h at 50% or 4 hr at 70% relative humidity are required. In the case of these cylinders, the time from when wet-winding commenced to when the mandrel was sealed in the metal canopy and rolled into the oven was ~4 hr. The humidity levels measured in the laboratory area during wet-winding were 30% for the SR-0037 cylinder fabrication and 37% for the SR-0034PST cylinder fabrication.

The shear moduli at 25°C (77°F) are 0.85 Msi for the SR-0034PST cylinder and 0.79 Msi for the SR-0037 cylinder. These shear moduli are comparable to the shear modulus values for hoopwound carbon fiber/epoxy resin composites tested by DMA.

3.5.2.7 Composite Process Trials Summary

The combination of data collected as part of the Composite Process Trials Subtask indicate that conducting elevated temperature cure cycles in an inert environment primarily benefits the composite ring tensile strength. High(er) average tensile strengths with lower data scatter were achieved more frequently in these process trials than in previous studies in which the cure cycles were conducted in air. It is believed that the inert atmosphere cure minimizes potential resin degradation at the composite cylinder OD due to reaction of the cyanate ester resin with moisture and air at elevated temperatures. The highest average ring tensile strengths achieved with this method and for this lot of T1000G carbon fiber were on the order of 660 to 670 ksi, with several individual rings failing above 700 ksi. Based on these results, fiber strength translations of 89% are achievable with these methods and materials.

Conversely, the concave up transverse flexural strength data for cylinders cured in an inert atmosphere are, on average, comparable to the low(er) range of strengths measured for the composite cylinders cured in air. It is speculated that the blackened OD resin layer typical of polycyanate resin composites that are postcured in air may have had a somewhat higher modulus than comparable resin cured in an inert atmosphere. This reacted surface resin layer may have artificially biased higher the concave up transverse flexural strength values obtained in previous ORNL studies.

The data also show that (for the most part) there is a broad process envelope for curing composites with RS-14 and RS-14A resin. With some exceptions, equivalent ring tensile strengths and moduli, interlaminar shear strengths and transverse flexural strengths were obtained for composites cured using (1) a 280°F precure step prior to postcure; (2) a 380°F precure step prior to postcure, and (3) a cure cycle with no precure step in which the composite is ramped directly to the postcure temperature.

Similarly, the mechanical properties of T1000G carbon fiber composites wet-wound with RS-14A and RS-14 resin are equivalent. Composition data and photomicrographs confirm that high fiber fraction composites with low void levels are achievable with the RS-14A resin system. T1000G fiber wettability during wet-winding has therefore not been impaired by removal of the zirconate coupling agent.

The data do show a slight correlation between low(er) interlaminar shear strength and concave up transverse flexural strength values for composites cured (or thermally cycled) to the 280°F precure temperature prior to postcure. However, there are inconsistencies in these data. Therefore, at present there is no conclusive evidence that curing composites with a 280°F precure step prior to postcure is necessarily detrimental to the composite.

The data also show that (with some exceptions), equivalent ring tensile strengths and moduli, interlaminar shear strengths and transverse flexural strengths were obtained for composites thermally cycled (1) four times to the 280°F precure temperature prior to postcure; (2) four times to the 380°F precure temperature prior to postcure, and (3) four times to the 500°F postcure temperature.

The data do show that the concave up transverse flexural strengths were statistically lower for the cylinders that received (1) four precure cycles to 380°F followed by postcure and (2) four postcure cycles. In the majority of these cases, however the concave up transverse flexural strengths

for the thermally cycled cylinders are still higher than 10,600 psi. Inconsistencies in these data, too, make it difficult to state definitively that these process schedules are detrimental to the composite.

The most significant finding is that the T_g data for the composite are significantly lower than for the neat RS-14 and RS-14A resin. The evidence to date show no obvious explanation for this phenomena but the T_g reductions are suggestive of moisture contamination (hydrolysis) of the cyanate ester resin. The reason for the lower composite T_gs is currently under investigation.

3.6 Cure Process Selection

In Section 3.5, it was demonstrated that (for the most part) there is a fairly broad process envelope for curing composites that are wet-wound with RS-14 or RS-14A cyanate ester resin. This provides some process flexibility for the fabrication of thick, stage-cured composites. Based on these results, and the neat resin results in Section 2, the suggested process for the fabrication of thick composite rings and cylinders is similar to the baseline process used previously by ORNL[23] to fabricate thick cylinders, *with the exception that all curing be conducted in an inert atmosphere.*

The baseline process therefore is to wind nominal 1/4 in. wall thickness increments (stages) each day and precure each stage for 3 hr at 380°F. After the entire wall thickness has been wound and precured, the cylinder is then postcured on the mandrel for 4 hr at 500°F. The rationale for selecting this cure schedule is presented below.

The 380°F precure temperature is selected over the 280°F precure temperature for several reasons. The first is that there is lower risk of inadvertently undercuring the composite at the higher postcure temperature. This risk arises from the difficulty of maintaining an exact temperature set point in the composite wall thickness due to thermal lags and gradients associated with the heavy steel mandrel being heated under the metal canopy. Current estimates are that this set point can be maintained between ±10°F. The 280°F precure temperature is believed to be a minimum temperature for adequate gelation of the cyanate ester to occur. If the cure temperature were inadvertently lower than this by more than 10°F, the resin in the composite might not gel properly.

A second reason is based on DSC analyses of the heat of reaction associated with the precure step (Section 2.2.1). The data show that the measurable exothermic heat of reaction for an RS-14A sample that has been precured 3 hr at 380°F is between 2 to 9% of its original (non-precured) value.

By comparison, an RS-14A sample that has been precured 3 hr at 280°F still liberates 25 to 30% of its original heat. This residual heat may have significance for thick composite parts where transport mechanisms to conduct excess heat away from the composite are limited.

Finally, the data in Section 3.5.2 demonstrated that composite cured with a 380°F precure step followed by a 500°F postcure temperature yield good composite properties. The highest average ring tensile strength (673 ksi) was for a composite (SR-0037) that was cycled four times to the 380°F precure temperature prior to postcure. Although inconclusive, the data in Section 3.5.2 also showed a weak correlation between low(er) interlaminar shear strength and concave up transverse flexural strength values for composites cured (or thermally cycled) to the 280°F precure temperature prior to postcure.

The decision to postcure the entire cylinder wall thickness rather than each individual stage is based on the thermal cycling results of the neat RS-14 and RS-14A resin (Section 2.3). These results demonstrated that the RS-14 and RS-14A resin darken with continued exposure to elevated temperature, even when curing is conducted in an inert atmosphere. The change occurs to the bulk resin, as opposed to being a surface phenomena. Multiple postcure cycles to 510°F also produced slightly higher tensile and shear moduli and lower tensile elongations in the neat resin.

The results of Section 3.5 showed that multiple postcure cycles to 500°F did not degrade composite properties with the exception, (perhaps), of the concave up transverse flexural strength, which is a property that is dominated by the OD surface resin layer of the composite. The combination of neat resin and composite data therefore suggest that multiple postcure cycles to the inner stages of a thick composite cylinder might have an inadvertently adverse affect on the ***resin*** (and its composite) properties. Limiting the composite resin's exposure to the elevated postcure temperature is best accomplished by postcuring the entire cylinder wall thickness once.

3.7 B-basis Cylinder

The purpose of this activity was to determine the B-basis mechanical properties for a composite fabricated using the processes and materials that have been recommended for manufacturing T1000G/RS-14A composite. A summary of the composite fabrication procedure, evaluation and results are provided in the following sections.

3.7.1 Fabrication

The B-basis composite cylinder (SR-0039) was wet-wound on the 24 in. internally heated steel mandrel using T1000G fiber (Lot No. 615022) and RS-14A resin (YLA Reference No. FB5K176). The cylinder was hoopwound to a nominal 1/8 in. wall thickness using the wet-winding parameters described in Section 3.3.

After winding, the cylinder was cured in an inert atmosphere per the procedure described in Section 3.4. The cylinder was precured for 3 hr at 380°F and then postcured for 4 hr at 500°F which is per the cure process recommended for thick cylinder fabrications (Section 3.6).

This cylinder fabrication differed from the previous composite process trials conducted in this study in that the resin pot was shielded from the ambient air environment by the plexiglass box described in Section 2.4.5. The box (Figure 2.4.5-1) was purged with nitrogen gas continuously during the winding process to prevent contact of the hot cyanate ester resin with the ambient air. Measurements made with a hygrometer indicate that the box was effective at reducing the humidity level in the vicinity of the pot from the ambient 45 to 50% relative humidity level measured in the facility when the B-basis cylinder was fabricated to below the lower limit of the hygrometers measurement capability (25%). A separate measurement made using the Bacharach Oxor II oxygen deficiency monitor confirmed that the ambient air environment was reduced effectively by the nitrogen purge. Oxygen levels in the box were reduced from a nominal 21% (ambient conditions) to levels below 3%.

Samples were taken of the resin remaining in the pot after winding was completed as well as from the surface of the next-to-the last layer wound on the composite. These resin samples were evaluated by DSC analysis to determine the effects of the winding process on the resin properties.

The DSC analysis was performed using equipment and procedures described in Section 2.2.1. Nominal 10 mg resin samples were encapsulated in aluminum pans and placed in the DSC sample cell. The samples were ramped at 2°C/min from 25° to 260°C (500°F) and held at the upper temperature for 4 hr to cure the resin. The samples were then cooled to 25°C and retested at 5°C/min to determine the T_g of the resin.

The DSC results showed that the final T_g of the resin sample obtained from the wet-out pot was 270°C (518°F). The T_g of the resin sample wiped from the composite surface was slightly lower (263°C or 505°F). Both results are consistent with the DSC T_g data presented in Table 2.4.3.1-2 for RS-14A resin samples that have had minimal (30% or less) exposure to relative humidity.

3.7.2 Evaluation

The SR-0039 cylinder was cut into specimens and tested for ring tensile strength and modulus, interlaminar shear strength and transverse flexural strength using the procedures and test geometries described in Section 3.5.2. Testing was conducted at both 140° and 275°F. Interlaminar shear and transverse flexural strength testing was also performed at the ambient (~68°F) temperature for comparison. In addition to mechanical property tests, the SR-0039 cylinder was evaluated for composition and by DMA. The DMA results are presented in the next section.

Table 3.7.2-1 are the results of mechanical property and composition testing conducted on the SR-0039 cylinder. Averages and B-basis values were calculated using STAT17. The B-basis value shown is from the two-parameter weibull calculation.

A minimum of ten specimens was tested for each condition with the exception of the measurement of ring tensile modulus. That is because removing the extensometer from the split D fixtures at an intermediate load would have interfered with the temperature in the test chamber. (It is necessary to remove the extensometer from the split D fixtures prior to the ultimate break load so that it is not destroyed when the ring fails.) Instead, three to four rings were tested with an extensometer to 12,000 lb (~205 ksi ring tensile stress) to generate a load-deflection curve. The rings were then unloaded and the chamber was opened to remove the extensometer. The chamber was then resealed and brought back to temperature. At that point, the rings were taken to failure. The strength data from ring specimens tested using this procedure showed that this did not affect the ultimate strength of the composite.

The average ring tensile strength of the SR-0039 cylinder at 140°F is 653.9 ksi with a 2.2% coefficient of variation. This value is comparable to the room temperature ring tensile strengths measured for other T1000G/RS-14A cylinders (Table 3.5.2-2) in this study and indicates no appreciable change in this property at 140°F. The B-basis value for this set is 613.9 ksi. At 275°F,

Table 3.7.2-1. T1000G/RS-14A composite properties of SR-0039 cylinder.

Test Temperature	68°F		140°F		275°F	
STAT17 Result	Average	B* Value	Average	B* Value	Average	B* Value
Ring Tensile						
Strength (ksi)	NA	NA	653.9 (2.2)	613.9	615.3 (1.4)	587.6
Modulus (Msi)	NA	NA	32.5	NA	32.5	NA
SBS Strength (psi)	8,318 (4.7)	7,397	8,223 (4.3)	7,207	7,389 (4.4)	6,488
Transverse Flex. Strength						
Concave Up (psi)	10,906 (5.3)	9,127	10,065 (5.1)	8,756	9,500 (6.0)	8,003
Concave Down (psi)	6,490 (10.1)	4,878	6,510 (8.7)	4,800	5,797 (11.2)	3,930
Composition						
Density (gm/cm3)	1.6574	NA	1.6574	NA	1.6574	NA
Volume % Fiber	78.6	NA	78.6	NA	78.6	NA
Volume % Resin	20.9	NA	20.9	NA	20.9	NA
Volume % Voids	0.5	NA	0.5	NA	0.5	NA

Number of specimens is 10 minimum for ring tensile strength, SBS strength and transverse flexural strength.
Number of specimens is 3-4 for ring tensile modulus.

*** B value is from two-parameter weibull calculation.**
( ) Number in parentheses is percent coefficient of variation.
NA - Not available

the average ring tensile strength decreases by 6% to 615.3 ksi with a 1.4% coefficient of variation. There is an extremely small amount of data scatter in this set of rings. The B-basis value is 587.6 ksi.

The average ring tensile moduli at 140° and 275°F are 32.5 Msi, which is comparable to the room temperature ring tensile moduli measured for the other T1000G/RS-14A cylinders in this study. This is as expected because ring tensile modulus is a fiber dominated property and should not change appreciably with temperature.

The average interlaminar shear strength of the SR-0039 cylinder at room temperature is 8,318 psi, which is among the lower values measured in this study. At 140°F, the shear strength is statistically unchanged (based on a STAT17 analysis) and is 8,223 psi with a B-basis value of 7,207 psi. At 275°F, the average interlaminar shear strength is reduced by 11% from its room temperature level to 7,389 psi and has a B-basis value of 6,488 psi.

The average concave up transverse flexural strength of the SR-0039 cylinder at room temperature is 10,906 psi, which is in the mid-range of values measured in this study. At 140°F, the strength is reduced by 8% to 10,065 psi with a B-basis value of 8,756 psi. At 275°F, the average concave up transverse flexural strength is reduced by 13% from its room temperature level to 9,500 psi and has a B-basis value of 8,003 psi.

The average concave down transverse flexural strength of the SR-0039 cylinder at room temperature is 6,490 psi, which is the lowest value measured in this study. The reason for the low room temperature strength is unknown. There is a high degree of data scatter associated with the concave down transverse flexural strength measurement and the percent coefficient of variation for the room temperature data set is 10.1%. This scatter may be caused by machining flaws and variations in the resin layer thickness at the cylinder ID.

At 140°F, the average concave down transverse flexural strength is statistically unchanged (based on a STAT17 analysis) and is 6,510 psi with a B-basis value of 4,800 psi. At 275°F, the average strength is reduced by 11% from its room temperature level to 5,797 psi and has a B-basis value of 3,930 psi.

3.7.3 DMA

Figure 3.7.3-1 are the DMA results for a specimen cut from the SR-0039 composite cylinders. The specimen and test methodology are comparable to those described in Section 3.5.2.6. The data show that the T_g as calculated by the G' line-fit intersection method (441°F) is lower than that of the neat RS-14A resin and comparable to the 443°F T_g measured for cylinder SR-0037 (Table 3.5.2.6-1).

Additional DMA specimens were cut from the SR-0039 cylinder and given an additional 4 hr postcure at 500°F to determine if the T_g could be increased with additional cure time. (The rationale was that perhaps the composite resin was undercured due to a thermal lag associated with the thick steel mandrel). The cure was conducted in an autoclave under a nitrogen environment using procedures comparable to those used to cure the RS-14 and RS-14A resin panels. After the additional postcure, the composite OD was a darker brown color (but not black) indicating that the composite resin had changed slightly with the additional postcure cycle. This color change was similar to that observed with neat RS-14 and RS-14A resin panels that were given additional postcure cycles as part of the resin thermal cycling study.

Figure 3.7.3-2 are the DMA results for one specimen (SR-0039PST) that received a second postcure cycle. The results show that the T_g (415°F) is lower than for the specimen which was postcured once on the mandrel. The results are summarized in Table 3.7.3-1 and suggest that (1) the composite was not undercured during its initial cure cycle on the steel mandrel, and (2) the additional time at the postcure temperature may foster a degradation mechanism in the composite.

Table 3.7.3-1. DMA of SR-0039 composite cylinder.

Specimen I.D.	G' @ 77°F (Msi)	T_g (°F) G' Line-Fit	G" Peak	Tan Delta Peak
SR-0039*	0.94	441	466	488
SR-0039PST**	0.87	415	442	468

*SR-0039 cylinder precured 3 hours @ 380°F and postcured 4 hours @ 500°F.

**SR-0039PST is a section of SR-0039 composite that has been given a second posture of 4 hours @ 500°F.

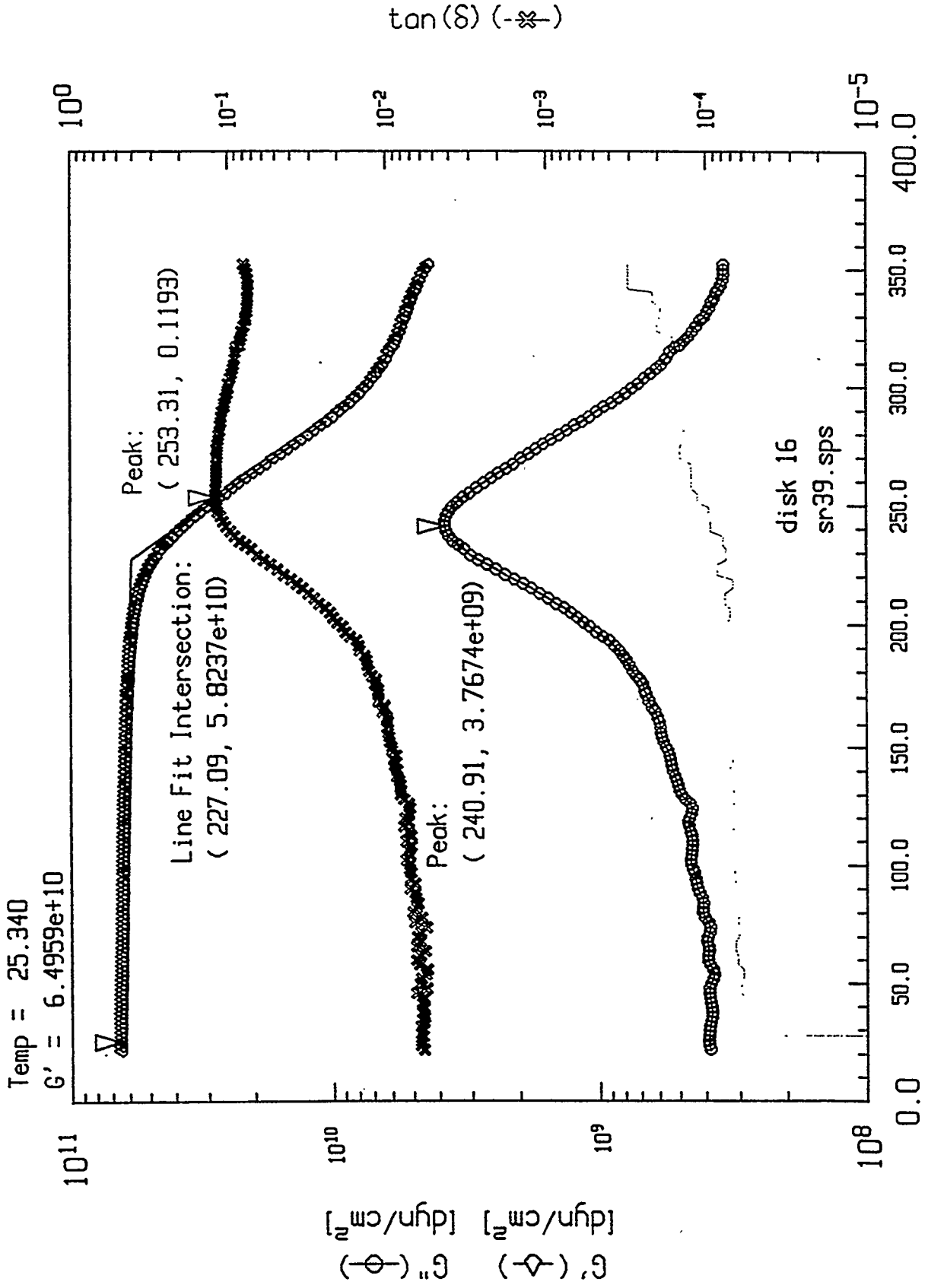

Figure 3.7.3-1. DMA plots for SR-0039.

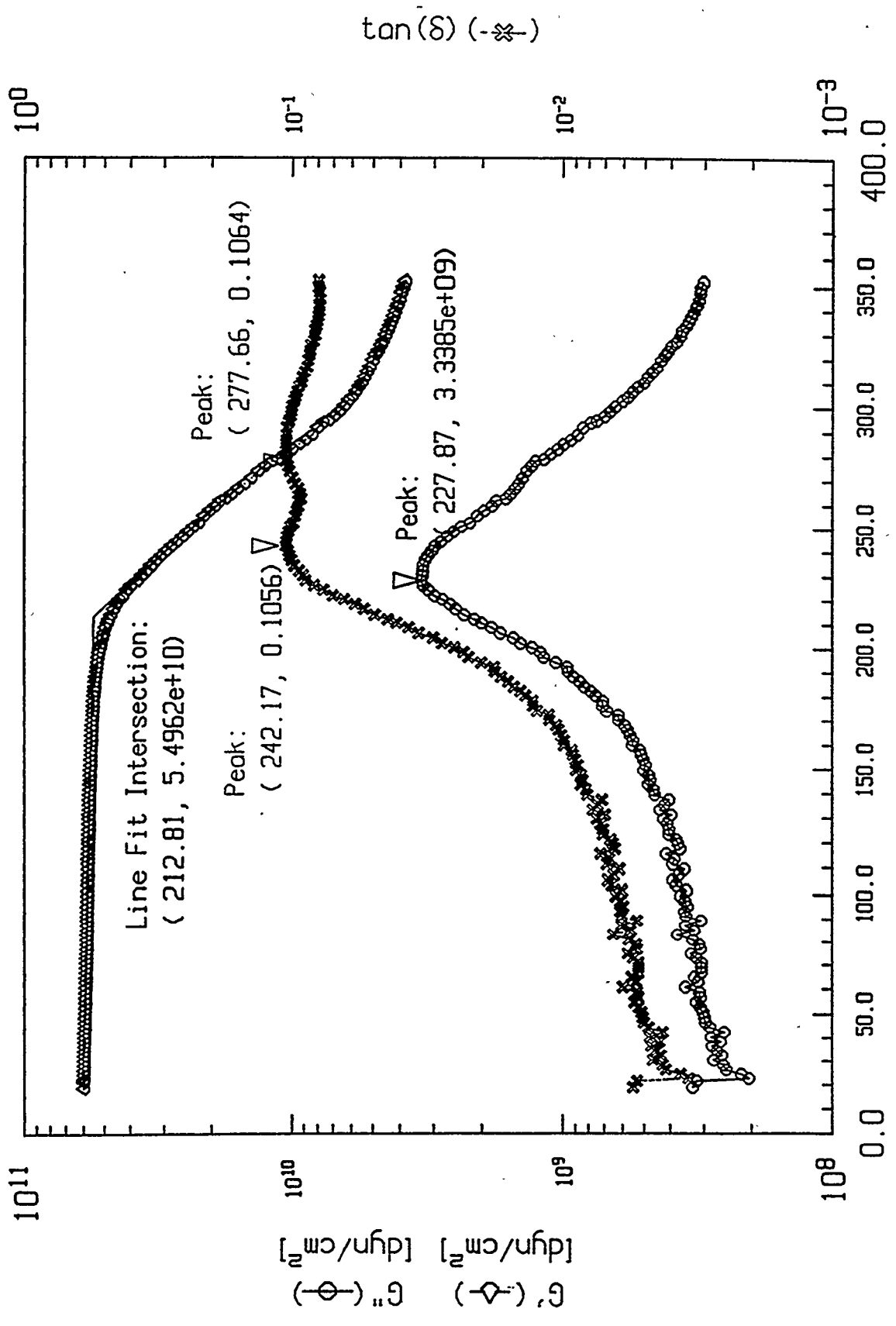

Figure 3.7.3-2. DMA plots for SR-0039PST.

Another interesting phenomena is that the SR-0039PST specimen that was postcured twice developed a second peak in the vicinity 270° to 300°C that was not apparent in the original SR-0039 composite. This peak may correspond to a polymer relaxation mode but at present its precise source has not been identified.

The shear modulus at 25°C (77°F) of the SR-0039 composite specimen tested after the initial cure was 0.94 Msi. The shear modulus was 0.87 Msi for the specimen given a second postcure cycle. There is insufficient data to determine whether the difference in the two measurements is significant for this type of specimen and test.

4. T1000G/RS-14 DEMONSTRATION CYLINDER FABRICATION

The objective of this activity was the fabrication of a nominal 1 in. thick hoopwound T1000G/RS-14 cylinder using the process described in Section 3.6 and with all composite precure and postcure operations performed in an inert atmosphere environment. This section describes the fabrication and cure of this cylinder.

4.1 Fabrication Parameters

The demonstration cylinder was wet-wound on an internally heated steel mandrel comparable in design to the process trial mandrel described in Section 3.2, with the exception that the mandrel OD was nominally 14 in. The cylinder was wet-wound using T1000G fiber (Lot No. 615111) and RS-14* resin (YLA Reference No. FB3K265).

The 1 in.-thick cylinder was wound in nominal 1/4 in.-thick stages per day over a 4-day period. Each stage took ~4 hr to complete before the mandrel could be moved from the winding machine to the oven. To minimize the potential for carbamate formation from exposure of the resin to ambient humidity in the vicinity of the winding machine, winding was accomplished on days when the relative humidity in the laboratory was 40% or less.

As in previous ORNL T1000G/RS-14 composite fabrications, the pot temperature was maintained between 175°–180° F and the fiber tension was 12 lb. Every layer was compacted and wiped during winding. An additional two compaction passes with wiping were also applied after every five-layer winding increment.

The internal heaters of the mandrel were used to maintain the mandrel OD surface temperature between 170°–180° F. The composite surface temperature was also maintained between 170°–180°F. As the winding progressed, the thickening composite acted as an insulation layer and an external strip heater was required to maintain the composite surface temperature.

---

*RS-14A resin was under evaluation at the time of this activity and was therefore not selected to fabricate the demonstration cylinder.

The last carbon fiber layers wound on the first, second, and third stages were wiped dry prior to moving the mandrel to the oven for precure. The purpose was to remove excess resin so that there would not be an excessively thick resin layer between the composite stages after cure. Excess resin that bled out during the precure was sanded to roughen the surface and degreased with acetone prior to winding the next stage. The last layer of the fourth and final stage was left slightly resin rich to protect the carbon fiber at the OD of the composite.

4.2 Cure Schedule

After the completion of each 1/4 in.-thick stage, the mandrel was moved from the winding machine to the rotisserie cart and sealed within the metal canopy. The canopy was purged with nitrogen gas and the mandrel temperature was raised to 380°F at ~0.5-1°F/min and held at that temperature for 3 hr to complete the precure.

After the precure of the fourth and final stage, the mandrel was allowed to return to ambient temperature and the seal of the metal can was inspected to ensure that there would be no air leakage into the canopy during the elevated temperature postcure. Following inspection, the canopy was purged with nitrogen gas and the mandrel temperature was raised to 500°F at ~0.5-1°F/min and held at that temperature for 4 hr to complete the postcure of the composite.

Oxygen levels were measured with an oxygen analyzer during the 500°F portion of the cure cycle and ranged between 1 to 2%. The outer resin layer of the composite cylinder was examined visually and had a brown tint instead of the dark black color typical of cylinders that have been postcured in air. This information suggests that the process used to fabricate the T1000G/RS-14 demonstration cylinder was successful at preventing resin surface oxidation during the cure cycle.

4.3 Demonstration Cylinder DMA

Figure 4.3-1 are the DMA results for a specimen cut from the T1000G/RS-14 demonstration cylinder. The test methodology is the same procedure described in Section 3.5.2.6. The torsion rectangular geometry specimen was cut with the 1.75 in.-long axis of the specimen corresponding

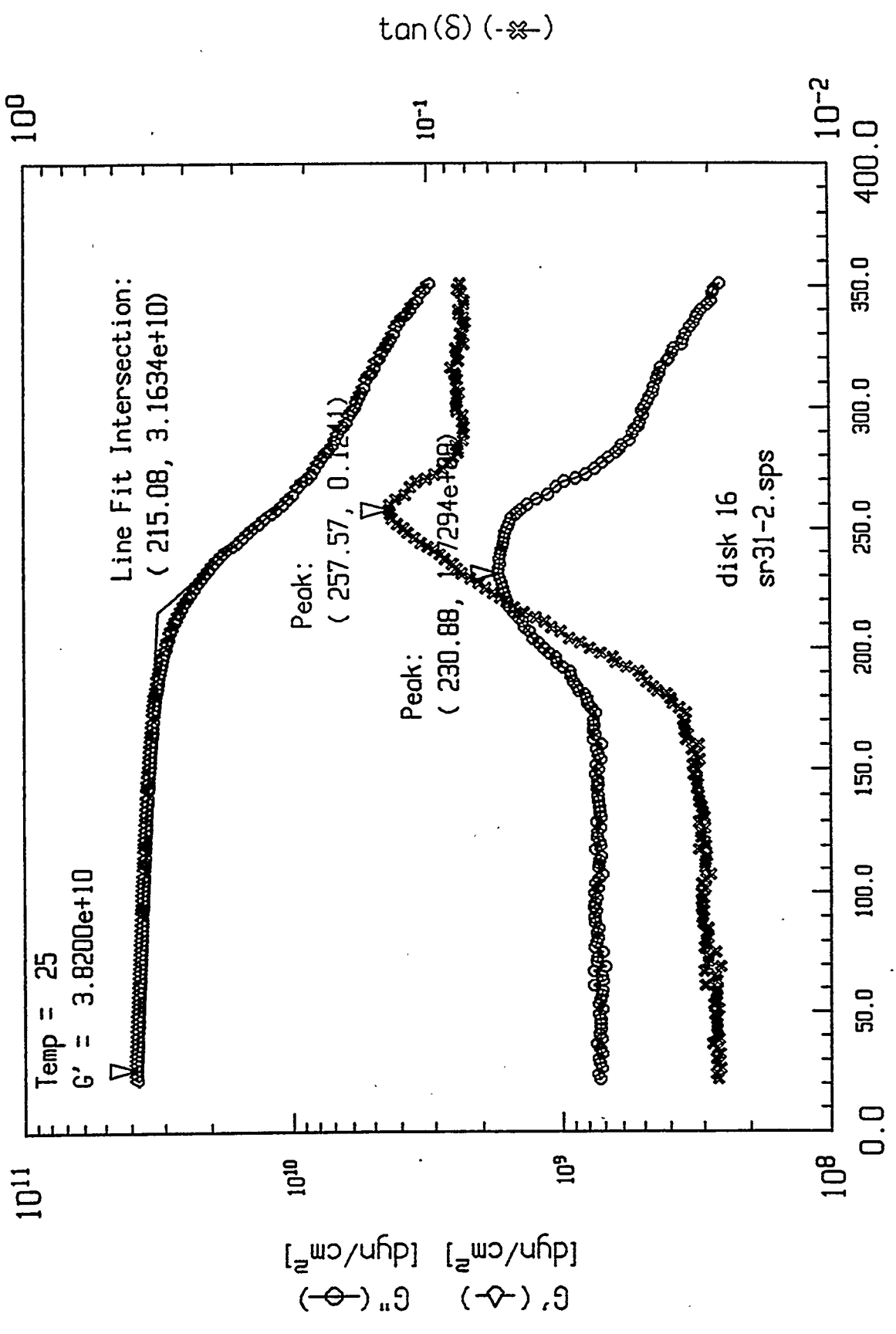

Figure 4.3-1. DMA plots for T1000G/RS-14 demonstration cylinder.

to the axial length (z-direction) of the cylinder and the 0.5 in. width corresponding to the circumferential (theta-direction). The 0.125 in. specimen thickness corresponds to the radial (r-direction). The specimen was taken near the middle of the cylinder wall thickness and is comprised mainly of composite from the first and second stages. This specimen was cut with flat (non-curved) surfaces.

The data show that the T_g as calculated by the G' line-fit intersection method (419°F) is similar to that obtained from the other composite DMA measurements and is also lower than the T_g of the neat RS-14 resin. The shear modulus at 25°C (77°F) is 0.55 Msi which is substantially lower than the DMA shear modulus measured for other composite specimens. The reason for the low shear modulus value is unknown at present but may be related to the sample geometry because of the way the specimen was cut.

5. CONCLUSIONS

This study has shown that a cyanate ester resin can be wet-filament wound with carbon fiber to produce high-strength hoop-wound composites. Optimum mechanical and thermal properties are achievable when the manufacturing and cure environments are controlled. The following is a summary of the conclusions from the RS-14/RS-14A resin optimization study, composite process trials and the T1000G/RS-14 demonstration cylinder fabrication sections of this report.

The process envelope for obtaining equivalent cured RS-14 and RS-14A resin properties is flexible. Comparable mechanical properties were obtained for RS-14 resin cured with (1) either a 380° or a 280°F precure step prior to postcure, (2) a cure cycle with no precure step that ramps directly to the postcure temperature, and (3) either a 480°F or a 510°F postcure temperature.

The precure temperature (or lack of a precure step) as well as the heatup (ramp) rate to the cure temperature also have no effect on the RS-14 resin ultimate T_g. Similarly, postcure cycles of either 4 hr at 480° or 510°F yield equivalent T_gs for the RS-14 resin. The long (4 hr) thermal soak is believed to provide time for the resin to reach a comparable degree of cure at the lower postcure temperature.

DSC analyses showed that the measurable exothermic heat of reaction for an RS-14A sample that has been precured 3 hr at 380°F is between 2 to 9% of its original (non-precured) value. By comparison, an RS-14A sample that has been precured 3 hr at 280°F still liberates 25 to 30% of its original heat.

Evaluations of RS-14 and RS-14A neat resin showed that their mechanical and physical properties are equivalent. The tensile strength is in the range of 11.7 to 13.0 ksi with elongations at failure between 4.1 to 5.8%. The tensile modulus ranges between 377 to 406 ksi. The room temperature shear modulus (G') is on the order of 150 to 165 ksi. The RS-14 and RS-14A cured resin density is 1.20 g/cm^3.

The RS-14 and RS-14A resin lots evaluated for this study did show an unexpected and significant difference in T_g between the two materials. The RS-14 resin T_g (G' line-fit method) is 470° to 490°F when postcured for 4 h between 480° to 510°F. The RS-14A resin T_g is higher and ~505°F. It is not known whether this difference is due to normal batch-to-batch variability for these

materials or because the RS-14 came from an older lot of resin. Removal of the zirconate coupling agent from the resin formulation may also have had an effect on the RS-14A resin's T_g.

RS-14 and RS-14A resin properties are affected by the presence of ambient air during the elevated temperature portions of the cure cycle. RS-14 resin specimens cycled four times to the 380°F precure temperature in air prior to postcure had tensile strengths that were only 60% of the tensile strength of the non-thermally cycled specimens. The reduction is attributed to degradation of the resin surface layer when exposed to air and humidity at the 380°F precure temperature. The specimens also had slightly elevated tensile and shear moduli, suggesting that the degraded surface resin has a significantly higher modulus than the bulk resin. The T_g of these specimens was roughly 20°F lower than the range of T_g values measured for non-thermally cycled RS-14 resin. The T_g reduction is attributed to degradation of the resin surface layer when contacted with air and humidity at the 380°F precure temperature.

The T_g, tensile strength, modulus and percent elongation of RS-14A resin specimens that were cycled four times to the 280°F precure temperature in air prior to postcure were not substantially different from those of the non-thermally cycled specimens. Surface resin degradation as a function of the cyanate ester resin reacting with air and humidity either does not occur at this low a temperature or occurs at too slow a rate to be significant for these exposure times.

It was also observed that RS-14 and RS-14A resin panels exhibit significant darkening of the bulk resin with multiple postcure cycles to 510°F, even when testing is performed in a nitrogen (inert) environment. The darkness goes all the way through the panel thickness, indicating that the color change is caused by temperature rather than by reaction with the ambient atmosphere. Panels that cycled multiple times to the 480°F postcure temperature in nitrogen also show darkening of the resin with each cure cycle but to a much lesser degree than samples cycled to 510°F. The chemical basis for the color change is unknown at this time.

However, no change in the tensile strength was observed for RS-14 and/or RS-14A resin specimens that were cycled four times to 510°F in nitrogen; four times to 480°F in nitrogen; and cycled four times to the 380°F precure temperature in nitrogen prior to postcure. The tensile moduli of RS-14 panels that were thermally cycled at either the precure temperature or postcure temperature tended to be slightly higher than their non-thermally cycled counterparts. The average percent

elongation at failure for panels cycled four times to 510°F in nitrogen was also slightly lower.

The combination of results from the moisture preconditioning study indicate that the most significant effect from exposure to ambient humidity is depression of the resin T_g after postcure. The analyses of preconditioned RS-14A resin indicates that the cyanate ester resin is susceptible to moisture at the 175°F temperature for exposure levels as low as 8 hr at 30% relative humidity. More significant T_g reductions were encountered at exposures >4 hr at 40% relative humidity for the RS–14A resin system and at exposures >2 hr at 40% relative humidity for the RS-14 resin.

RS-14 and RS-14A resin are similarly affected by moisture exposure prior to cure indicating that the removal of the zirconate coupling agent has not affected (improved) the moisture resistance of the uncured cyanate ester resin. Resin tensile properties are largely unaffected, provided that excessive bubbles or voids are not produced in the resin panels during postcure as a result of carbamate decomposition.

The preliminary data indicate that cured RS-14 resin can be subject to chemical degradation when exposed for long periods to elevated temperature in an air environment. The result is a brittle, black material on the outside surface that has a significantly lower T_g, higher modulus and higher density. This reacted resin layer has a significantly low(er) ductility and promotes premature failure in tensile specimens. Heating above the resin T_g causes the reacted surface layer to decompose into at least one gaseous product, believed to be CO_2, a known by-product from the decomposition of carbamates.

The evidence from this study also suggests that this surface layer is permeable and that continued reaction with the ambient environment will continue, causing the reacted resin thickness to grow deeper into the cyanate ester resin substrate with time. These phenomena were observed for a RS-14 resin panel that was postcured in an air environment. These results require validation using resin panels that are first postcured in an inert atmosphere and to the maximum level of cyanate group conversion. This is to ensure that the reacted resin layer is not the result of a reaction of the ambient air and moisture with free cyanate groups or the products of free cyanate groups (carbamates) with ambient moisture.

The results of the composite process trials show that conducting elevated temperature composite cure cycles in an inert environment primarily benefits the ring (hoop) tensile strength.

High(er) ring tensile strengths with lower data scatter were achieved more frequently in this study than in previous fabrications in which the cure cycles were conducted in air. It is believed that the inert atmosphere cures minimizes potential resin degradation at the composite cylinder OD due to reaction of the cyanate ester resin with moisture and air at elevated temperatures. The highest average ring tensile strengths achieved in this study were on the order of 660 to 670 ksi, with several individual rings failing above 700 ksi. Based on these results, T1000G fiber strength translations of 89% are achievable with these methods and materials.

Conversely, the concave up transverse flexural strength data for cylinders cured in an inert atmosphere are comparable to the low(er) range of strengths measured for the composite cylinders cured in air. It is speculated that the blackened OD resin layer typical of polycyanate resin composites that are postcured in air may have had a somewhat higher modulus than comparable resin cured in an inert atmosphere. This reacted surface resin layer may have artificially biased higher the concave up transverse flexural strength values in previous studies.

Similarly to the neat resin results, there is a broad process envelope for curing composites with RS-14 and RS-14A resin. Equivalent ring tensile strengths and moduli, interlaminar shear strengths and transverse flexural strengths were obtained for composites cured using (1) a 280°F precure step prior to postcure; (2) a 380°F precure step prior to postcure, and (3) a cure cycle with no precure step in which the composite is ramped directly to the postcure temperature. The mechanical properties of T1000G carbon fiber composites wet-wound with RS-14A and RS-14 resin are also equivalent. T1000G fiber wettability during wet-winding has not been impaired by removal of the zirconate coupling agent.

Equivalent ring tensile strengths and moduli, interlaminar shear strengths and transverse flexural strengths were obtained for composites thermally cycled (1) four times to the 280°F precure temperature prior to postcure; (2) four times to the 380°F precure temperature prior to postcure; and (3) four times to the 500°F postcure temperature.The majority of the concave up transverse flexural strengths were statistically lower for the cylinders that received (1) four precure cycles to 380°F followed by postcure and (2) four postcure cycles. However, the strengths of these thermally cycled cylinders are still higher than 10,600 psi.

One key finding is that the T_g values for the composite are significantly lower (~440°F, or less) than for the neat RS-14 and RS-14A resin. It is speculated that either (1) the carbon fiber sizing or (2) moisture associated with the carbon fiber and/or its sizing may be responsible for the reduced T_g values in the composite. The T_g reductions are suggestive of moisture contamination (hydrolysis) of the cyanate ester resin.

The average ring tensile strength of a T1000G/RS-14A cylinder tested at 140°F was 653.9 ksi and is comparable to the room temperature ring tensile strengths of other T1000G/RS-14A cylinders in this study. The B-basis value (two-parameter Weibull calculation) for this set was 613.9 ksi. At 275°F, the average ring tensile strength decreased by 6% to 615.3 ksi with a B-basis value of 587.6 ksi. The average ring tensile moduli of a T1000G/RS-14A cylinder tested at 140° and 275°F are 32.5 Msi, which is comparable to the room temperature ring tensile moduli measured for the other cylinders in this study.

At 140°F, the shear strength of a T1000G/RS-14A cylinder was not statistically different from its room temperature strength and was 8,223 psi with a B-basis value of 7,207 psi. At 275°F, the shear strength was reduced by 11% to 7,389 psi and had a B-basis value of 6,488 psi.

With respect to flexural strength data, the average concave up transverse flexural strength of a T1000G/RS-14A cylinder at 140°F was reduced by 8% from its room temperature level to 10,065 psi with a B-basis value of 8,756 psi. At 275°F, the reduction was 13% from its room temperature value to 9,500 psi with a B-basis value of 8,003 psi. The average concave down transverse flexural strength at 140°F, on the other hand, was statistically unchanged from its room temperature strength and was 6,510 psi with a B-basis value of 4,800 psi. At 275°F, the reduction as 11% from its room temperature level to 5,797 psi with a B-basis value of 3,930 psi.

6. RECOMMENDATIONS

The following is a summary of the recommendations from the RS-14/RS-14A resin optimization study, composite process trials and the thick T1000G/RS-14 demonstration cylinder fabrication sections of this report.

The combination of neat resin and composite process trial data compiled in this study indicate that the properties of both RS-14 and RS-14A cyanate ester resins are sensitive to the process and cure environment. It is recommended that the cure of RS-14A resin and its composites be conducted in an inert atmosphere. (Precuring at temperatures up to 280°F in air ***may*** be permissable provided that the curing environment is dry and the total exposure time is limited.)

Similarly, processing of RS-14A should be conducted in a dry environment. Practical humidity exposure limits for the RS-14 and RS-14A resins at the 175°F wet-winding process temperature are recommended to be 8 hr maximum at 30% relative humidity or 4 hr maximum at 40% relative humidity. The susceptibility of the cyanate ester resin to degradation as a result of contact with ambient humidity indicates that the resin pot should be maintained in as dry an environment as possible. Use of the nitrogen-purged, plexiglass housing to shield the pot from ambient humidity is therefore recommended for future wet-winding operations with cyanate ester resins.

It is recommended that additional studies be conducted on the long-term physical aging behavior of RS-14/RS-14A resin to determine the effects on such resin and composite properties as creep resistance, modulus and density. The test specimens should be cured in an inert atmosphere and to the maximum level of cyanate group conversion to prevent surface degradation due to contact with air and moisture. All elevated temperature testing should be conducted in an inert atmosphere as well to prevent chemical degradation of the surface. Doing this will make it possible to study the effects of physical aging on RS-14 and RS-14A resin separately from the effects of chemical degradation.

Until further studies are performed to validate/confirm the resin surface degradation phenomena that arises from long-term exposure to air at elevated temperature, it is recommended

that RS-14A cyanate ester resin and its composites be maintained in either a vacuum or inert environment when exposed for prolonged periods to elevated temperatures.

The fabrication process recommended for fabricating thick hoopwound composite cylinders with T1000G/RS-14A resin consists of winding nominal 1/4 in. wall thickness increments (stages) each day followed by precuring each stage for 3 hr at 380°F. After the entire wall thickness has been wound and precured, the cylinder is then postcured on the mandrel for 4 hr at 500°F. All precure and postcure operations are to be conducted in an inert atmosphere.

It is recommended that additional studies be conducted to determine the reason(s) for the low(er) T_g values measured for T1000G composites that are wet-wound and cured with the RS-14 and RS-14A resin systems.

7. ACKNOWLEDGEMENTS

The author wishes to acknowledge and thank D. Skidmore and K. D. Yarborough for fabricating the composite specimens and for their contributions to the composite process development and equipment modifications described in this report; C. L. Knaff for performing the neat resin characterization, sample preparation and testing; T. White and C. H. Linginfelter of the General Manufacturing Division for machining the composite specimens; A. R. Ellis and D. C. Howard of the Technical Division for preparation of the humidity-exposed resin samples and for providing the composite specimen test data; C. A. Willis and J. D. Brown of the Development Division for their contributions to the DSC and DMA analyses; W. L. Bolinger of the Analytical Services Organization for performing the SEM/EDX analyses; and to J. R. Phillips for editing, preparation and distribution of this report. Special thanks and appreciation are also extended to S. M. Robitaille of YLA Incorporated for providing all of the FTIR analyses performed as part of this study as well as for sharing her considerable knowledge and experience with polycyanate resins.

8. REFERENCES

1. Frame, B. J. and Starbuck, J. M., "Preliminary Investigation of Polycyanate Resins for Wet-Filament Wound High-Strength Composites," *41st International SAMPE Symposium* (1996).

2. Frame, B. J., "Processess Study of Polycyanate Resin for Wet-Filament Wound High-Strength Composites," ORNL/TM-13387, Oak Ridge, Tennessee (1997).

3. Bauer, M. and Bauer, J., "Aspects of the Kinetics, Modeling and Simulation of Network Build-Up During Cyanate Ester Cure," from *Chemistry and Technology of Cyanate Ester Resins*, edited by I. Hamerton, Chapman, & Hall, New York, 1994.

4. Snow, A. W., "The Synthesis, Manufacture and Characterization of Cyanate Ester Monomers," from *Chemistry and Technology of Cyanate Ester Resins*, edited by I. Hamerton, Chapman, & Hall, New York, 1994.

5. Shimp, D. A., Christenson, J. R., and Ising, S. J., "Cyanate Esters – An Emerging Family of Versatile Composite Resins,"*34th International SAMPE Symposium* (May 8–11, 1989).

6. Bauer, M., Bauer, J., and Kuhn, G., *Acta Polym.*, **37**, 715 (1986).

7. Bauer, M., Thesis, *Academy of Sciences of the GDR, Berlin* (1986).

8. Alla, C., Thesis, Paris; further publication in preparation.

9. Shimp, D. A. and Ising, S. J., "Moisture Effects and Their Control in the Curing of Polycyanate Resins," ASC National Meeting, PMSE Division, San Francisco, April 1992.

10. Pascault, J., Galy, J., and Mechin, F., "Additives and Modifiers," from *Chemistry and Technology of Cyanate Ester Resins*, edited by I. Hamerton, Chapman ,& Hall, New York, 1994.

11. Rodriguez, F., *Principles of Polymer Systems*, McGraw Hill Book Company, 1970.

12. L. C. E. Stuik, "Physical Aging in Plastics and Other Glassy Materials," *Polym. Eng. Sci.*, **17** (1977).

13. Ising, S. J., Shimp, D. A., and Christenson, J. R., "Cyanate Cure Behavior and the Effect on Physical and Performance Properties," *3rd International SAMPE Electronics Conference,* (June 20–22, 1989).

14. Lee, Stuart M. (editor), *International Encyclopedia of Composites*, VCH Publishers Incorporated, New York, 1990.

15. Wang, J. Z, et al., "Studies on the Physical Aging Behavior of Cyanate Ester Resin and it Graphite Resin Compositess," *Reliability, Stress Analysis, and Failure Prevention Aspects of Composite and Active Materials,* DE-Vol. 79, ASME, 1994.

16. Wang, J. Z., et al., "Physical Aging Behavior of High-Performance Composites," C*omposite Science and Technology*, **54** (1995).

17. Parvatareddy, H., et al., "Environmental Aging of High-Performance Polymeric Composites: Effects on Durability," *Composite Science and Technology*, **53** (1995).

18. Hahn, D., et al., "Examination of Physical Aging on the Viscoelastic Properties of Cyanate Esters," *Polymeric Materials Science & Engineering, Polymeric Materials Science & Engineering,* ACS, Washington, D.C., Vol. 69 (1993).

19. Simon, S. L. and Gillham, J. K., "Physical Aging of a Dicyanate Ester/Polycyanurate Material," *Polymeric Materials Science & Engineering*, ACS, Washington, D.C., Vol. 66, (1992).

20. Simon, S. L. and Gillham, J. K., "Effects of Conversion and Temperature on the Physical Annealing of a high-Tg Dicyanate Ester/Polycyanurate Material," *Polymeric Materials Science & Engineering,* ACS, Washington, D.C., Vol. 63 (1990).

21. Shimp, D. A., Ising, S. J., and Christenson, J. R., "Cyanate Esters – A New Family of High Temperature Thermosetting Resins," *High Technology Conference on High Temperature Polymers and Their Uses*, (October 2–4, 1989).

22. *AROCY® Cyanate Ester Resins: Chemistry, Properties, and Applications,* Ciba Geigy Corporation Polymers Division, Hawthorne, New York.

23. Frame, B. J. and Dodge, W. G., "Wet-Filament Winding Fabrication of Thick Carbon Fiber/Polycyanate Resin Composite," ORNL-6917, Oak Ridge, Tennessee (June 1997).

Appendix A.1

FTIR ANALYSES OF RS-14 AND RS-14A RESIN

FTIR analyses were performed by YLA Incorporated using a Perkin Elmer Spectrum 1000 FTIR spectrophotometer with a zinc selenide sample trough. For all analyses, the sample compartment was purged with nitrogen and a minimum of 16 scans were used to collect sample and/or background data between 650 to 4000 cm^{-1}. The scans are the results of the sample scans after subtraction of the background baseline.

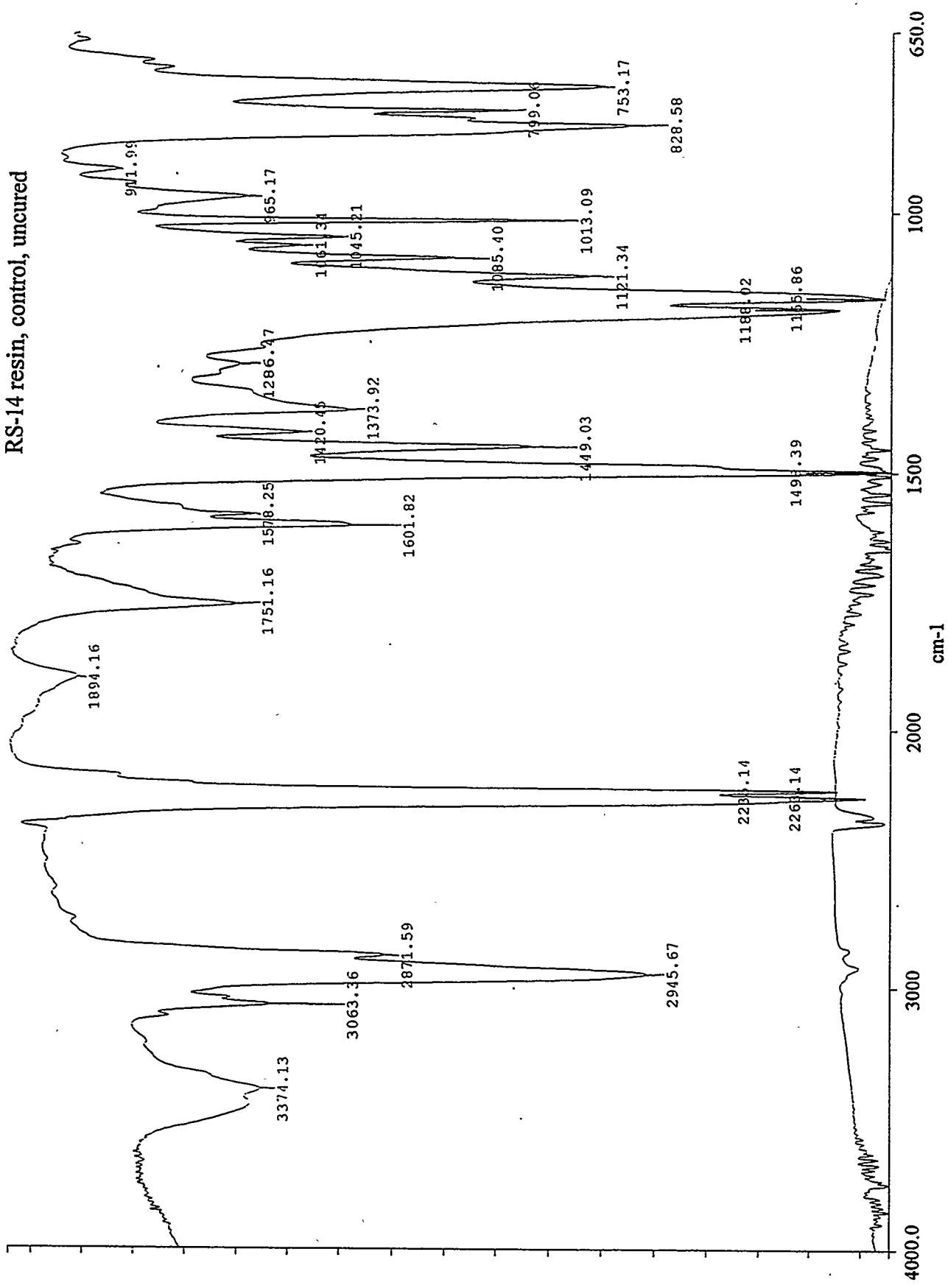
RS-14 resin, control, uncured
4000.0
3000
2000
1500
1000
650.0
cm-1
3374.13
3063.36
2871.59
2945.67
1894.16
1751.16
1578.25
1601.82
1449.03
1373.92
1286.47
1121.34
1013.09
828.58
753.17

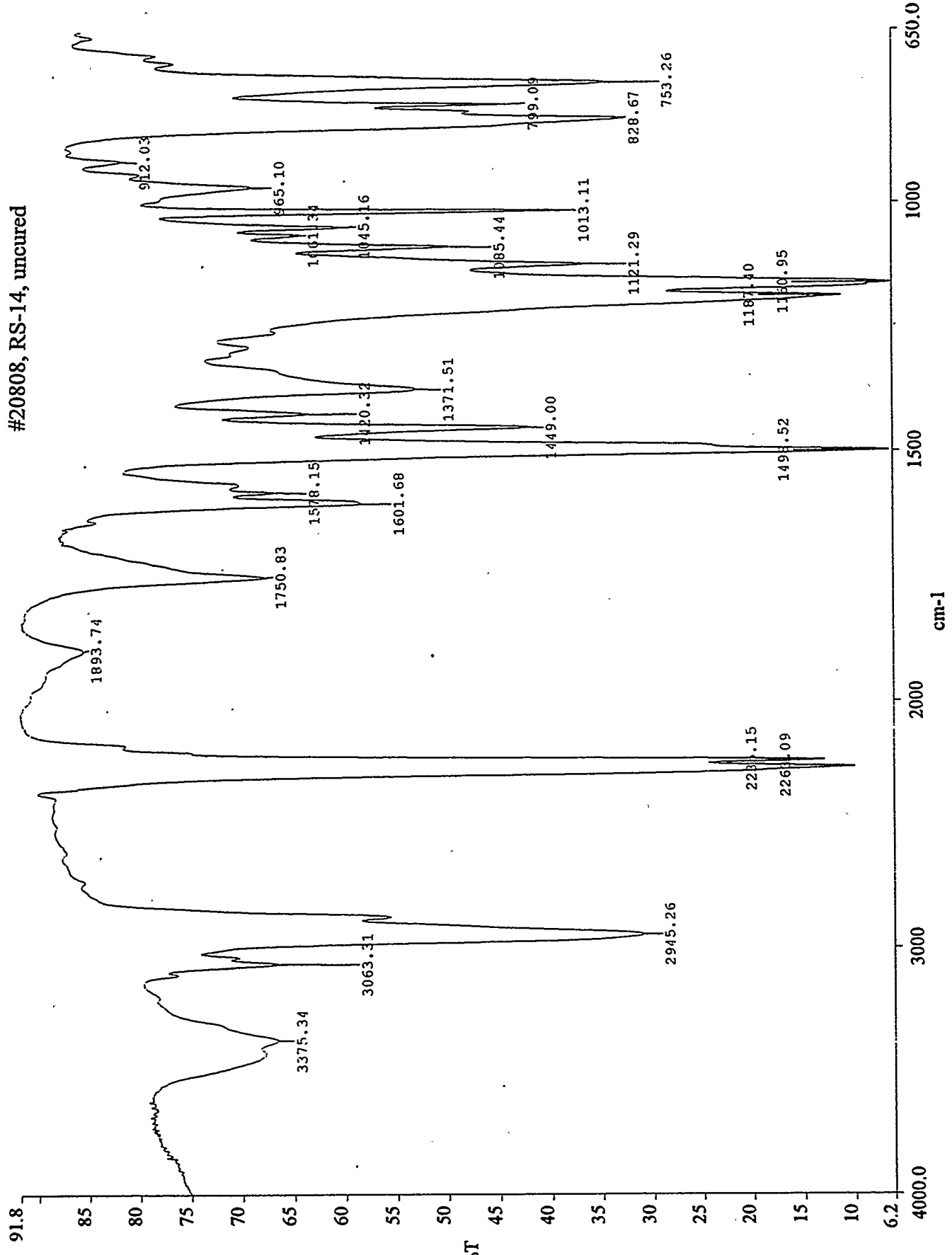
#20808, RS-14, uncured
91.8
6.2
%T
4000.0
3000
2000
1500
1000
650.0
cm-1
3375.34
3063.31
2945.26
2260.09
1893.74
1750.83
1601.68
1578.15
1449.00
1371.51
1121.29
1013.11
965.10
912.03
828.67
799.09
753.26

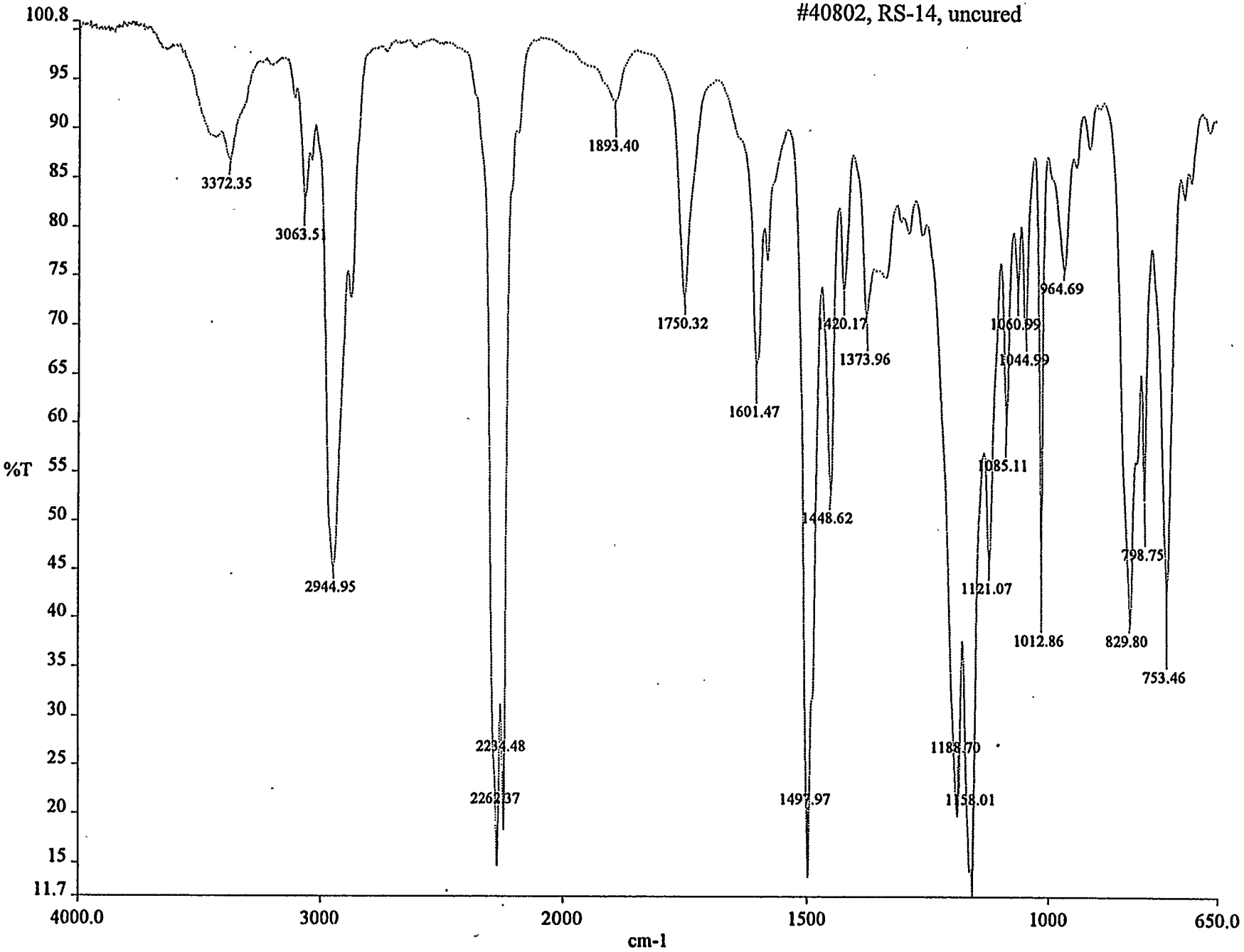
#40802, RS-14, uncured
100.8
95
90
85
80
75
70
65
60
55
50
45
40
35
30
25
20
15
11.7
%T
3372.35
3063.51
2944.95
2234.48
2262.37
1893.40
1750.32
1601.47
1497.97
1448.62
1420.17
1373.96
1188.70
1158.01
1121.07
1085.11
1060.99
1044.99
1012.86
964.69
829.80
798.75
753.46
4000.0
3000
2000
1500
1000
650.0
cm-1

A-4

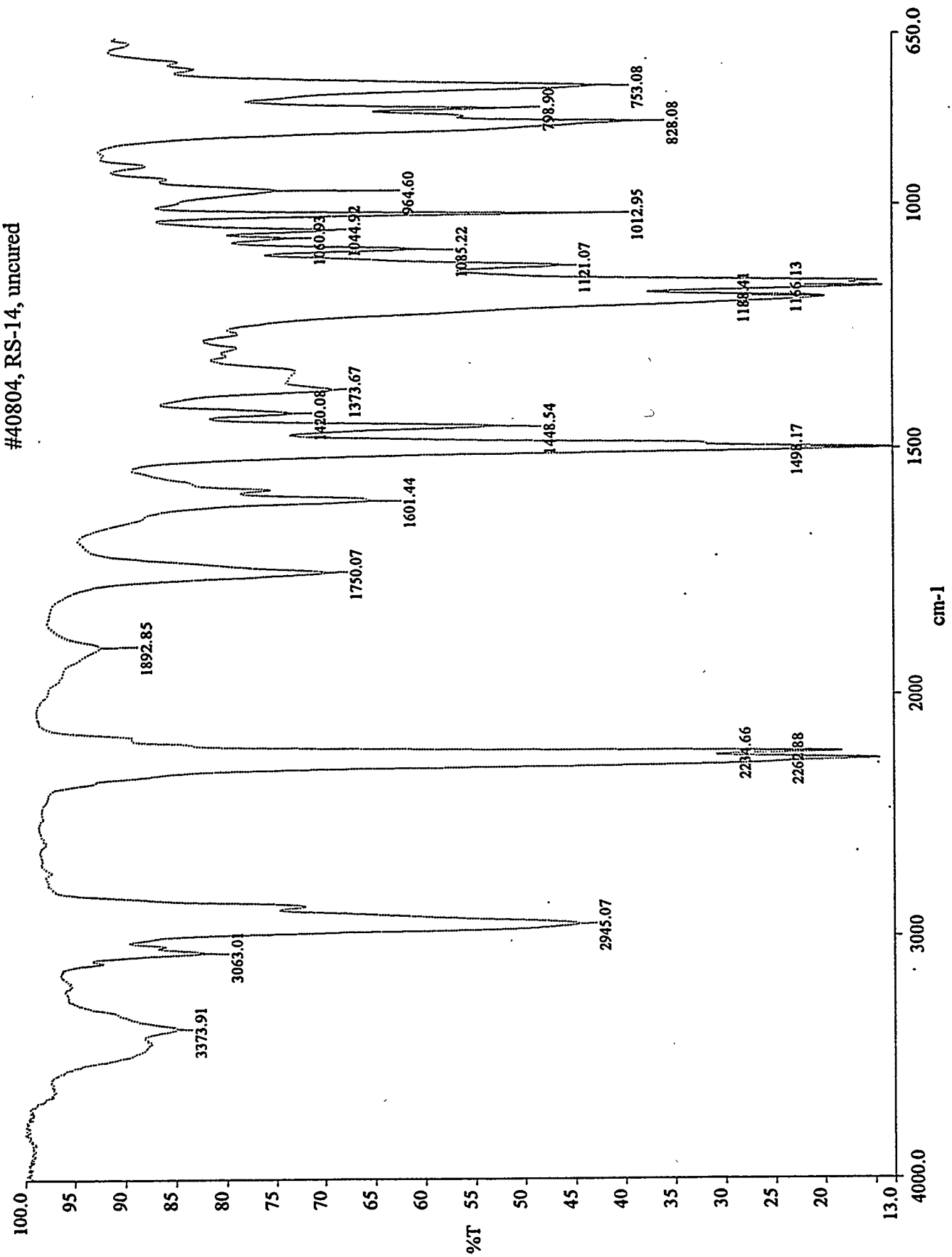
#40804, RS-14, uncured
100.0
95
90
85
80
75
70
65
60
55
50
45
40
35
30
25
20
13.0
%T
4000.0
3000
2000
1500
1000
650.0
cm-1
3373.91
3063.01
2945.07
1892.85
1750.07
1601.44
1498.17
1448.54
1420.08
1373.67
1188.41
1166.13
1121.07
1085.22
1060.93
1044.92
1012.95
964.60
828.08
798.90
753.08

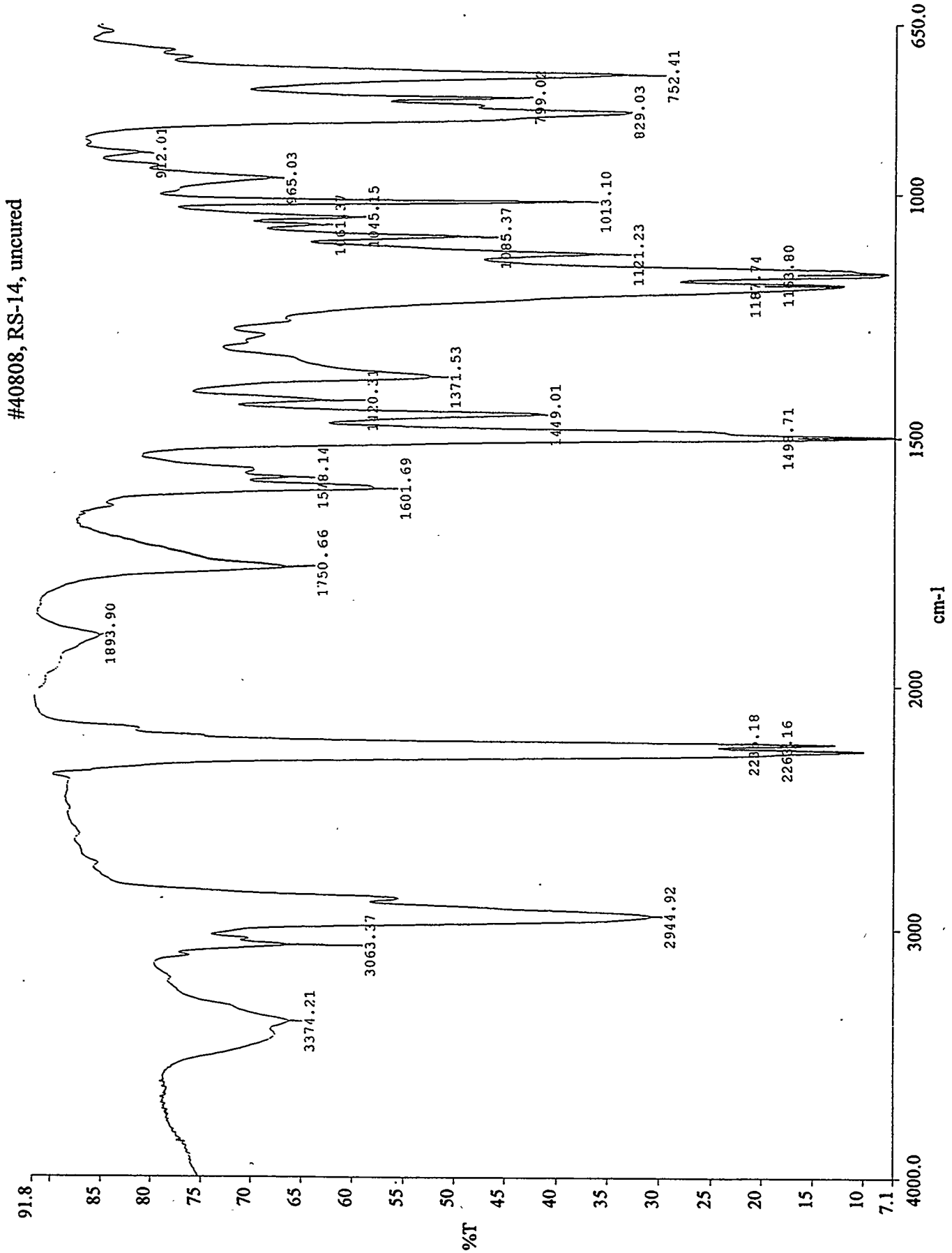
#40808, RS-14, uncured
%T
cm-1
4000.0
650.0
1000
1500
2000
3000
3374.21
3063.37
2944.92
1893.90
1750.66
1601.69
1498.71
1449.01
1371.53
1121.23
1013.10
912.01
829.03
752.41

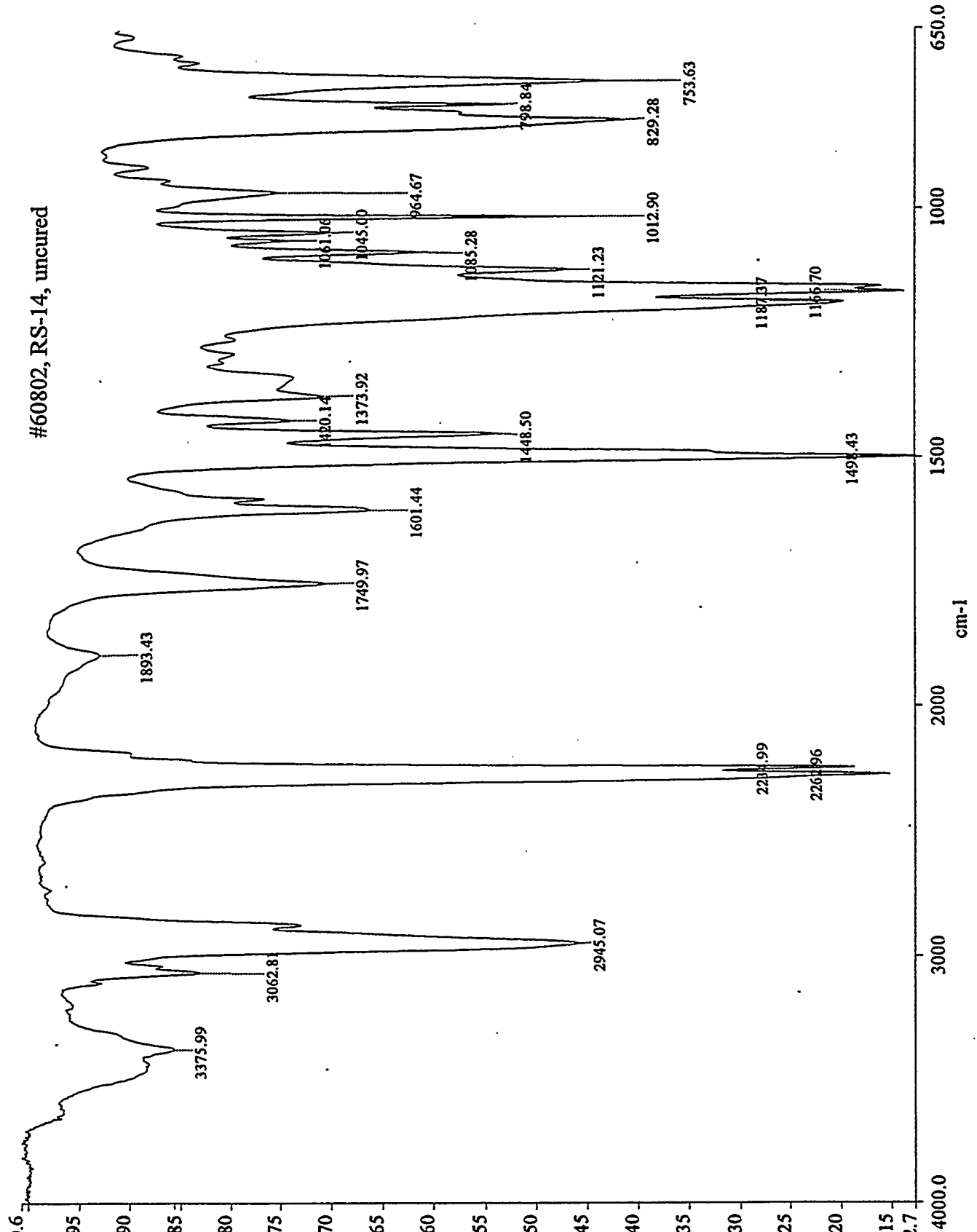
#60802, RS-14, uncured
100.6
95
90
85
80
75
70
65
60
55
50
45
40
35
30
25
20
15
12.7
%T
4000.0
3000
2000
1500
1000
650.0
cm-1
3375.99
3062.81
2945.07
2264.99
2261.96
1893.43
1749.97
1601.44
1498.43
1448.50
1420.14
1373.92
1187.37
1166.70
1121.23
1085.28
1061.06
1045.00
1012.90
964.67
829.28
798.84
753.63

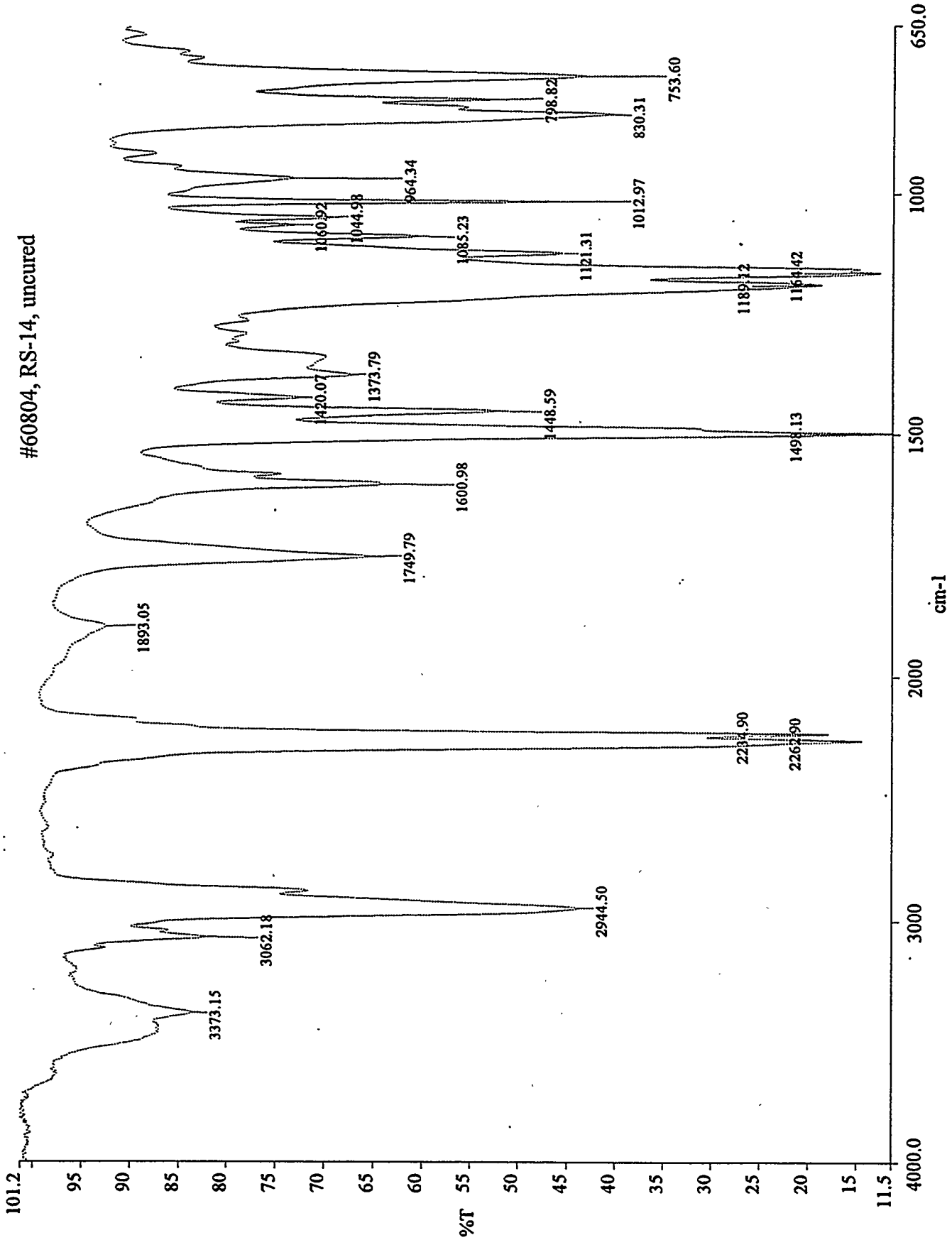
#60804, RS-14, uncured
%T
cm-1
101.2
95
90
85
80
75
70
65
60
55
50
45
40
35
30
25
20
15
11.5
4000.0
3000
2000
1500
1000
650.0
3373.15
3062.18
2944.50
1893.05
1749.79
1600.98
1448.59
1420.07
1373.79
1121.31
1085.23
1060.92
1044.98
1012.97
964.34
830.31
798.82
753.60

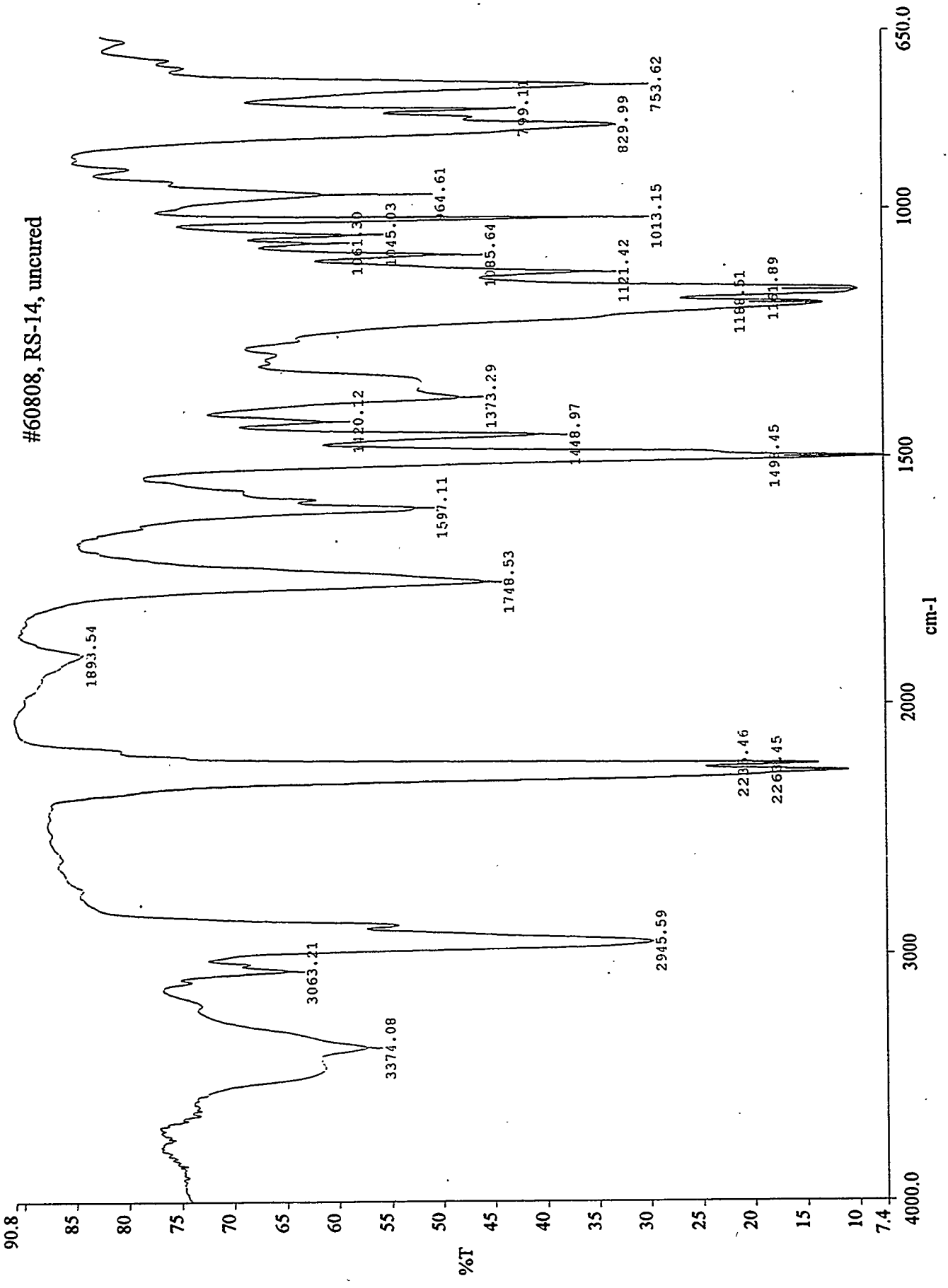
#60808, RS-14, uncured
%T
cm-1
4000.0
3000
2000
1500
1000
650.0
90.8
7.4
3374.08
3063.21
2945.59
1893.54
1748.53
1597.11
1448.97
1373.29
1120.12
1121.42
1013.15
829.99
753.62

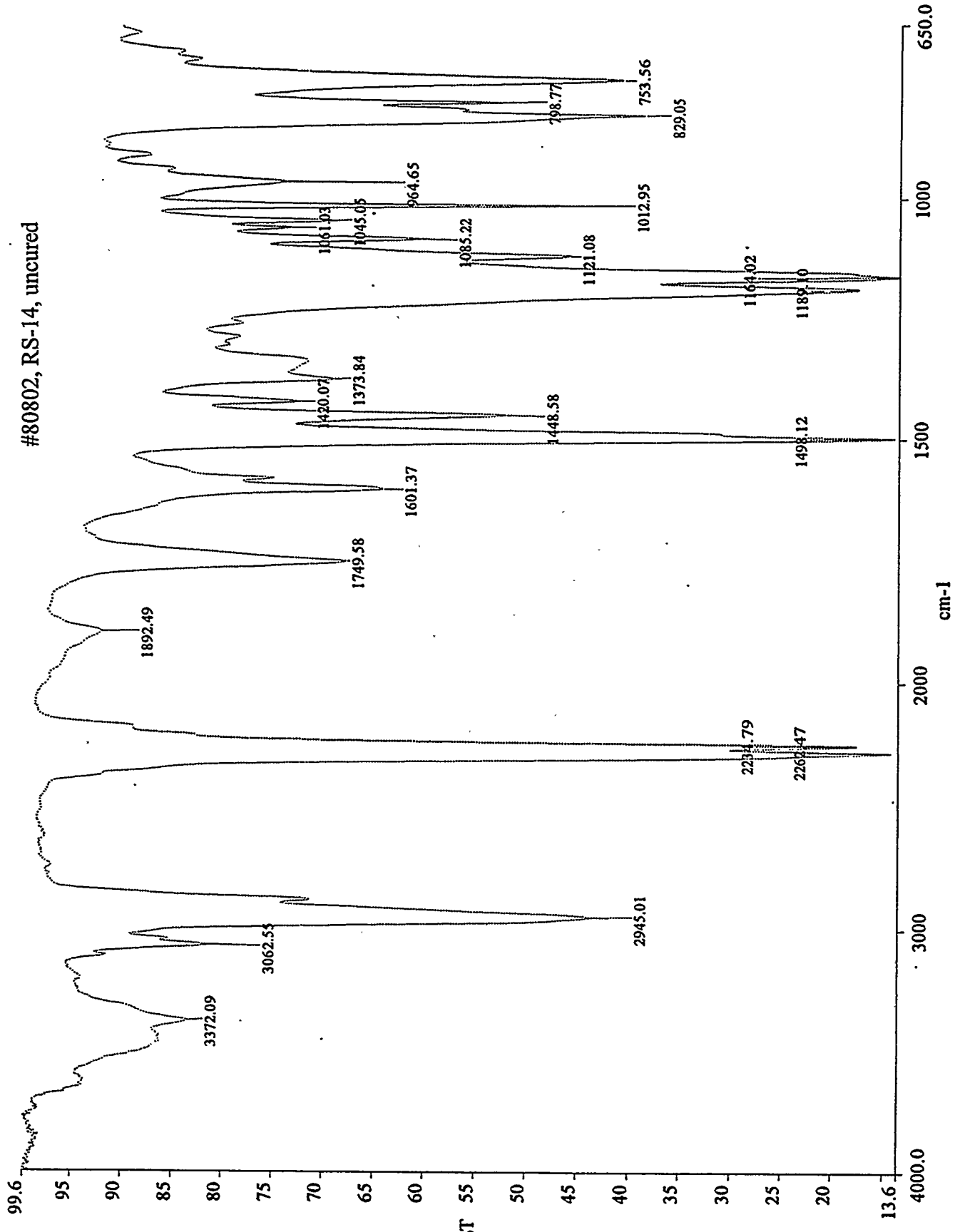
#80802, RS-14, uncured
%T
cm-1
99.6
95
90
85
80
75
70
65
60
55
50
45
40
35
30
25
20
13.6
4000.0
3000
2000
1500
1000
650.0
3372.09
3062.55
2945.01
2231.79
2264.47
1892.49
1749.58
1601.37
1498.12
1448.58
1420.07
1373.84
1189.10
1164.02
1121.08
1085.22
1061.03
1045.05
1012.95
964.65
829.05
798.77
753.56

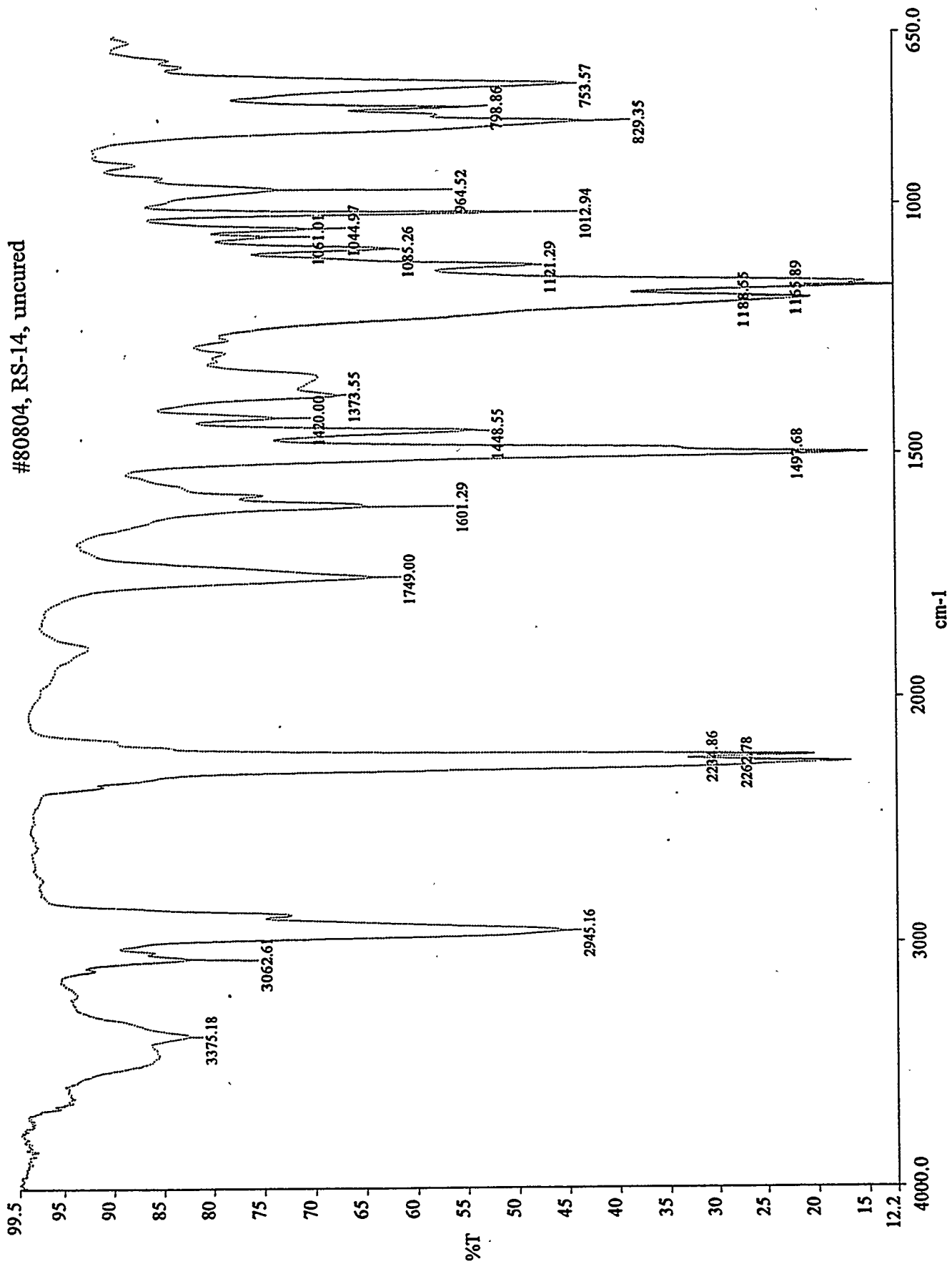
#80804, RS-14, uncured
%T
cm-1
99.5
95
90
85
80
75
70
65
60
55
50
45
40
35
30
25
20
15
12.2
4000.0
3000
2000
1500
1000
650.0
3375.18
3062.6
2945.16
2234.86
2262.78
1749.00
1601.29
1497.68
1448.55
1420.00
1373.55
1188.55
1155.89
1121.29
1085.26
1061.05
1044.97
1012.94
964.52
829.35
798.86
753.57

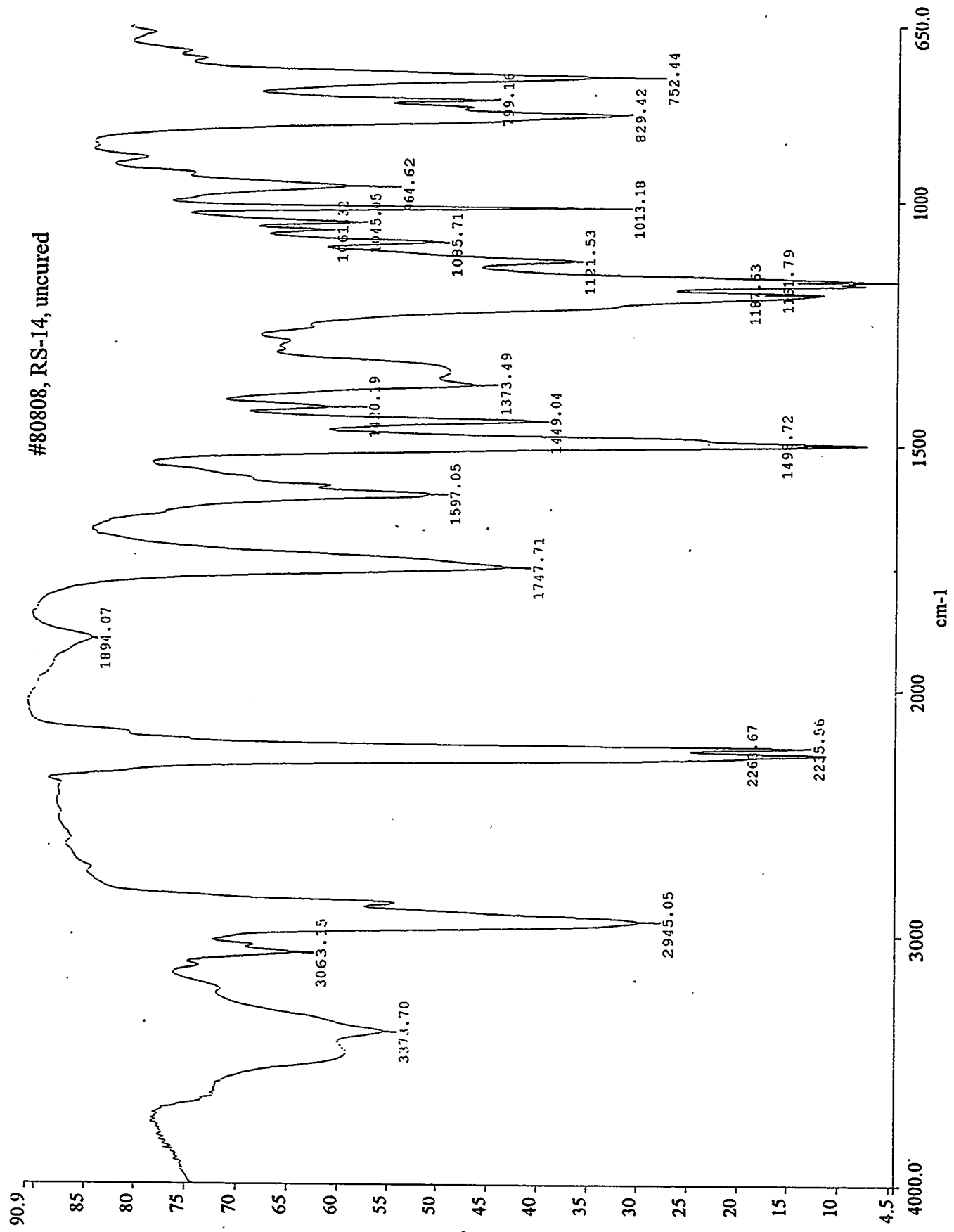
#80808, RS-14, uncured
%T
cm-1
4000.0
650.0
1894.07
1747.71
1597.05
1373.49
1449.04
2945.05
3063.15
1013.18
829.42
752.44
1085.71
1121.53
1013.18
964.62
829.42
752.44

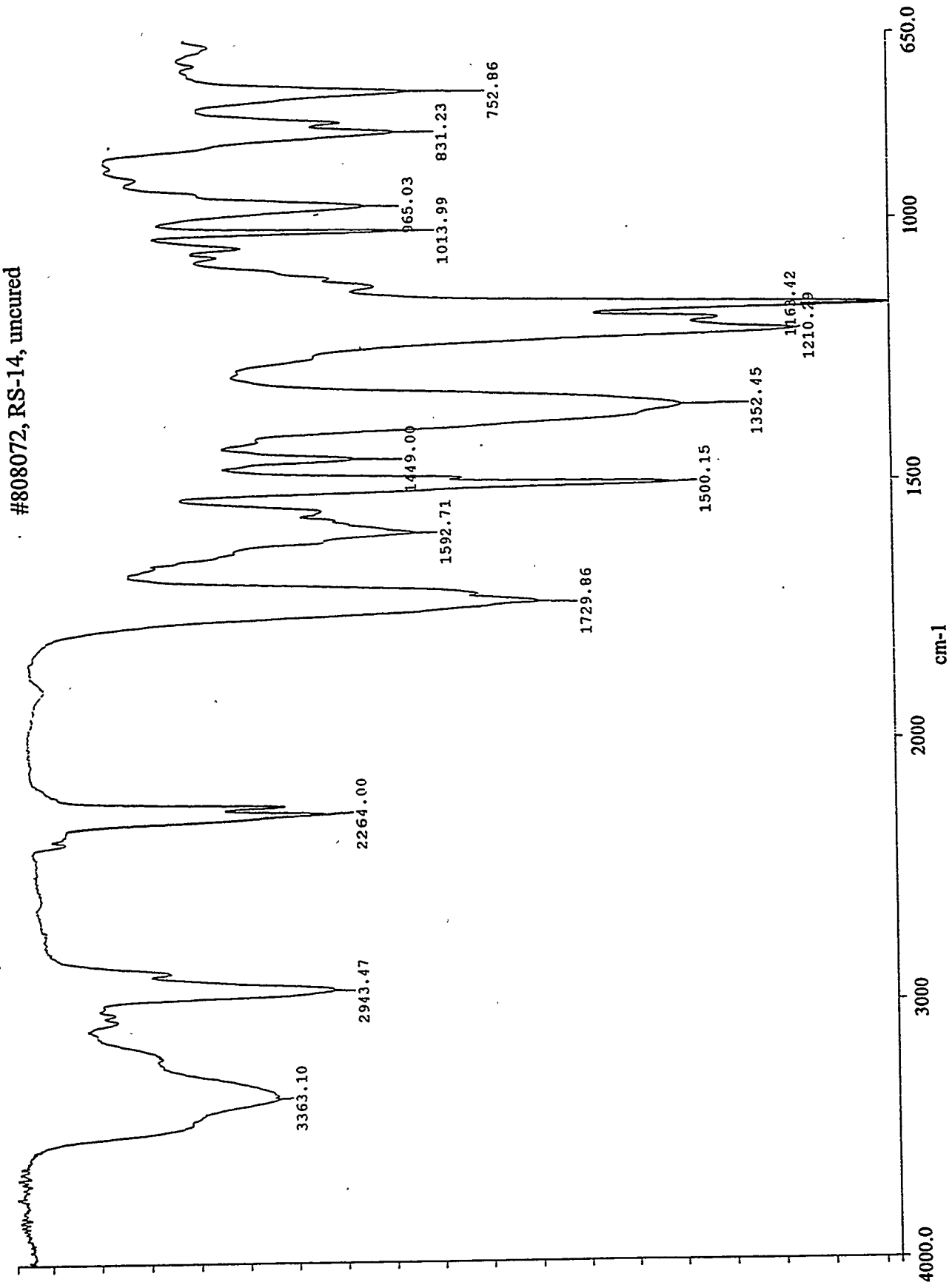
#808072, RS-14, uncured
4000.0
3000
2000
1500
1000
650.0
cm-1
3363.10
2943.47
2264.00
1729.86
1592.71
1500.15
1449.00
1352.45
1210.29
1168.42
1013.99
965.03
831.23
752.86

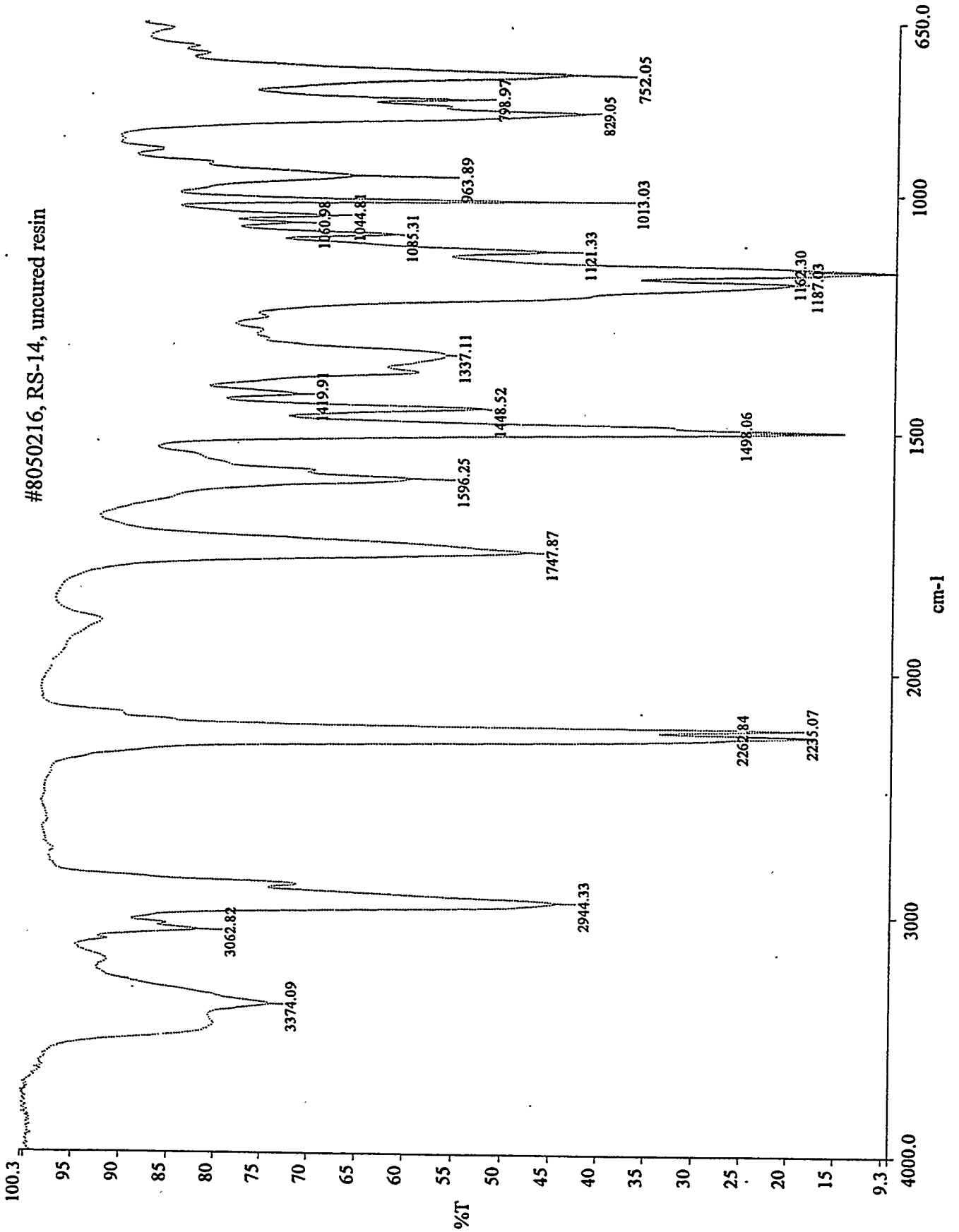
#8050216, RS-14, uncured resin
100.3
95
90
85
80
75
70
65
60
55
50
45
40
35
30
25
20
15
9.3
%T
4000.0
3000
2000
1500
1000
650.0
cm-1
3374.09
3062.82
2944.33
2267.84
2235.07
1747.87
1596.25
1498.06
1448.52
1419.91
1337.11
1187.03
1157.30
1121.33
1085.31
1060.98
1044.81
1013.03
963.89
829.05
798.97
752.05

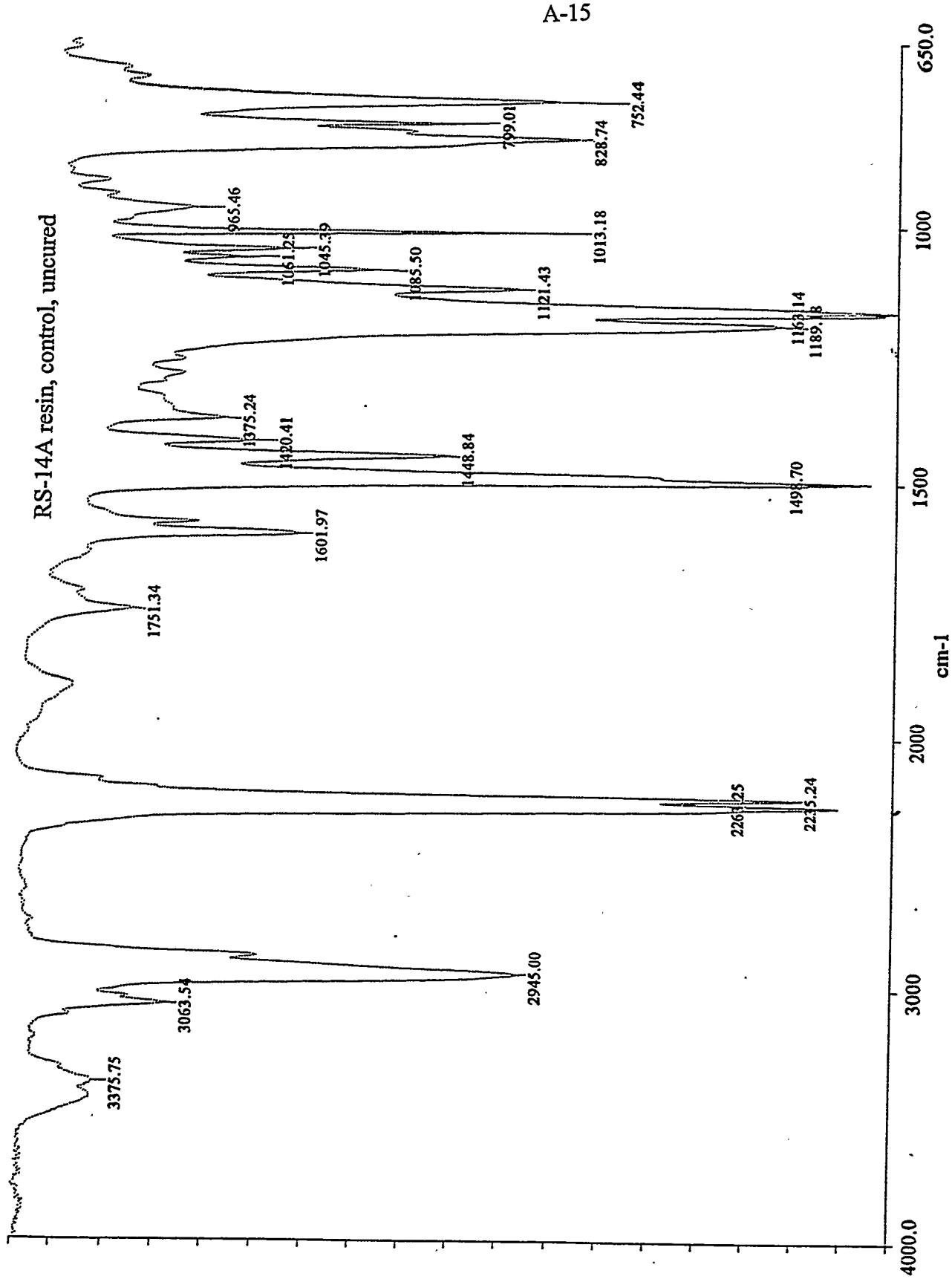
RS-14A resin, control, uncured
4000.0
3000
2000
1500
1000
650.0
cm-1
3375.75
3063.54
2945.00
2269.25
2235.24
1751.34
1601.97
1498.70
1448.84
1420.41
1375.24
1189.18
1168.14
1121.43
1085.50
1061.25
1045.39
1013.18
965.46
828.74
799.01
752.44

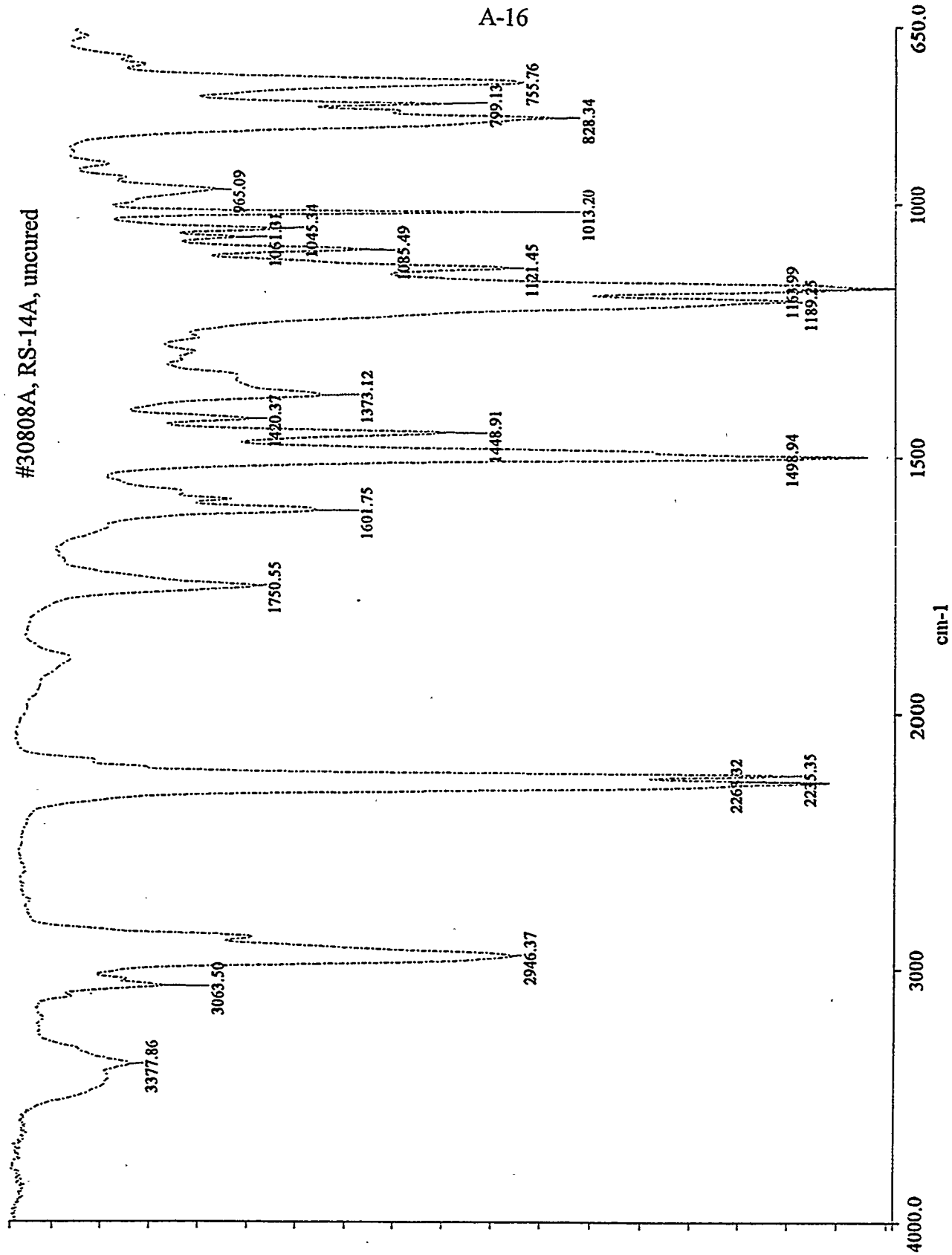
#30808A, RS-14A, uncured
4000.0
3000
2000
1500
1000
650.0
cm-1
3377.86
3063.50
2946.37
2269.32
2235.35
1750.55
1601.75
1498.94
1448.91
1420.37
1373.12
1189.25
1163.99
1121.45
1085.49
1045.14
1013.20
965.09
828.34
799.13
755.76

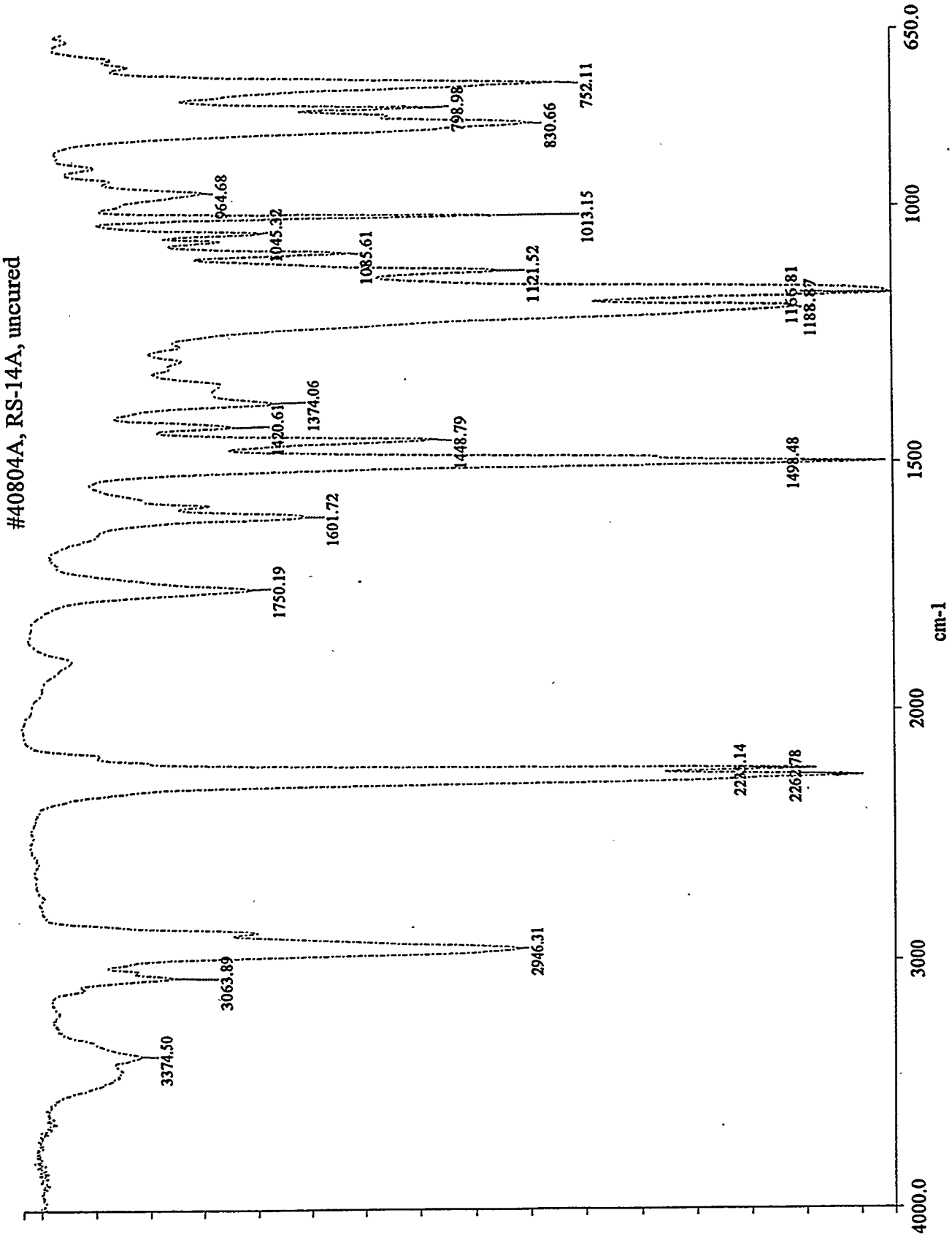
#40804A, RS-14A, uncured
4000.0
3000
2000
1500
1000
650.0
cm-1
3374.50
3063.89
2946.31
2265.14
2261.78
1750.19
1601.72
1498.48
1448.79
1420.61
1374.06
1188.87
1166.81
1121.52
1085.61
1045.32
1013.15
964.68
830.66
798.98
752.11

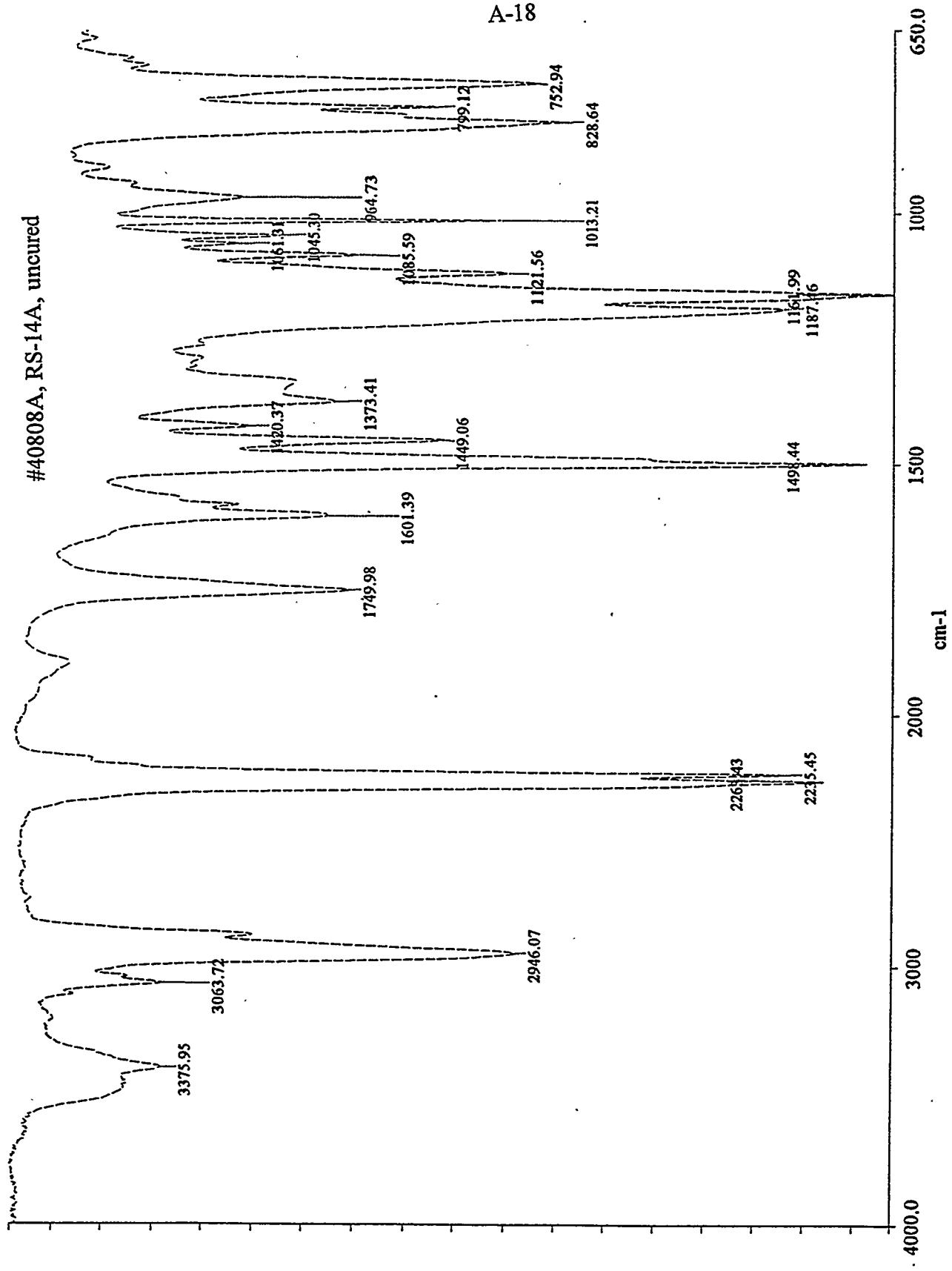
#40808A, RS-14A, uncured
4000.0
3000
2000
1500
1000
650.0
cm-1
3375.95
3063.72
2946.07
2265.43
2235.45
1749.98
1601.39
1498.44
1449.06
1420.37
1373.41
1187.16
1161.99
1121.56
1085.59
1045.30
1013.21
964.73
828.64
799.12
752.94

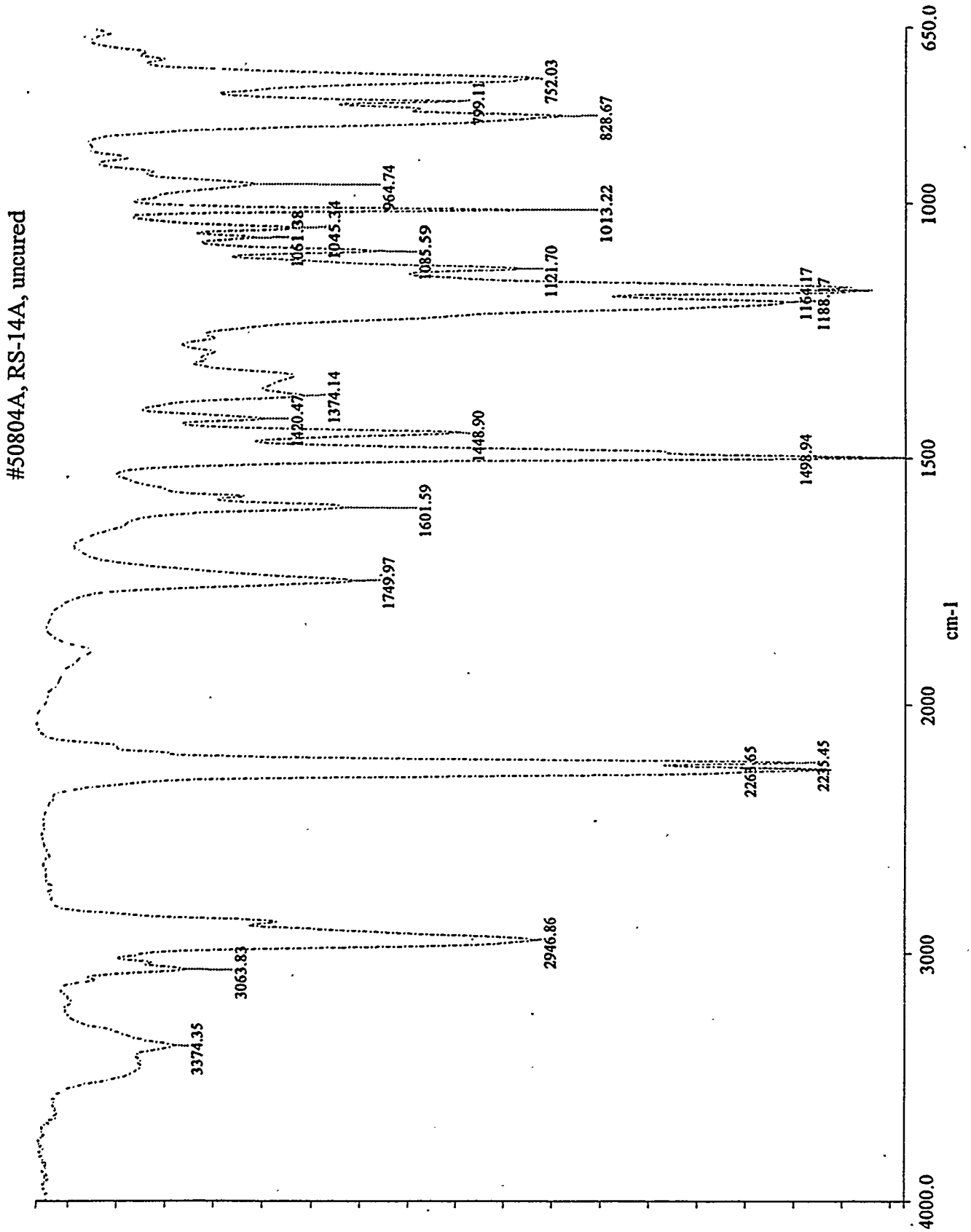
#50804A, RS-14A, uncured
4000.0
3000
2000
1500
1000
650.0
cm-1
3374.35
3063.83
2946.86
2263.65
2235.45
1749.97
1601.59
1498.94
1448.90
1420.47
1374.14
1188.17
1164.17
1121.70
1085.59
1045.14
1061.38
1013.22
964.74
828.67
799.11
752.03

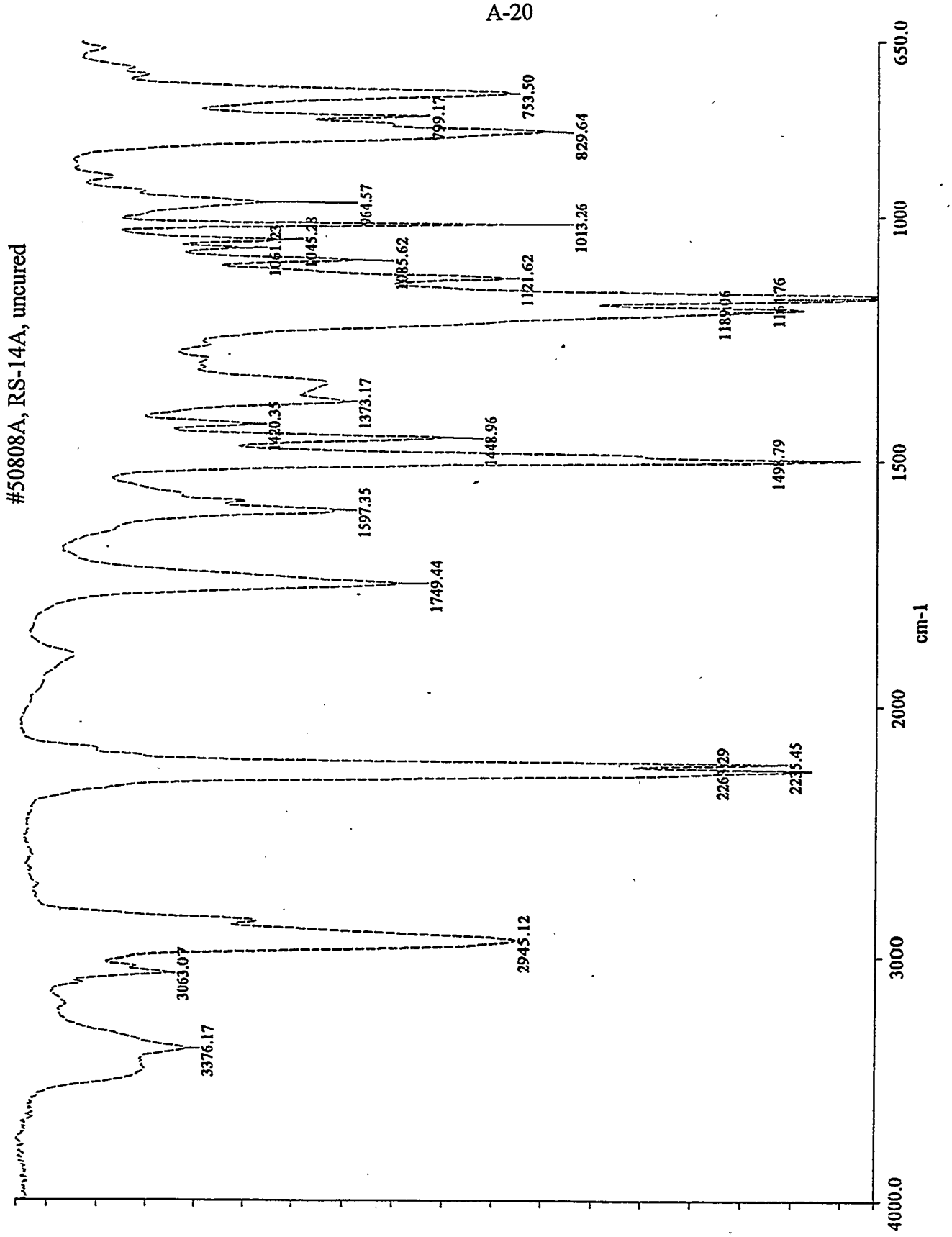
#50808A, RS-14A, uncured
4000.0
3000
2000
1500
1000
650.0
cm-1
3376.17
3063.07
2945.12
2261.29
2235.45
1749.44
1597.35
1498.79
1448.96
1420.35
1373.17
1189.06
1161.76
1121.62
1085.62
1045.28
1013.26
964.57
829.64
799.17
753.50

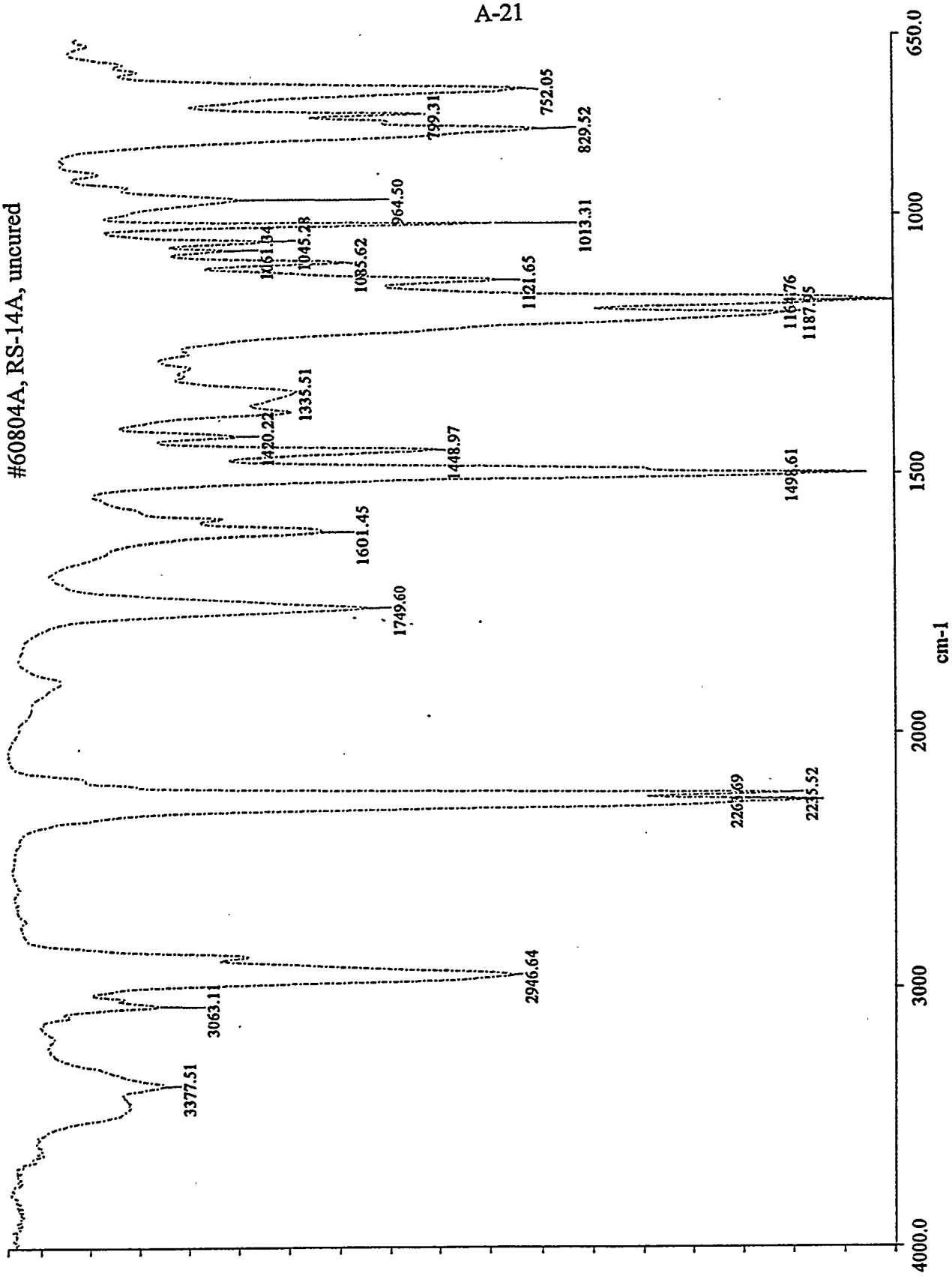
#60804A, RS-14A, uncured
4000.0
3000
2000
1500
1000
650.0
cm-1
3377.51
3063.11
2946.64
2263.69
2235.52
1749.60
1601.45
1498.61
1448.97
1420.22
1335.51
1187.95
1164.76
1121.65
1085.62
1045.28
1013.31
964.50
829.52
799.31
752.05

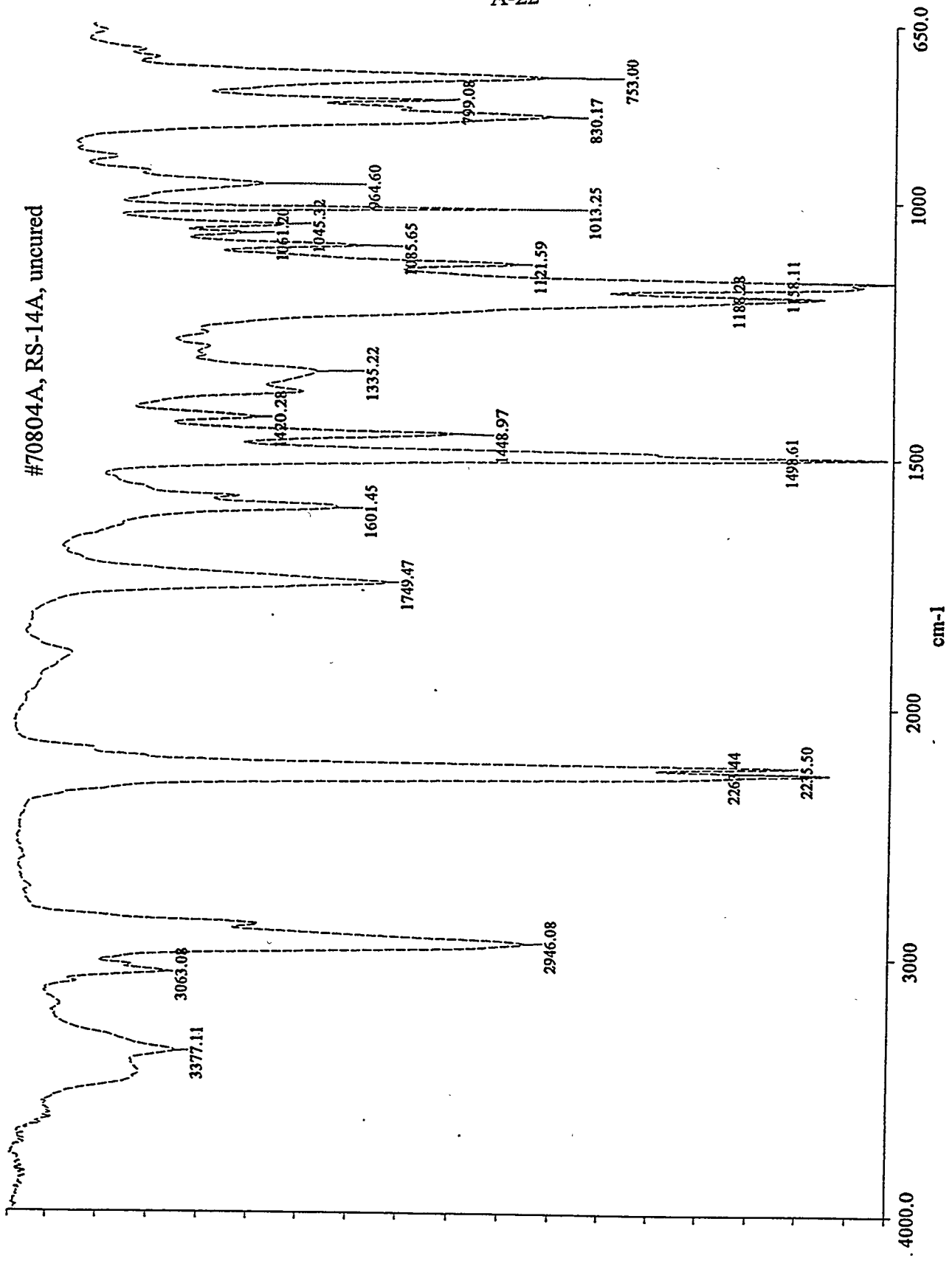
#70804A, RS-14A, uncured
4000.0
3000
2000
1500
1000
650.0
cm-1
3377.11
3063.08
2946.08
2261.44
2235.50
1749.47
1601.45
1498.61
1448.97
1420.28
1335.22
1188.23
1158.11
1121.59
1085.65
1061.20
1045.32
1013.25
964.60
830.17
799.08
753.00

Appendix A.2

FTIR REFERENCE SCANS OF RS-14, XU71787.07L AND AroCy L-10 RESINS

Reference scans of the RS-14 resin and its two major constituents (XU71787.07L from the Dow Chemical Company and AroCy L-10 from Ciba Geigy) have been provided by YLA and are included for comparison.

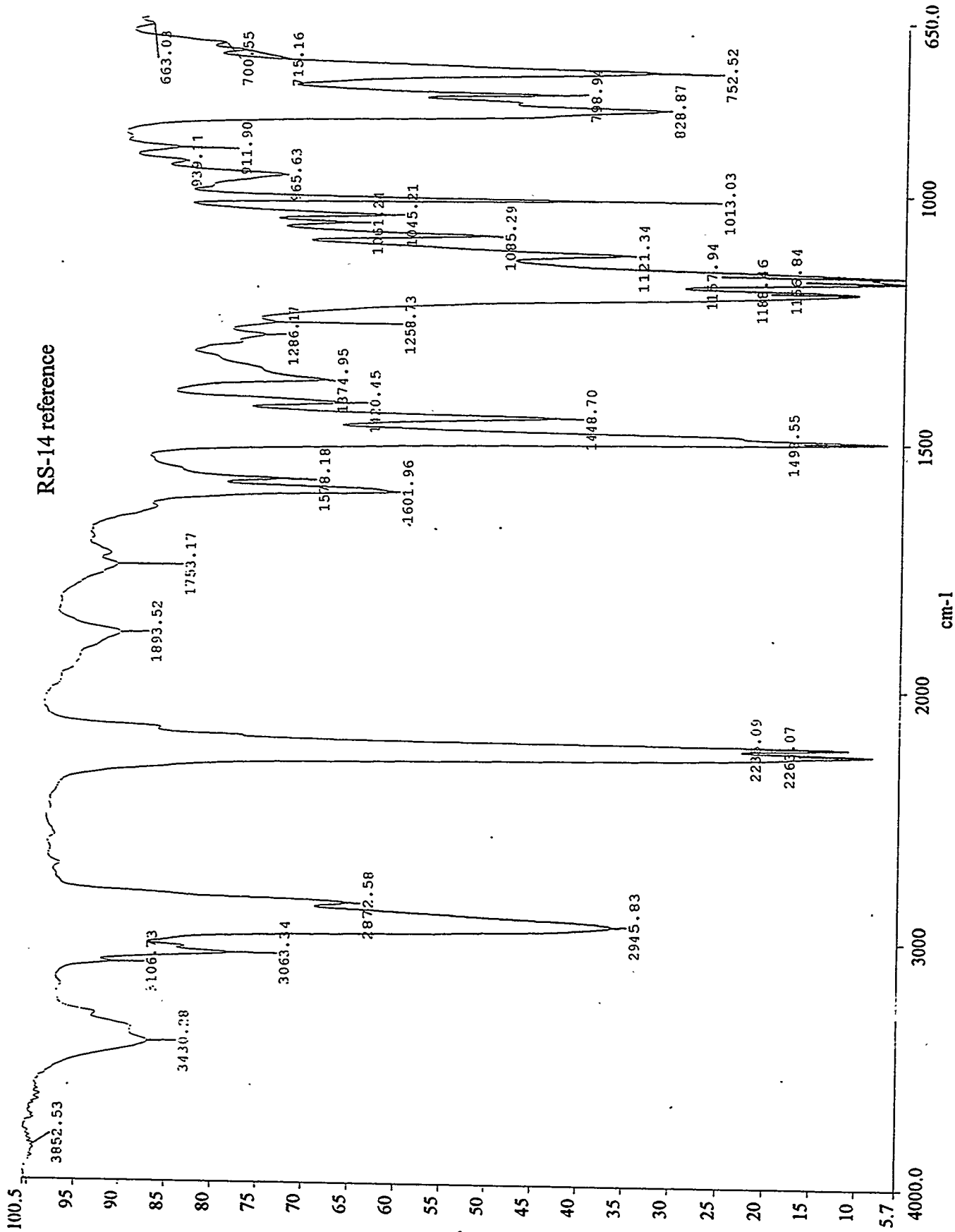
RS-14 reference
%T
cm-1
100.5
95
90
85
80
75
70
65
60
55
50
45
40
35
30
25
20
15
10
5.7
4000.0
3000
2000
1500
1000
650.0
3852.53
3430.28
3106.73
3063.34
2945.83
2872.58
2263.07
1893.52
1753.17
1601.96
1578.18
1448.70
1374.95
1286.17
1258.73
1085.29
1045.21
1013.03
911.90
828.87
798.94
752.52
715.16
700.55
663.08

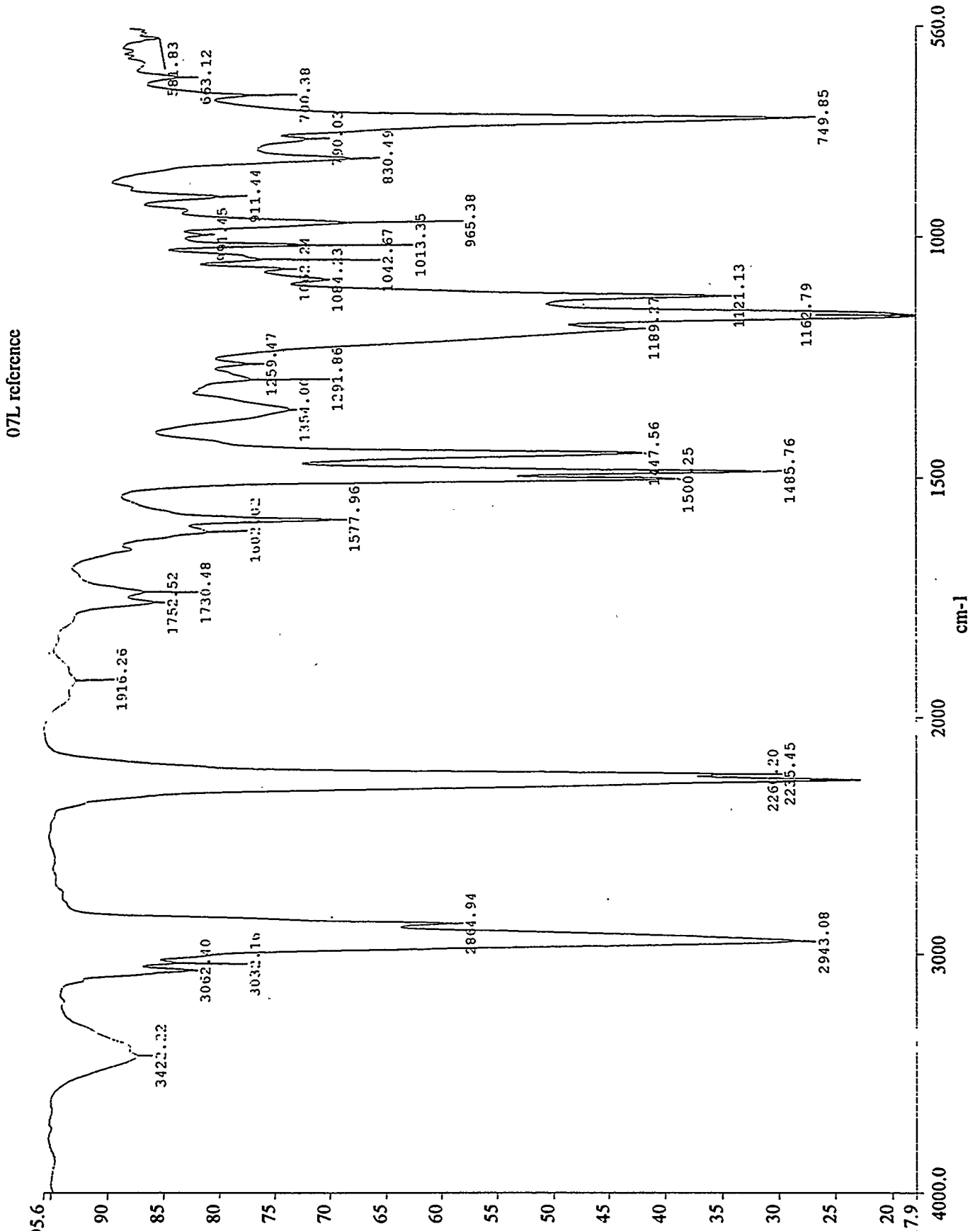
07L reference
%T
cm-1
95.6
17.9
4000.0
560.0
3422.32
3062.40
3032.16
2943.08
2864.94
2260.20
2235.45
1916.26
1752.52
1730.48
1577.96
1485.76
1500.25
1447.56
1354.06
1291.86
1259.47
1189.27
1160.79
1121.13
1084.13
1042.67
1013.35
965.38
911.44
830.49
749.85
700.38
663.12

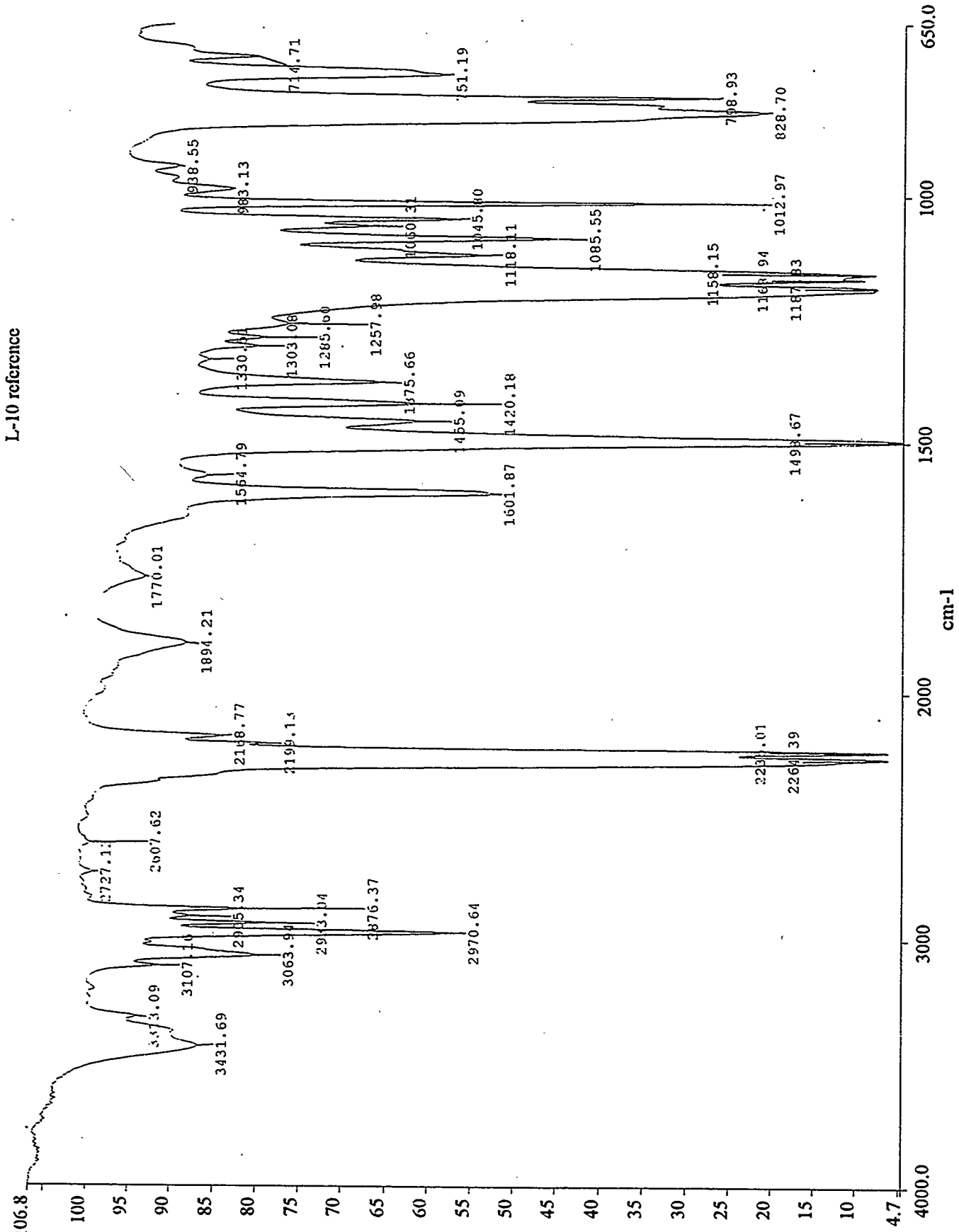
L-10 reference
106.8
100
95
90
85
80
75
70
65
60
55
50
45
40
35
30
25
20
15
10
4.7
%T
4000.0
3000
2000
1500
1000
650.0
cm-1
3431.69
3107.10
3063.99
2970.64
2876.37
2727.12
2607.62
2264.39
1894.21
1770.01
1601.87
1564.79
1498.67
1420.18
1375.66
1330.00
1303.08
1257.98
1158.15
1118.11
1085.55
1045.80
1012.97
983.13
938.55
828.70
798.93
751.19
714.71